Aus der Klinik für Frauenheilkunde,
Geburtshilfe und Reproduktionsmedizin
Universitätsklinikum des Saarlandes, Homburg/Saar
Direktor: Prof. Dr. med. E.-F. Solomayer

Cyclopentanolates of Aluminium Hydride /Chloride and Synthesis & Characterization of Superhydrophobic Surfaces for Biomedical Applications

Dissertation
zur Erlangung des Grades eines Doktors der Naturwissenschaften
der Medizinischen Fakultät
der UNIVERSITÄT DES SAARLANDES
2016

Vorgelegt von: Awadelkareem Abdelrahman Ali Mohamed
geb. am: 01.01.1981 in Algalgala, Sudan

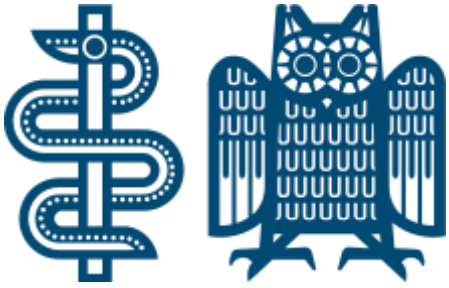

This thesis was performed at INM-Leibniz Institute for New Materials and biology laboratory of Paediatric Cardiology Department at Medical Faculty of Saarland University located at the same institute.

Table of contents

Abstract

The first approach of this thesis is dedicated to the synthesis of aluminum based precursors with exactly known structures to be used for the preparation of nano materials for further application. Six different compounds were prepared from the reaction of $LiAlH_4$ with $AlCl_3$ and cyclopentanol in different molar ratios: $[H_2Al(O\text{-}C_5H_9)]_6$ $[H(Cl)Al(O\text{-}C_5H_9)]_2$ **1**, $[H_6Al_4(O\text{-}C_5H_9)_6]$ **2**, $[Cl_6Al_4(O\text{-}C_5H_9)_6]$ **3**, $[Al(O\text{-}C_5H_9)_3]_4$ **4**, $[H_5Al_5(O)(O\text{-}C_5H_9)_8]$ **5**, and $[H_{4.5}Cl_{0.5}Al_5(O)(O\text{-}C_5H_9)_8]$ **6**. All these compounds were obtained in a crystalline form and their molecular structures have been determined by using single crystal X-ray structure analysis as well as ^1H and ^{13}C NMR, IR spectroscopy and elemental analysis.

The second approach of this dissertation is the modification of 1D Al/Al_2O_3 core/shell nano-wires with a fuoro-organophosphazene polymer. We have developed a super-hydrophobic surface by a dual surface treatment of 3D Al/Al_2O_3 nano-wire assemblies using chemical vapour deposition technique followed subsequently by surface modification with Poly[bis(2,2,2-trifluoroethoxy)phosphazene] (PTEFP). The so modified surfaces were fully characterized by SEM, XPS, Contact angle, and IR spectroscopy. This approach leads to the formation of stable ultra-hydrophobic surfaces without altering the general topographic nature of the surface initially created by the inorganic backbone. Exemplary properties and applications of the new hybrid surfaces versus different liquids are presented.

This thesis is dealing with chemical and physical methods and results to develop such stable ceramic surfaces for potential use in patients with congenital and acquired heart disease.

The developed ceramic surface in combination of nano-wires and polymer has proven to be mechanically and chemically stable and can be easily manufactured on metal mostly used for stents, such as stainless steal, nitinilol, or cobalt chrome.

Zusammenfassung

Der erste Teil dieser Doktorarbeit beschäftigt sich mit der Synthese von molekularen Precursoren mit Aluminium als Zentralelement und mit möglichst genau bestimmten Strukturen, die zur weiteren Anwendung für die Herstellung von Nanomaterialien verwendet werden sollen. Es wurden sechs verschiedene Verbindungen durch Reaktionen von $LiAlH_4$ mit $AlCl_3$ und Cyclopentanol, in unterschiedlichen Molverhältnissen umgesetzt, erhalten: $[H_2Al(O\text{-}C_5H_9)]_6$ $[H(Cl)Al(O\text{-}C_5H_9)]_2$ **1**, $[H_6Al_4(O\text{-}C_5H_9)_6]$ **2**, $[Cl_6Al_4(O\text{-}C_5H_9)_6]$ **3**, $[Al(O\text{-}C_5H_9)_3]_4$ **4**, $[H_5Al_5(O)(O\text{-}C_5H_9)_8]$ **5**, und $[H_{4.5}Cl_{0.5}Al_5(O)(O\text{-}C_5H_9)_8]$ **6**. Alle diese Verbindungen lagen in kristalliner Form vor und ihre Molekularstrukturen wurden durch Einkristall-Röntgenstrukturanalyse sowie ^1H und ^{13}C NMR, IR-Spektroskopie und Elementaranalyse bestimmt.

Der zweite Teil dieser Dissertation ist die Veränderung von 1D Al/Al_2O_3-Kern/Schale-Nanodrähten mit einem Fluor-Organorphosphazen-Polymer. Wir konnten eine super-hydrophobe Oberfläche auf Substraten generieren, indem wir zunächst 3D Al/Al_2O_3-Kern/Schale-Nanodraht Strukturen durch chemische Gasphasenabscheidung bildeten und darauf nachträglich als weitere Schicht Poly[bis(2,2,2-trifluoroethoxy)phosphazene] (PTEFP) ablagerten. Die derart modifizierten Oberflächen wurden vollständig durch REM, XPS, Kontaktwinkelmessung und IR-Spektroskopie charakterisiert. Dieser Ansatz führt zur Bildung von stabilen ultra-hydrophoben Oberflächen, ohne die topographische Beschaffenheit der vormals anorganischen Schicht zu verändern.

Exemplarische Eigenschaften und Anwendungen der neuen, hybriden Ober-flächen gegenüber unterschiedlichen Flüssigkeiten werden vorgestellt.

Diese Arbeit beschäftigt sich mit chemischen und physikalischen Methoden. Final wurden stabile keramische Oberflächen für eine spätere potenzielle Anwendung bei Patienten mit angeborenen oder erworbenen Herzfehlern entwickelt.

Es konnte gezeigt werden, dass die entwickelten keramischen Oberflächen in Kombination mit Al/Al2O3-Nanowiren und PTFP über eine mechanische und chemische Stabilität verfügen. Ferner ist eine einfache Herstellung auf metallischen Substraten, die auch zur Produktion von Stents eingesetzt werden, wie Edelstahl, Nitinolol oder Chrom-Kobald-Gemischen, möglich**.**

Research Motivation:

Interventional percutaneous implantation of different devices to treat vessel stenosis and recanalization of obstructed vessels is increasingly used instead of surgical therapy in different congenital and acquired cardiovascular diseases.

In the last year's percutaneous implantation of stent valves are replacing the surgical implantation of mechanical biological and mechanical valve in adults.

In addition to the wildly used stents in adults with acquired coronary heart disease, intervention in children with congenital heart and vessel disease has improved the survival and quality of life in these patients. However, implantation of small stents in the small vessels is still challenging due to thrombosis and In-Stent stenosis as well as intima-proliferation. In children with growing small vessels stent implantation is also challenging, due the rapid intimal proliferation and failure to dilate the stents in further age.

Congenital aortic and pulmonary valve disease in infants and children are primarily treated with balloon dilatation. However, in some case the need to implant mechanical prosthesis in aortic as well as mitral valve position may become necessary, when surgical reconstruction and repair failed.

The leading complications in association with these therapeutic procedures are still the poor blood surface biocompatibility and, even in the presence of extensive anticoagulation's. In addition, Anticoagulation therapy is associated with the risk of bleedings as well as thrombosis.

To overcome such complication coating oft he surface of all implanted devise such as stents and valves may enhance the biocompatibility and reduced such associated complications.

Thus, this thesis was concentrated on the development of chemical and physical ceramic surfaces in order to improve the blood surface biocompatibility. The testing of the biological aspects and the haem-compatibility on this surface was studied in other thesis in the same institution.

1. Introduction:

Biomaterials - artificial objects placed in direct contact with biological tissues, organisms or systems [1] are primary components of medical implants which support or substitute failing organs and tissues of the body. Despite the macroscopic dimensions of the implants and the human body, the interactions between biomaterials and biological media are taking place on a wide range of length scales: starting from angstrom and nanometer level where the atomic structure of the implant surface interact with biological ions and molecules (e.g. water, salts, amino acids, peptide sequences, proteins), continuing with micrometer size surface irregularities interacting mostly with cells, and ending with millimeter and centimeter size features being in functional contact with tissues or organs of the body [2].

In recent years researchers from different disciplines conducted various studies to understand the interactions between the biological environment and artificial materials. Biomaterial science and technology bring up new innovations where the main attention is given on both continuous functionality of an artificial device and proper biological host response. Biomaterials are used in tissue engineering scaffolds, biosensors and bioanalytical devices, non-fouling coatings in marine and food industries. Most of such applications are dependent on the nanoscopic and microscopic surface properties and processes, because the latter are involved at the very start of a complex sequence of physical, chemical and biological interactions occurring at the biosystem-material interface and therefore strongly affect the macroscopic outcome. For example, successful long-term performance and positive host tissue reaction to metallic orthopedic implants, e.g. artificial hip or knee joints, depends a lot on their surface microscopic parameters, such as surface oxide thickness and roughness determining the intensity of internal friction and wear, stress distribution and transmission to surrounding tissues, as well as the amount of microscopic

defects in the oxide layer, which can be corrosion and/or toxic ion leakage sites [3].

Former studies pointed out that the surface nano-architecture plays essential rule in the determination of the amount and conformation of adsorbed proteins and some cellular responses [4-9], while surface chemical and topographic microstructure affects cell morphology and physiology [4, 6, 7, 9-13], adhesion strength of single cells [14, 15] or whole macro-organisms [16], as well as influences tissue responses such as inflammatory reaction and fibrous capsule formation [17-19]. Having the means to induce and vary microscopic material characteristics in controlled manner, it becomes possible to study the role of each characteristic in the final outcome of the material interactions with surrounding media, and therefore to utilize the microscopic processes for inducing/improving overall functionality of the material, e.g. general biocompatibility, fouling resistance, sensing ability. The well-controlled systematic variation of most relevant surface microscopic characteristics may help to tune or optimize the surfaces for their best functional performance in a specific application, even in the situations where biological reactions are caused by synergistic effects of several material characteristics and the variation of individual microscopic characteristics does not provide enough information to understand the mechanisms behind the effect.

Various types of materials varying from organic compounds to metal/metal alloys have been used to fabricate implants. Most of the current orthopedic and cardiovascular implants are made of metal or metal alloys [20]. For instance exposure of such metallic surfaces to environmental conditions leads to oxide layer formation. So in this context properties of such metal oxide surfaces are crucial for the design of an implant. Various metal and metal oxides were shown to exhibit a high degree of biocompatibility [21].

On the other hand the corrosion problem of metals leads the scientists to explore new stable oxides which can tackle this problem and improve the biocompatibility of the implants in same time. In case of oxide based coatings,

surface chemistry and topography play a critical role for the performance of the implant. It has been shown that micro-nano structured oxides improve the cell adhesion and proliferation [22].

Various synthetic methods such as sol-gel, chemical vapor deposition, physical vapor deposition and their combinations have been used to synthesize micro-nano structured oxide thin films for implant applications. CVD is one of the most promising approaches due to ultra-thin layer deposition capability and conformity which is critical for coating 3D complex shaped implants.

One of the main problems in CVD coatings is the control of the stoichiometry and purity especially in case of multi-component systems. For the synthesis of multi-component materials using single source precursors (SSP) provides a clear advantage due to its ease of use and control [23]. In this context CVD of SSP brings out new possibilities for implant other biomedical applications.

1.1Metal alkoxides:

Metal alkoxides are a class of compounds with the general formula $[M(OR)_x]_n$ (where M = Metal or metalloid with valency x; R = simple alkyl, substituted alkyl, or alkenyl group; n = degree of molecular association). These types of compounds were observed for the first time in 1840 for the reaction of sodium and potassium with alcohol [24]. In the same year the term alkoxides was used by Kuhlmann [25] for the alkaline derivatives of alcohols. Later on there has been growing interest in the chemistry of this type of compounds due to their numerous applications especially in the fields like catalysis [26], sol- gel [27] and MOCVD (metal organic chemical vapour deposition) as precursors for the synthesis of pure metal oxides [28], precursors for nano materials, ceramics etc [23]. Metal alkoxides are very attractive for materials researchers, which is due to their unique features such as: easy accessibility, low cost, easy removability of alkoxide ligands via thermal treatments. More over their thermal deposition or

decomposition processes can be performed at relatively low temperatures compared to conventional methods involving other inorganic salts. These features play an essential rule in the properties of the obtained metal oxides from alkoxides precursors. These oxides are mostly highly pure, with high hardness, with a chemical and mechanical resistance, and have high temperature stability.

The synthesis of new different alkoxides precursors can lead to alternate the unique features of the structural frame work which influences the chemical and physical properties of the final metal oxide product.

Due to the characteristic features mentioned above, it is clear that metal alkoxides are very favourable and they posses a key role for the synthesis of new materials.

1.2 General synthesis methods of metal alkoxides:

Metal alkoxides are in general very sensitive to air and moisture, therefore essential precautions must be taken during their synthesis and handling. These include, drying of all reagents, solvents and the apparatus of production. Furthermore the environment above the reactants and products must be kept inert.

Different methods have been applied for the synthesis of metal alkoxides and their derivatives [24]. The main factor affecting the selection of the method for the synthesis is the ionization energy of the metal, which also affects the formation of alkoxide. The less electronegative ions with valences up to 3 (alkalie, alkaline earth metals, and lanthanides) react directly with alcohols liberating hydrogen and forming the corresponding metals alkoxides [29]. On the other hand the reaction of alcohols with more electronegative metals such as magnesium, aluminium and etc requires a catalyst (I_2 or $HgCl_2$) for the successful synthesis of their alkoxides [30, 31]. For other metals, more complicated

reactions need to be applied. Below here we describe briefly the most common methods used for the synthesis of metal alkoxides and their derivatives.

1.2.1 Direct reaction of metals with an alcohol:

The direct reaction of metals with alcohols is quite successful for the synthesis of the alkoxide of alkali metals that is due to their high electropositivity. These metals react vigorously with alcohols by replacement of the hydroxylic hydrogen and liberating hydrogen gas (eq.1), while the reaction is slowed down with increasing branches of the alkyl group [32, 33].

$$M + nHOR \longrightarrow 1/m\left[M(OR)_n\right]_m + n/2\ H_2 \qquad (1)$$

M= Li, Na, K, Rb, Cs, Ca, Sr, etc.. ; R = primary or secondry or tetiray alkyl group

This method has been used also for the synthesis of the alkoxides of alkaline earth metals, but the reaction is much slower than with the alkali metals due to their less electropositive character. For the synthesis of the alkoxides of Be and Mg a catalyst must be used [34].

1.2.2 Reaction of metal halides with alcohols:

Large number of metal alkoxides was synthesized using this method. In this reaction, the halide anion around the metal is substituted with alkoxy group forming appropriate metal alkoxide (eq.2)

$$MX_n + nHOR \longrightarrow 1/m\left[M(OR)_n\right]_m + nHX \qquad (2)$$

M= B, Si, Th, Ti, Zr, etc.. ; R = primary or secondry or tetiray alkyl group

Depending on the solvent, molar ratio of reagents, and temperature, the reaction of alkaline earth, lanthanides, actinides, and later 3d (Mn, Fe, Co, Ni) metal halides with alcohol can lead to the formation of different compounds in the form of molecular adducts [35].

1.2.3 Reactions of metal hydroxides and oxides with alcohols:

A dozen of alkoxides of s and p block metals were synthesized using this method. In this technique the metal hydroxides and oxides behave as oxyacids or acid anhydrides and react with alcohol to form esters (alkoxides of these metals) (eq.3& 4).

$$MOH_n + nHOR \rightleftharpoons 1/m\left[M(OR)_n\right]_m + nH_2O \qquad (3)$$

$$MO_n + 2nHOR \rightleftharpoons 1/m\left[M(OR)_n\right]_m + 2nH_2O \qquad (4)$$

M = Tl, V, Cr, Mo, etc, R = promary, or secondry, or tetiary alkyl group

Due to reversible nature of this reaction, water must be removed from the reaction system in order to yield the final alkoxides products [36].

1.2.4 Reactions of alcohols with metals dialkylamides:

The reaction of alcohol and metals dialkylamide was firstly reported by White et al in the preparation of metal alkoxides in liquid ammonia solution [37]. Metal alkyamides reacted with alcohol to form the alkoxide and eliminating dialkyl amine (eq. 5)

$$M(NR_2)_n + n\,R'OH \longrightarrow 1/m\left[M(OR')_n\right]_m + R_2NH\uparrow \qquad (5)$$

M= Cr, V, Sn, Al, U, etc.. R = primary, or secondry , or tetiary alkyl group

This method is very successful for the synthesis of alkoxides of those metals which have a great affinity to oxygen. The resulting alkoxides using this method are obtained in high purity, which is due to the high volatility of the liberated dialkylamine, which can be removed easily from the reaction environment [38].

1.2.5 Ligands exchange reactions (alcoholysis):

One the characteristic properties of metal alkoxides is their ability to undergo a facile ligand exchange reaction with alcohols (eq.6)

$$M(OR')_n + nROH \longrightarrow 1/m\left[M(OR)_n\right]_m + nR'OH \quad (6)$$

M= Li, Na. K, Rb, Al, La. etc R´ = primary, or secondry, or tetiary alkyl group, etc

This method has been used for the synthesis of different hetero and hetroleptic metal alkoxides [39]. There are three important factors that influence the extent of the substitution. The first factor is steric demand of the alkyl part of alcohols.The substitution of bulky groups with less steric groups could be achieved quickly. However, the replacement of less steric groups with higher steric groups is always slow and difficult. The second factor is the O-H bond energies of the reactant and product alcohol. The third factor is the relative M-O bond of the reactant and product metal alkoxides [40].

1.2.6 Electrochemical method:

The synthesis of metal alkoxides using electrochemical reactions was firstly reported by Szilard [41] for the synthesis of methoxides of copper and lead , later extensively used by lemakuhl [42] for the synthesis of $M(OR)_2$ complexes (where M is Fe^{2+}, Co^{2+}, Ni^{2+}; R = Me, Et, ^{n}Bu, ^{t}Bu).

This technique of synthesis is quite successful and promising for the synthesis of the alkoxides of less electropositive metals. This process has the advantages of

simplicity and high productivity as well as continuous and none – polluting character [43].

1.3 **Synthesis of aluminium hydride alkoxides:**

After the existence of Al-H bond for the first time in a reported work in 1940 [44], a lot of efforts have been done to synthesize new stable compounds for aluminum hydrides and its derivatives. The isolated derivatives were either alane with organic bases or as substitution products of hydrogen atom with halogen and organic radicals such as amino, alkoxy, mercapto groups [45].

Due to the unusual reducing properties of these synthesized derivatives, they were used extensively in the applications in organic synthesis and as stereo specific polymerization catalysts [45]. The hydride aluminium alkoxides were extensively studied by Nöth and H. Suchy [46]. Aluminium hydride AlH_3 reacts with alcohol to from the corresponding aluminium hydride alkoxide and gaseous hydrogen. As the AlH_3 is unstable, it is produced within the reaction by mixing metal aluminium hydride ($MAlH_4$ where M= Li, Na, K) and aluminium chloride $AlCl_3$ (eq 7).

$$3LiAlH_4 + AlCl_3 \longrightarrow \{4AlH_3\} + 3LiCl$$
$$\{AlH_3\} + nROH \longrightarrow [H_{3-n}Al(OR)_n] + n\,H_2 \qquad (7)$$

This method was used for the synthesis of aluminium hydride alkoxides using different alcohols [46, 47]. It is also used for the synthesis of heterometal hydride alkoxides of aluminium [48].

1.4 **Structures of metal alkoxides:**

The structure of metal alkoxides depends mainly on the nature of metal atom and the steric demand of the alkoxo group. Alkoxides with a lower primary or secondry alkyl group has a tendency to polymerization, which is lead to formation of a coordination polymer $(Al(OR)_x)_y$ (where y is the degree of polymerazion. Due to the tendency of polymerization the physical properties of the alkoxides vary from non-volatile insoluble solid to volatile soluble solid [24]. The alkoxides with large polymeric framework are non volatile and insoluble while those with small oligomeric units are volatile and soluble.

The tendency of the polymerization in alkoxides is dependent of the oxygen atom of the alkoxy anions which can form a terminal or bridging bond between two and even more metal centers (Fig 1.1). Alkoxides with more bulky group have fewer tendencies to associate.

Another parameter which affects the structures of the alkoxides is the oxidation state and the size of the metal atom. Metals with low oxidation states need more bridges in order to reach a given coordination number as compared to that with higher oxidation state: the metal with large size can accommodate easily a bulky alkoxy groups and so increases its coordination number.

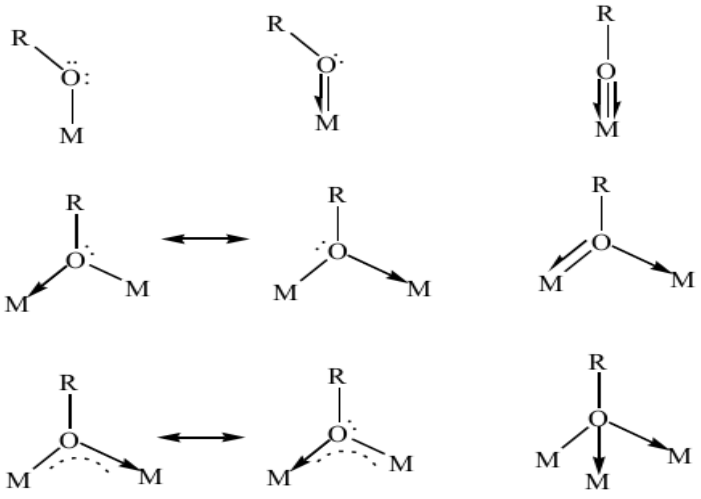

Figure 1.1: Coordination modes of alkoxy ligand [49]

The versatile coordinating abilities of the alkoxy ligands are responsible for the structure diversity of the alkoxides wide range from simple bimetallic compounds to very complex aggregates. Alkoxides are in general interesting from a structural point of view and it would be very difficult to formulate a precise rule that could fully predict the final geometry of the formed alkoxide complex. As mentioned above, the metal alkoxide complexes can have very complex structures due to formation of oligomeric and sometimes even polymeric aggregates. Formation of alkoxy bridges, M-O(R)-M', help the complexes to obtain maximal and preferred coordination even though the number of bonded ligands per metal is poor. Complexes are categorized, based on number of metal atoms in the complex. Optimal coordination is obtained by chelating ligand or by a shared (bridging) ligand atom [49].

Monomer alkoxides are obtained for highly charged metal ion where the coordination number is high and needs to be satisfied by a number of alkoxy ligands, the ligands are often large and branched. The steric demand of the alkoxy ligand shielding the central metal ion is crucial for hindering the coordination of the oxygen of the alkoxy ligand. A number of monomeric alkoxides have been synthesized for a number of metals with different steric alkoxy group [50-52].

The dimeric structure is a common structure of metal alkoxides, which is in fact two monomers bridged via alkoxy group and forming a central four membred ring M_2O_2. The structure of the dimers can be adopted in different stereo configurations based upon the oxidation state of the metal ion [24] figure (1.2).

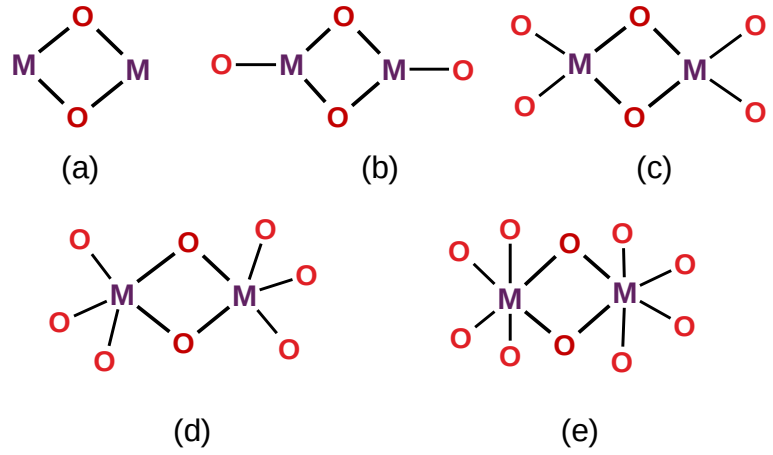

Figure 1.2: Adopted configurations of dimeric metal alkoxides

Trimeric metal alkoxides are often triangular structures, linear or non linear chains. With same type of connection that are observed for dimeric alkioxides [24].

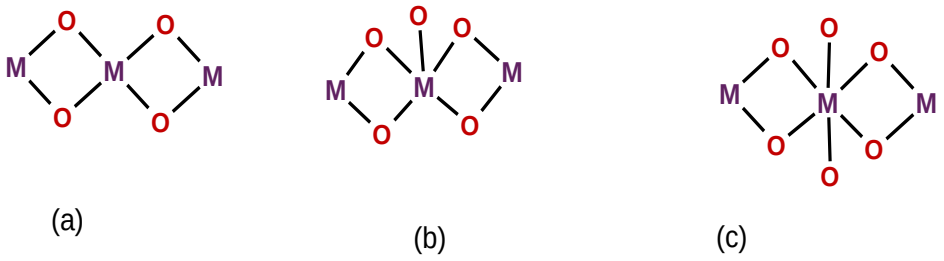

Figure 1.3: Possible configurations of trimeric metal alkoxides.

Tetrameric metal alkoxide have been reported with a large variety of configurations: Tetrahedral configuration with a core μ_4 O connected with four metal atoms; cubane like structure with 4 μ_3 O core ; planar [M_4] rhombs structure with 2 μ_3 O and 4 μ O; an octahedron sharing ages with 3 tetrahedra (M_4 $(OR)_{12}$) (this type of structure have been reported for $[Al(OPr^i)_3]_4$ predicted by Bradley [53] using NMR and confirmed by X-ray of single crystal study later [54]. Analogues structures with same the ligand have been also reported for Er [55].

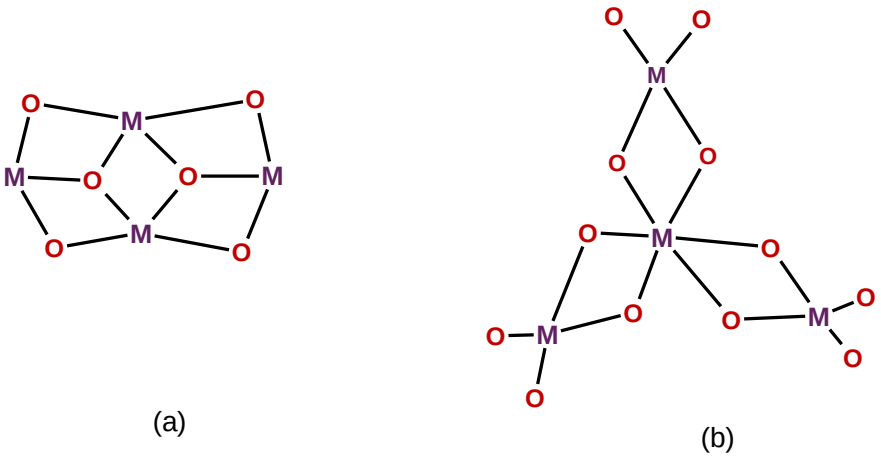

Figure 1.4: Possible configurations of tetrameric metal alkoxides.

Metal alkoxides containing more than 4 metal atoms are very often conglomerates of smaller stable fragments mentioned and described above.

1.5 Structures of aluminium hydride alkoxides:

The molecular structures of these compounds are similar to that of metal alkoxides, are varying from monomer to tetramer and low polymer. Monomer is obtained only, by applying highly bulky alkoxy groups with additional donor ligands [56]. The most common structure is dimmeric and different hydride alkoxides of aluminum and gallium have been reported with this structure [47, 56, 57]; for example tert butoxy aluminum dihydride, $[H_2Al\ (OtBu)]_2$ [47] is dimmeric having a central Al_2O_2 four membered ring. Trimeric and tetrameric structures for aluminum hydride alkoxides have also been reported. In trimeric structures the aluminium central atom was penta cordintated by four bridging oxygen atoms and one terminal hydrogen [57], while the reported tetrameric structure is made up of two dimmers associated via hydrogen bridges [57, 58].

1.6 Chemical vapour deposition CVD:

Chemical vapour deposition (CVD) is one of the widely used techniques for the synthesis of nano materials. The majority of its applications include coating of solid thin films to surfaces, production of highly pure bulky materials and of powders [59]. CVD may be defined as the deposition of solid material on a heated substrate through a chemical reaction in the gaseous state, and it can be described simply as following: flowing a precursor gas into a reaction chamber containing a heated substrate to be coated. Chemical reactions occur on and near the hot surfaces, resulting in the deposition of a thin film on the surface. This is accompanied by the production of chemical byproducts that are pumped out of the reaction chamber along with unreacted precursor [59].

1.6.1 Advantages and disadvantages of CVD:

A characteristic feature of CVD is it's use for the deposition of a large variety of materials for a wide range of applications; there are many variants of CVD. It can be done in hot-wall reactors and cold-wall reactors, at sub-torr total pressures to above-atmospheric pressures, with and without carrier gases, and at temperatures typically ranging from 200-1600°C [59].

CVD has a number of advantages which make it the favourable techniques for the deposition of nano materials. These advantages are: CVD films are generally quite conformal; this means that films can be applied to elaborately shaped pieces, including high-aspect ratio holes and other 3D structure can also be coated. Another advantage of CVD is that, besides the wide variety of materials that can be deposited, they can be deposited with very high purity. Other advantage of CVD is the high deposition rate [59].

On the other hand CVD has a number of disadvantages. A major disadvantage is the properties of precursor: the ideal precursors must have a high vapour

pressure, and this is not possible for a number of elements in the periodic table. Some precursors can also be toxic, explosive, or corrosive. The by-products of the CVD reactions can also be hazardous and must be neutralized and this increase the cost of the operation [59].

1.6.2 Chemical vapour deposition processes:

CVD processes are extremely complicated, and involve a series of gas phase and surface reactions. A more detailed picture of the basic physicochemical steps in an overall CVD reaction is illustrated in Figure 1.5., which indicates several key steps [60]:

1. Evaporation and transport of precursors into the reaction chamber.
2. Gas phase reactions of precursors in the reaction chamber to produce reactive intermediates and gaseous by-products;
3. Mass transport of reactants to the substrate surface;
4. Adsorption of the reactants on the substrate surface;
5. Surface diffusion to growth sites, nucleation and surface chemical reactions leading to film formation;
6. Desorption and mass transport of remaining fragments of the decomposition away from the reaction chamber.

In traditional thermal CVD, the film growth rate is determined by several parameters, the primary ones being the temperature of the substrate, the operating pressure of the reactor and the composition and chemistry of the gas-phase.

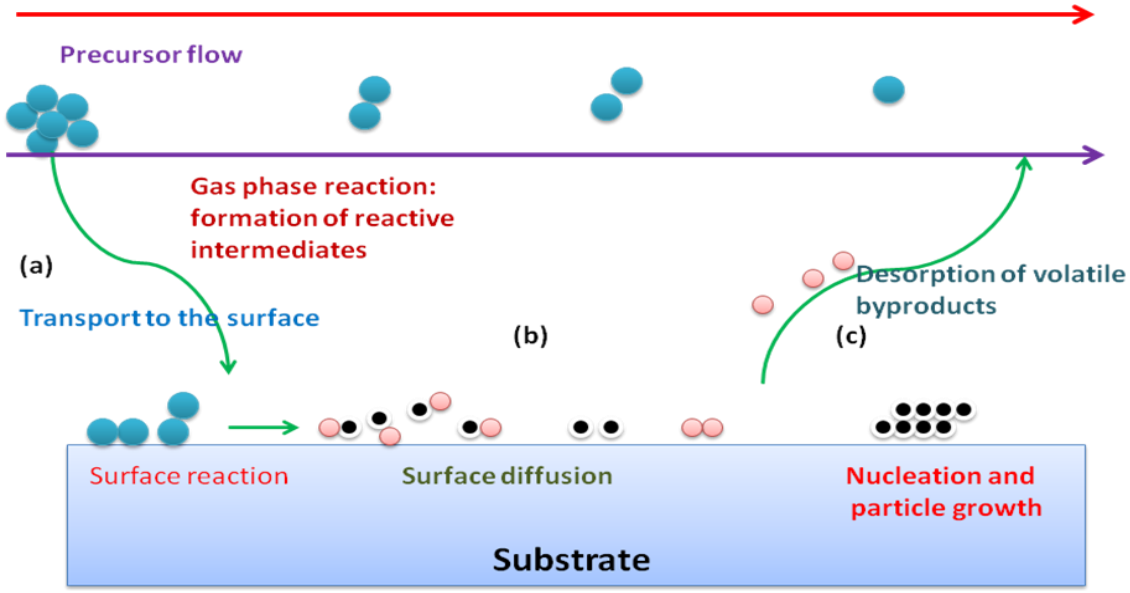

Figure 1.5: Schematic representation of CVD process: (a) transport of gaseous precursors to the surface; (b) reaction, diffusion and nucleation on the surface; (c) removal of the gaseous byproducts from the surface [60].

1.7 Uses of aluminium hydride alkoxides as single source precursor:

The use of the single-source precursor concept to thin film development facilitates greater control over the stoichiometry of the film and can also create more homogenous materials [23, 61]. This precursor must be simple and volatile and must contain all the appropriate atoms required for the film. Hydride-aluminum alkoxides of the general formula, $[H_nAl(OR)_{3-n}]_x$ were extensively used as potential single source precursors for chemical vapor deposition in the group of Prof. Michael Veith in Saarbruecken. The versatilities of these compounds can be exemplified by $[H_2Al\ (O^tBu)]_2$ which is used as single source precursor for preparation of nano-materials by chemical vapor deposition (CVD) process. It gives different nano-materials in terms of morphology and chemical compositions at different decomposition temperatures as shown in scheme 1.1[62-64].

At >550°C:

$$[\ ^{t}BuOAlH_2\ ]_2 \longrightarrow 2(CH_3)_2C{=}CH_2 + 3H_2 + 2/3\ Al/Al_2O_3$$

Nano-wires

At 370 ~ 450°C:

$$[\ ^{t}BuOAlH_2\ ]_2 \longrightarrow 2(CH_3)_2C{=}CH_2 + 3H_2 + 2/3\ Al/Al_2O_3$$

Nano-balls

At 300 ~ 320°C:

$$[^{t}BuOAlH_2]_2 \longrightarrow 2H_2 + 2\ H_2C{=}C(CH_3)_2 + 2\ HAlO$$

Scheme 1.1: Thermal decomposition of $[H_2Al\ (O^tBu)]_2$ on CVD Reaction

Aluminum hydride alkoxides were proved to be ideal precursors for CVD process due to their smart features which includes high volatility, easy purification via crystallization, sublimation at ambient temperatures etc. Besides lower decomposition temperature, high purity, adopted composition and microstructure are the distinguished advantages of the molecular precursor route over classical solid state production of materials. However, the library of this type of compounds is limited to a few numbers of structurally well characterized compounds.

1.8 Biocompatibility of aluminium oxide:

Aluminium ceramics are known as excellent biocompatible materials, that is due to their good mechanical properties and log-term durability [65]. Different studies on alumina based implants have been shown that the alumina implants surfaces topography play the essential rule in enhancing the performance of implants. [66].During the last two decades Michael Veith and his co- workers and students

pioneered the study of cell interaction and biocompatibility of the surfaces prepared by CVD of one the homologue hydride metal alkoxides precursors $[H_2Al^tBuO]_2$. As mentioned above this precursor gives two different materials in terms of morphology and chemical composition HAlO and Al/Al_2O_3. In order to study the cell interactions and commutability of the 1D-Al/Al_2O_3 nano-wires, numerous in-vitro investigations using different cell lines were carried out [67-70]. These results revealed that these surfaces can be effective for selective adhesion and proliferation of one type of cell depending on the nano and micro features produced on the surfaces [67]. The surfaces were also treated with laser and depending on the laser intensity and pulse numbers various structures composed of both nano and micro features were produced. It was observed that the cell density increases when the surface topography is adjusted in the right way [69]. In the same way, typical nano and micro structures accelerate cell proliferation [70]. The developed 1D-Al/Al_2O_3 nano-wires surfaces exhibit a high biocompatible character and could be used as a coating material for medical implants

1.9 Fluorinated phosphazene polymers:

Poly phosphazenes are macro molecules with phosphorus – nitrogen backbone and organic or inorganic side groups as illustrated in figure (1.6). They posses a number of characteristic features that make them highly attractive for biological applications [71]. First the inorganic backbone is capable for hydrolytical degradation, which can be modulated through selection of an appropriate side group. Second, the unique synthetic path way of these polymers allows huge selection of substituents to be introduced by common organic chemistry methods. Other unique feature is the unique flexibility of the backbone and its ability to participate in noncovalent bonding and formation of supermolecular assemblies creating new opportunities for an interface with biological systems [71].

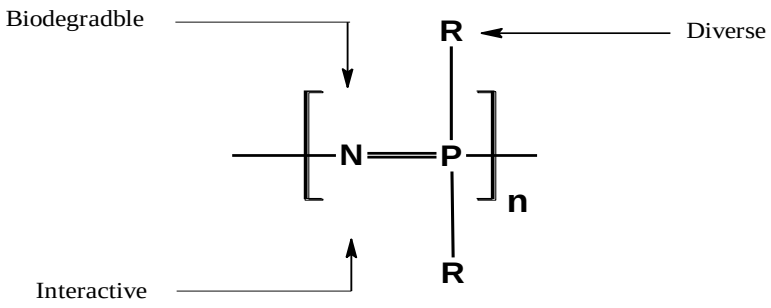

Figure 1.6: Polyphosphazenes

Among all synthesized poly phosphazene, fluorinated poly phosphazenes have attracted interest and attention since they have been synthesized for the first time in the last century by Allcock and Kugel et al [72]. The advantage of using fluorinated phosphazenes, rather than other poly phosphazene polymers, is their solubility in common organic solvents such as tetrahydrofuran, acetone, or methylethyl ketone which make them easier to handle [73].

Poly[bis (2,2,2-trifluoroethoxy)phosphazene] (PTFEP) is one of the remarkable fluorinated organo phosphazene polymers (fig. 1.7) that is extensively used as biodegradable and biocompatible polymer [74] for various applications such as drug delivery [75, 76], inert biomaterials [77] and super hydrophobic surface coatings [78, 79] .

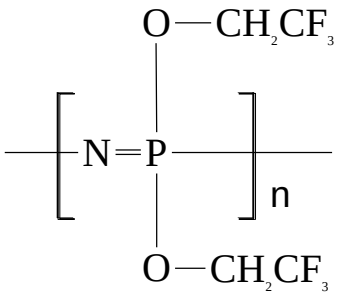

Figure 1.6: Formula of poly [bis (2, 2, 2-trifluoroethoxy) phosphazene] (PTFEP).

The basic structure of this polymer consists of trifluoroethoxy side groups linked to a backbone of alternating phosphorus and nitrogen atoms. The combination of fluorinated side groups with an inorganic backbone generates a number of

interesting properties many of which are specific to fluorinated polyphosphazenes. For example, films of PTFEP are hydrophobic, are resistant to many chemicals, are bio inert, and have high fire resistance and radiation stability [73]. They are also easy to fabricate into microfibers and films. These unique properties of PTFEP are the reason for their use in membranes research [80], biomedicine, and surface coatings [71].

1.10 Using of PTFEP films in surfaces modification:

Films obtained from PTFEP have high thermal stability, good mechanical properties, hydrolytic stability [81]and of course biological properties. One of the challenges in applying these films on the top of substrate surfaces for further applications is poor adhesion to the surface because of the hydrophobic character of PTFEP [82]. To overcome this problem surface modification reactions were studied extensively to increase the adhesion properties of these polymers to other substrate surfaces [71].

In general there are two ways for achieving that. The first one is altering the chemistry of the PTFEP films by introducing different side groups replacing the present trifluoroethoxy side group, which can undergo nucleophilic exchange reactions because of its electron-withdrawing character, and relatively small size [83-86]. In most cases this approach is critical, as the surface reactions should not alter the bulk property of the polymer, and it is not an easy reaction to be performed.

The second approach is modifying the surface of organic or inorganic substrates through the introduction of free hydroxyl group through oxidation reaction of the substrate surface using Caro's acid (1:3 mixture of H_2O_2 30% and concentrated H_2SO_4) [71]. Using this approach films of PTFEP were able to be deposited on the surface of medical devices through methatetetical exchange reactions using variety of pathways as illustrated in scheme (1.2).

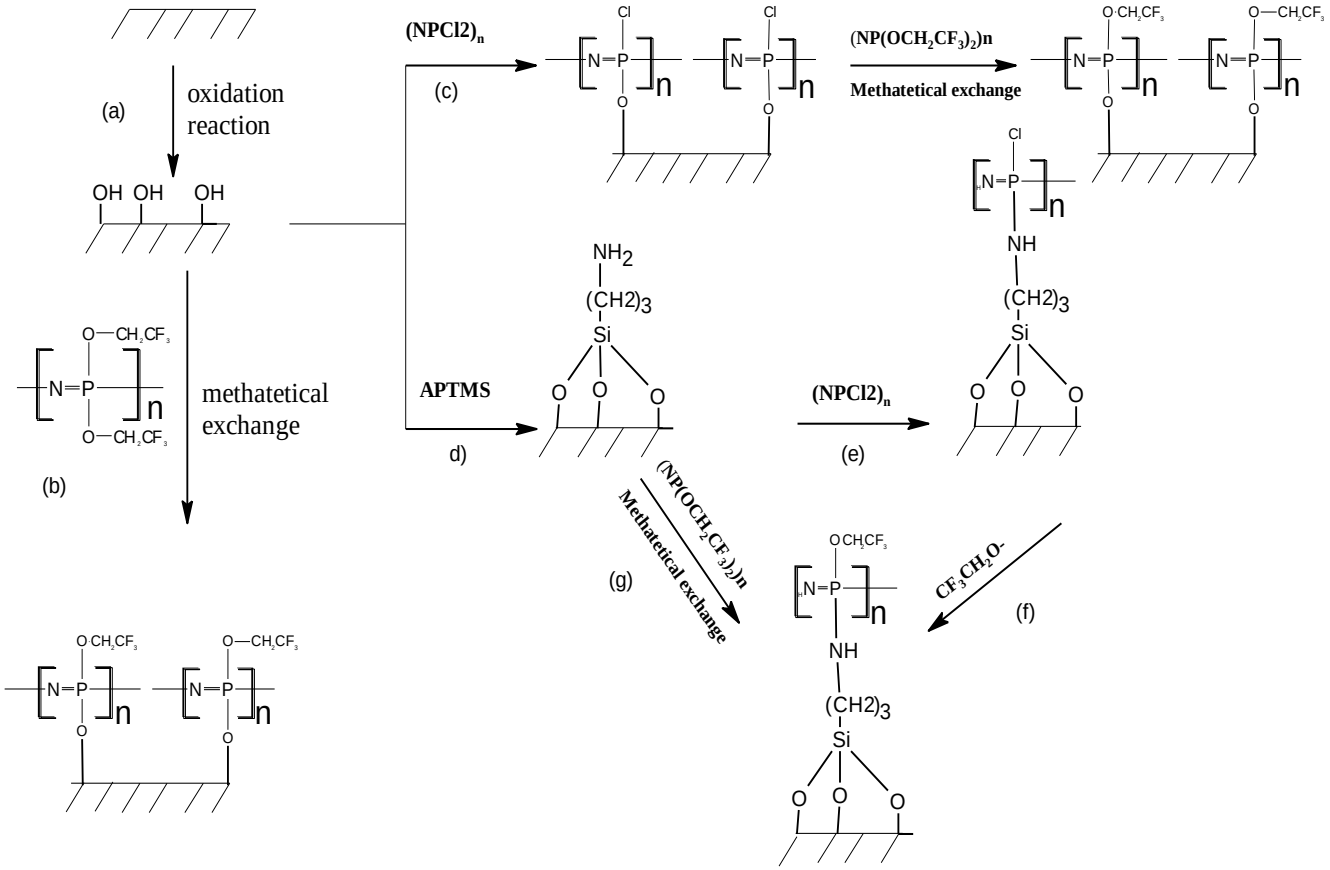

Scheme 1.2: Surface functionalizations of oxidized biomedical devices with PTFEP [71].

1.11 Biocompatibility of PTFEP:

PTFEP were known to show a good blood and tissue computability, both in bulk and as a coating material [87]. This property of poly phosphazene was reported to be due to the selective absorption of high quantities of albumin from blood plasma and selective rejection of some of the proteins that stimulate coagulation [88], the surfaces of PTFEP films or coating therefore appeared to be passivated against platelet adhesion. As a consequence it was thought that PTFEP has some potential applications in biomedicine field as material for blood contacting device such as stent, prostheses and dental implants.

Surfaces obtained by PTFEP coatings showed outstanding mechanical features, antithrombogenic characteristics and good biocompatibility [89, 90]. They also posses the ability to prevent or reduce the secondary injuries following implantation and re-stenosis in implanted stents and inflammatory reactions following the introduction of the implants to the human body [91-94]. PTFEP coating have been also applied to cover the surfaces of special alloys like nitinol (alloy based on nickel and titanium metals that posses thermal and mechanical shape memory) which is used for the preparation of medical implants such as stents and catheters [95].

1.12 Aim of the work

It is now quite widely accepted that surface modification processes lead to the preparation of materials showing completely different surface properties while maintaining the bulk physical and mechanical features of the pristine substrates. This may avoid research on completely new materials having totally unknown general characteristics, saving effort, time and money. In this context Al/Al_2O_3 core/shell nano-wires surfaces were shown to exhibit high biocompatibility as characterized with different cell lines. These surfaces were obtained by the CVD reaction of hydride aluminium tert-butoxide as it gives highly porous nano-structures of Al/Al_2O_3 upon decomposition at temperature above 450°C in a CVD chamber. However the number of well characterized aluminium hydrides/ alkoxides precursors which is shown to be ideal precursors for CVD and sol-gel is limited to few.

The aims of the present thesis can be sort as:

1). Synthesis and Characterization of further aluminium hydride/alkoxides for their use as precursors in high purity CVD or Sol/Gel processes for the formation of alumina or aluminium/alumina composites.

2). Development of micro and nano structured surfaces of 1D Al/Al_2O_3 nano-wires on , using CVD of single source precursors.

3). Modification / functionalization of the obtained 1D Al/Al_2O_3 nano-wires surfaces for another type of biocompatibility and for further application using PTEFP without altering their morphology and overall surface topography.

4).The developed hybrid surfaces are expected to represent potential coating for further cardiovascular implant applications.

Chapter two

Materials and Methods

2.1 Precursors synthesis:

2.1.1 Materials:

$LiAlH_4$ was used as obtained from Sigma-Aldrich without further purification, while $AlCl_3$ from Sigma-Aldrich was sublimed before used. Cyclopentanol was distilled from magnesium turnings and kept under nitrogen. Diethyl ether was freshly distilled from Na/benzophenone and kept under N_2.

2.1. 2. Methods:

The experimental work was carried out under dry N_2 by using modified Schlenk techniques due to the sensitivity to air and moisture. Elemental analyses were determined on Vario micro cube Analyzer. The infrared (IR) spectra were recorded in solid state on Bruker tensor 27 FTIR spectrophotometer in the 4000 – 400 cm^{-1} range. The ^{1}H, ^{13}C NMR spectra were recorded on a Bruker 300, using C_6d_6 as a solvent. The chemical shifts (δ) in ppm were measured relative to tetramethylsilane (TMS).

2.1.2.1 Compound 1 $[H_2Al(O\text{-}C_5H_9)]_6[H(Cl)Al(O\text{-}C_5H_9)]_2$:

0.4270 g (11.25 mmol) of LiAIH4 were dissolved in 50 cm^3 of diethyl ether in a flask with a reflux condenser. Aluminiumtrichloride 0.5040 g (3.78 mmol) were dissolved under cooling with ice in 50 cm3 of diethyl ether and added to the lithium aluminium hydride in a steady flow at room temperature. LiCl precipitates from the mixture. To this suspension, 2.604 g (30.24 mmol) of cyclopentanol were added dropwise and formation of hydrogen gas was

observed. The reaction was completed by stirring the reaction mixture at ambient temperature for 4-5 h. After filtration of the lithium chloride, the filtrate was reduced to around 10 cm3 under reduced pressure and kept in the refrigerator at +5°C. Colourless crystals of $[H_2Al\ (O\text{-}C_5H_9)]_6[H(Cl)Al(O\text{-}C_5H_9)]_2$ were obtained overnight.

Yield: 89.70 % (3.07 g) ; ^{1}H-NMR(C_6D_6): δ=4.72 ppm (b, Al-H), δ=4.36 ppm (m, -O-CH-), δ=1.74-2.14 ppm (-CH_2-ring); ^{13}C-NMR: δ= 77.06 ppm (-C1), 34.93 ppm (-C2), and 23.46 ppm (C3); IR: ν=1807 cm^{-1} (br, Al-H). $C_{40}H_{86}Al_8Cl_2O_8$ (981.89 g/mol); elemental analysis: found (calc.): C 48.14 (48.93) , H 8.51 (8.83), Cl 5.00 (7.22). As a side product we could also isolate $[H_2Al\ (O\text{-}C_5H_9)]_5\ [H(Cl)Al(O\text{-}C_5H_9)]_3$ in low yield (50 mg) with anlytical data: $C_{40}H_{85}Al_8Cl_3O_8$ (1016.31 g/mol); elemental analysis: found (calc.): C 45.06 (47.27) , H 8.61 (8.43), Cl 9.36 (10.47).

2.1.2.2 Compound 2 $[H_6Al_4\ (\mu_2\text{-}OC_5H_9)_6]$:

0.4555 g (12.00 mmol) of $LiAlH_4$ were dissolved in 50 cm^3 of diethyl ether in a flask with a reflux condenser. Aluminiumtrichloride 0.5333 g (4.00 mmol) were dissolved under cooling with ice in 50 cm^3 of diethyl ether and added to the lithium aluminium hydride in a steady flow at room temperature. LiCl precipitates from the mixture. To this suspension, 2.7652 g (32.00 mmol) of cyclopentanol were added dropwise and formation of hydrogen gas was observed. The reaction was completed by stirring the reaction mixture at ambient temperature for 4-5 h. After filtration of the lithium chloride, the filtrate was reduced to around 10 cm^3 under reduced pressure and kept in the

refrigerator at +5°C. Colourless crystals of [H_6Al_4 (μ_2-OC_5H_9)$_6$] were obtained overnight.

Yield: 91.41 % (2.24 g) ; ^{1}H-NMR(C_6D_6): δ=4.86 ppm (b, Al-H), δ=4.48 ppm (m, -O-CH-), δ=1.83-2.14 ppm (-CH_2-ring); ^{13}C-NMR: δ= 76.32 ppm (-C1), 34.84 ppm (-C2), and 23.88 ppm (C3); IR: ν=1814 cm^{-1} (br, Al-H). $C_{30}H_{60}Al_4O_6$ (624.72 g/mol); elemental analysis: found (calc.): C 54.03 (57.68), H 8.95 (9.68).

2.1.2.3 Compound 3 [Cl_6Al_4 (μ_2-OC_5H_9)$_6$]:

0.2850 g (7.5 mmol) of $LiAlH_4$ were dissolved in 50 cm^3 of diethyl ether in a flask with a reflux condenser. Aluminiumtrichloride 1.00 g (7.5 mmol) were dissolved under cooling with ice in 50 cm^3 of diethyl ether and added to the lithium aluminium hydride in a steady flow at room temperature. LiCl precipitates from the mixture. To this suspension, 2.584 g (30.0 mmol) of cyclopentanol were added dropwise and formation of hydrogen was observed. The reaction was completed by stirring the reaction mixture at ambient temperature for 4-5 h. After filtration of the lithium chloride, the filtrate was reduced to around 10 cm^3 under reduced pressure and kept in the refrigerator at +5°C. Colourless crystals of [Cl_6Al_4(μ_2-OC_5H_9)$_6$] were obtained overnight.

Yield: 84.60% (5.28 g) ; ^{1}H-NMR(C_6D_6): δ=4.66 ppm (m, -O-CH-), δ=1.60-1.99 ppm (-CH_2-ring); ^{13}C-NMR: δ= 80.91 ppm (-C1), 34.95 ppm (-C2), and 23.62 ppm (C3) . $C_{30}H_{54}Al_4Cl_6O_6$ (831.39 g/mol); elemental analysis: found (calc.): C 41.77 (43.33), H 5.98 (6.50), Cl 25.03 (25.59).

2.1.2.4 Compound 4 [$Al(OC_5H_9)_3]_4$:

0.775g (19.90 mmol) of $LiAlH_4$ were dissolved in 50 cm^3 of diethyl ether in a flask with a reflux condenser. Aluminiumtrichloride 0.885 g (6.60 mmol) were dissolved under cooling with ice in 50 cm^3 of diethyl ether and added to the lithium aluminium hydride in a steady flow at room temperature. LiCl precipitates from the mixture. To this suspension, 6.82 g (79.20 mmol) of cyclopentanol were added dropwise and formation of hydrogen gas was observed. The reaction was completed by stirring the reaction mixture at ambient temperature for 4-5 h. After filtration of the lithium chloride, the filtrate was reduced to around 10 cm^3 under reduced pressure and kept in the refrigerator at +5°C. Colourless crystals of $[Al(OC_5H_9)_3]_4$ were obtained overnight.

Yield: 77.40 % (5.35 g) ; ^{1}H-NMR(C_6D_6): δ=4.04 ppm (m, -O-CH-), δ=1.49-1.67 ppm (-CH_2-ring); ^{13}C-NMR: δ= 74.71 ppm (-C1), 35.82 ppm (-C2), and 23.55 ppm (C3); $C_{60}H_{108}Al_4O_{12}$ (1129.42 g/mol); elemental analysis: found (calc.)C 62.73 (63.81), H 9.29 (9.63).

2.1.2.5 Compound 5 $[H_5Al_5(\mu_5\text{-}O)(\mu_2\text{-}OC_5H_9)_8]*OC_4H_{10}$:

0.4270g (11.25 mmol) of $LiAlH_4$ were dissolved in 50 cm^3 of diethyl ether in a flask with a reflux condenser. Aluminiumtrichloride 0.5004 g (3.78 mmol) were dissolved under cooling with ice in 50 cm^3 of diethyl ether (the diethyl ether solvent were not redistilled prior to use) and added to the lithium aluminium hydride in a steady flow at room temperature. LiCl precipitates from the mixture.

To this suspension, 2.604 g (30.24 mmol) of cyclopentanol were added dropwise and formation of hydrogen gas was observed. The reaction was completed by stirring the reaction mixture at ambient temperature for 4-5 h. After filtration of the lithium chloride, the filtrate was reduced to around 10 cm^3 under reduced pressure and kept in the refrigerator at +5°C. Colourless crystals of $[H_5Al_5$ (μ_5-O) (μ_2-$OC_5H_9)_8]$*OC_4H_{10} were obtained overnight.

Yield: 77.48 % (02.66 g) ; ^{1}H-NMR(C_6D_6): δ=4.83 ppm (b, Al-H), δ=4.51 ppm (m, -O-CH-), δ=1.96-2.46 ppm (-CH_2-ring); ^{13}C-NMR: δ= 74.51 ppm (-C1), 35.87 ppm (-C2), and 23.56 ppm (C3); IR: ν=1801 cm^{-1}(br, Al-H). $C_{29}H_{60}Al_5O_7$ (655.69 g/mol); elemental analysis: found (calc.): C 58.33 (58.01), H 9.39 (9.63).

2.1.2.6 Compound 6 $[H_{4.5}Cl_{0.5}Al_5$ (μ_5-O)(μ_2-$OC_5H_9)_8]$*OC_4H_{10}:

0.4555g (12.00 mmol) of $LiAlH_4$ were dissolved in 50 cm^3 of diethyl ether in a flask with a reflux condenser. Aluminiumtrichloride 0.5333 g (4.00 mmol) were dissolved under cooling with ice in 50 cm^3 of diethyl ether (the diethyl ether solvent were not redistilled prior to use) and added to the lithium aluminium hydride in a steady flow at room temperature. LiCl precipitates from the mixture. To this suspension, 2.7652 g (32.00 mmol) of cyclopentanol were added dropwise and formation of hydrogen gas was observed. The reaction was completed by stirring the reaction mixture at ambient temperature for 4-5 h. After filtration of the lithium chloride, the filtrate was reduced to around 10 cm^3 under reduced pressure and kept in the refrigerator at +5°C. Colourless crystals of $[H_{4.5}Cl_{0.5}Al_5$(μ_5-O)(μ_2-$OC_5H_9)_8]$*OC_4H_{10} were obtained overnight.

Yield: 54.40 % (1.85 g) ; ^{1}H-NMR(C_6D_6): δ=4.47 ppm (b, Al-H), δ=4.02 ppm (m, -O-CH-), δ=1.48-1.69 ppm (-CH_2-ring); ^{13}C-NMR: δ= 74.51 ppm (-C1), 35.88 ppm (-C2), and 23.65 ppm (C3); IR: ν =1779 cm $^{-1}$(br, Al-H). $C_{44}H_{86.5}Al_5Cl_{0.5}O_{10}$ (928.30 g/mol); elemental analysis: found (calc.): C 57.97 (56.93), H 9.49 (9.39), Cl 1.84 (1.91).

2.2 Superhydrophobic surface development:

2.2.1 Materials:

Poly bis 2,2,2-trifluoroethoxy phosphazene (PTFEP) and acetone were obtained from Sigma Aldrich. The polymer was used without further purification and its molecular weight was determined using chromatography; acetone was dried according to literature. tert-butanol was distilled from magnesium turnings and kept under nitrogen.

2.2.2 Methods:

2.2.2.1 Synthesis of the precursor [$H_2Al(O^tBu)]_2$:

The single source precursor, [$H_2Al(O^tBu)]_2$ was synthesized according to the reported procedure [24].

4.550 g (120 mmol) of $LiAlH_4$ were dissolved in 80 cm^3 of diethyl ether in a flask with a reflux condenser. Aluminiumtrichloride, 5.335 g (40 mmol), were dissolved under cooling with ice in 80 cm^3 of diethyl ether and added to the lithium aluminium hydride in a steady flow at room temperature. LiCl precipitates from the mixture. To this suspension, 11.859 g (160.0 mmol) of tert-butanol were added dropwise and formation of hydrogen was observed. The reaction was completed by stirring the reaction mixture at ambient temperature

for 5 h. After filtration of the lithium chloride, the solvent was removed from the filtrate under reduced pressure and condensed in a cold trap. The precursor was obtained as white powder and purified by sublimation at room temperature and lower pressure.

2.2.2.2 Al/Al_2O_3 nano-wires deposition by CVD of $[H_2Al(O^tBu)]_2$:

Al/Al_2O_3 nano-wires were synthesized following established route [68] by the decomposition of the molecular precursor $[^tBuOAlH_2]_2$ via chemical vapour deposition using a cold wall reactor as illustrated in Figure (2.1). Glass substrates were cleaned with iso-propanol and dried at 150°C for 1 hour to remove any organic residue. The substrates were placed on a graphite sample holder in order to be heated by the induction coil using a standard high frequency generator. Before the deposition process, the chamber was evacuated for more than 30 minutes until the vacuum reaches the $1.0x10^{-3}$ mbar, and then flushed with dry and pure nitrogen gas several times in order to eliminate the residual of water and oxygen. Afterwards the substrates were heated up to 630 °C and the precursor was flowed into the reaction chamber. The flow rate was controlled manually with a driven valve and a sensitive pressure detector. Al/Al_2O_3 nano-wires was deposited as thin film over the substrate, the volatile byproducts and unreacted precursors were flushed away using a vacuum pump Following 30 minutes deposition, the precursor valve was closed and substrates were cooled down to room temperature.

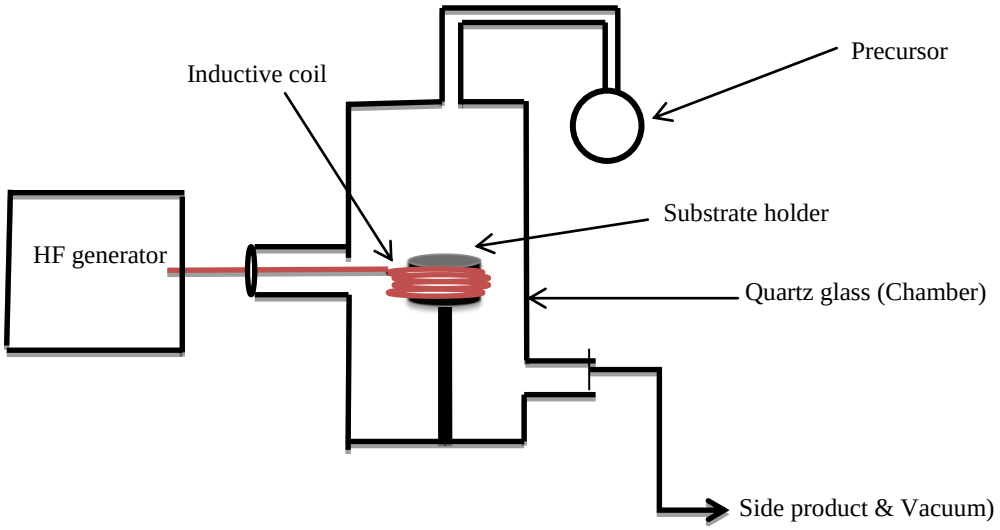

Figure 2.1: Schematic illustration of cold wall CVD reactor used for the deposition of Al/Al_2O_3 NWs at 630°C and 8.0 x 10^{-2} mbar pressure.

2.2.2.3 Al/Al_2O_3 nano-wires functionalization by PTFEP coating:

2.2.2.3.1 Polymer solution preparation:

PTFEP solution was prepared in concentrations of 1-3.0 % wt/v by dissolving PTFEP in dry acetone. The solution was stirred in a sealed beaker in order to avoid the evaporation of the solvent. The mixture was stirred over night to ensure uniform distribution of the polymer in solution. The solution was filtered with 0.2 μm filters just before use.

2.2.2.3.2 Dip coating:

The glass substrates covered with high density Al/Al_2O_3 nano-wires [68] were dip-coated by vertically immersing them into the solution at a rate of 10 mm/min, followed by a 20 s pause, and then withdrawal of the substrate from the solution at a rate of 1 mm/min. Samples were then dried for 2-3 hours in a vacuum oven at 30ºC to remove any residual solvent and then allowed to dry overnight in a covered beaker. The samples were washed with acetone and ethanol and dried over night in a vacuum oven at 80ºC.

2.2.2.4. Characterization of the developed surfaces:

2.2.2.4.1 Scanning Electron Microscope (SEM):

Scanning Electron Microscopy (SEM) analysis has been used specifically for the evaluation of the morphology and topography. The obtained surfaces were analysed in the following way: the deposited surfaces Al/Al_2O_3 nano-wires before and after coating with PTFEP were imaged with a scanning electron microscope (JEOL-JSM-6400F) at accelerating voltage of 15 kV. They were previously coated with gold using PVD sputter (JEOL-JFC-1300 Fine Coater, t = 30 s) to avoid charge on the surface.

2.2.2.4.2 Chemical characterization of the surfaces:

To determine the exact surface chemical state, we used infra red (IR) spectroscopy and X-ray Photoelectron Spectroscopy (XPS) techniques.

For further confirmation of the supposed hydrolysis reaction, ^{1}H and ^{13}C NMR analysis of the solution of the polymer before and after the immersion of Al/Al_2O_3 nano-wires was carried out.

2.2.2.4.3 Wetting angle properties measurements:

Static contact angle of the developed surfaces were measured using a video contact angle measuring system G2 (Kures GmbH, Germany) combined with a drop shape analysis software. Droplets, 6 μL in size, were placed on the surface and digital images of the drop were recorded with a video camera and analyzed on a computer. Reported contact angle values are the average of five measurements. Different liquids were applied: pure distilled water, ringer solution (which is known as artificial blood), and n-Hexadecane.

Chapter Three

Results and discussion

3.1 Aluminium Based precursors synthesis and characterization.

3.1.1 Synthesis:

The syntheses of aluminum alkoxides/hydrides precursors have been carried out following established [47] route. Lithium aluminum hydride, $LiAlH_4$, and aluminumtrichloride, $AlCl_3$, were mixed in diethylether as a solvent in an appropriate ratio (n/m either 1/3 or 1/1) to form lithium chloride and aluminum hydride as intermediates. The formed suspension was not isolated and when cyclo-pentanol was added, an immediate evolution of hydrogen gas was observed. Lithium chloride was removed via filtration; the solvent was removed under reduced pressure. The six compounds were obtained as white powders in high yields. Colorless crystals suitable for XRD analysis were grown at +5°C in a refrigerator using diethyl ether as solvent. In compounds **5**, and **6** due to some water residue in the solvent, the oxygen centred clusters were obtained. Overall reactions are shown in equation (3.1).

$$m\ LiAlH_4 + n\ AlCl_3 + 0\ C_5H_9\text{-}OH \longrightarrow o\ H_2 + n\ LilCl + [(C_5H_9\text{-}O)_0Al_{m+n}H_x$$

$$[(C_5H_9\text{-}O)_0Al_{m+n}H_xCl_y] \longrightarrow \begin{cases} [H_2Al(O\text{-}C_5H_9)]_6[H(Cl)Al(O\text{-}C_5H_9)]_2 & (\mathbf{1}) \\ [H_6Al_4(O\text{-}C_5H_9)_6] & (\mathbf{2}) \\ [Cl_6Al_4(O\text{-}C_5H_9)_6] & (\mathbf{3}) \\ [Al(O\text{-}C_5H_9)_3]_4 & (\mathbf{4}) \\ [H_5Al_5(O)(O\text{-}C_5H_9)_8] & (\mathbf{5}) \\ [H_{4.5}Cl_{0.5}Al_5(O)(O\text{-}C_5H_9)_8] & (\mathbf{6}) \end{cases}$$

$$m \approx 1,\ n \approx 3,\ o = 4 \text{ or } 8 \text{ or } 12$$

Eq. 3.1: Chemical reaction equation for the preparation of compounds **1-6**

The compounds **1**-**6** from equation (1) have been isolated as crystals and their compositions have been determined from analytical data as well as from crystal structure analyses. As may be seen, none of the products is compatible with a simple general formula like $H_2Al\text{-}O\text{-}C_5H_9$ or $HAl(O\text{-}C_5H_9)_2$. Instead, more complex compositions are found, which can be explained from reactions between the intermediate AlH_3 with 3 equivalents of $H_2Al\text{-}O\text{-}C_5H_9$ (**2**) or $AlCl_3$ with three equivalents of $Cl_2Al\text{-}O\text{-}C_5H_9$ (**3**). In the case of **1** $AlCl_3$ has not been completely transformed to AlH_3 and so besides $H_2Al\text{-}O\text{-}C_5H_9$ also $H(Cl)Al\text{-}O\text{-}C_5H_9$ is formed which combines with the former to a 6:2 adduct (H(Cl)Al-O-R with R= $^{c}HexMe^{-1}$ can be isolated in pure form as a dimer) [96]. Finally, in **5** and **6 ,** as the solvent used is not re-distilled a hydrolysis reaction took place and led to the formation of the clusters with a central oxygen atom connecting five aluminium atoms (see below) instead of the formation of $[H\text{-}Al(O\text{-}C_5H_9)_2]_n$. Examples of the same type of cluster are known with fluorine in the place of hydrogen like $F_5Al_5(O)(O\text{-iso-Prop})_8$ and are also believed to be due to partial hydrolysis [97]. Compound **6**, which is characterized by chlorine and hydrogen terminating ligands at the aluminium atoms, is a 1:1 mixture between **5** and $H_4(Cl)Al_5(O)(O\text{-}C_5H_9)_8$ in the crystal. The chlorine derivative has a chloride substituent in the place of one hydride. In principle a similar, precedent compound has been described before, with iso-propyl instead of the cyclo-pentyl group [98]). In contrast to the iso-propyl compound, which could be obtained in pure form, we could only isolate crystals with a mixture of $H_4(Cl)Al_5(O)(O\text{-}C_5H_9)_8$ and **5** [99].

3.1. 2 Spectroscopic Characterization:

All the six compounds (**1**-**6**) were obtained in high yields and have been characterized using 1H, ^{13}C NMR and IR spectroscopy. The ^{1}H- and ^{13}C-NMR Spectral data of compounds with assignments of relevant signals are compiled in

Table 3.1. The assignments are based on those made previously by other workers for structurally related compounds.

A broad peak at 4.72 has been observed in the ^{1}H-NMR spectrum of compound **1,** which is the characteristic peak of hydrido ligands at Al centre [47]. A multiplet with a centre at 3.97 ppm has been observed which can be assigned to the proton attached to α-carbon of the cyclopentyl ring. Multiple peaks in the range of 1.04 ppm to 2.34 ppm have been observed for the -CH_2- protons of the cyclopentylring, as the chemical environment of theses protons is similar, it is difficult to assign these peaks individually. In the ^{13}C-NMR spectra of **1** three peaks appeared for the three chemically different carbons. In the IR spectrum of compound **1** a broad peak at 1807 cm^{-1} has been observed, this peak can be attributed to the Al–H stretching vibration. The peak lies well in the Al–H stretching vibration reported range [47, 96].

The ^{1} H-NMR spectrum of compound **2** shows a broad peak at 4.86 ppm for the hydrogen atoms attached to the Al centre and the values lie well in the typically reported region [47]. A multiplet with the centre at 3.29 ppm has been observed for the proton attached to α-carbon. The peaks of –CH2- protons of the cyclopentyl ring appeared as multiple peaks in the range of 1.83 – 2.14 ppm. The chemical environments of these protons are quite similar. Therefore, the peaks are difficult to be resolved into clear and individual peaks for each –CH2- group. ^{13}C-NMR spectroscopy gives four peaks for the three chemically different carbons at 76.32, 34.84, and 23.88 ppm. This indicates that the organic moieties are identical.

The IR spectrum of **2** shows abroad peak for Al–H stretching vibration, at 1814 cm^{-1}.

The ^{1}H-NMR spectrum of compound **3,** shows a multiplet peak with the centre at 3.29 ppm for the proton attached to α-carbon. The peaks of –CH2- protons of the cyclopentyl ring appeared as multiple peaks in the range of 1.60 – 1.99 ppm.

^{13}C-NMR spectroscopy gives three peaks for the three chemically different carbons of the cyclopentyl group at 80.91, 34.95, and 23.62 ppm.

The ^{1}H-NMR spectrum of compound **4,** shows a multiplet peak with the centre at 4.04 ppm for the proton attached to α-carbon. The peaks of –CH2- protons of the cyclopentyl ring appeared as multiple peaks in the range of 1.49 – 1.67 ppm. The presence of the cyclopentyl group was also confirmed by ^{13}C-NMR spectroscopy, in which three different peaks could be seen for the three chemically different carbons of the cylclopently group.

In the ^{1}H-NMR spectra of compounds **5** and **6** in C_6D_6, the peak assigned to the protons attached to α-carbon, appeared as multiple peaks with a centre at 4.51 ppm in **5** and at 4.02 ppm in **6**. The peaks of –CH2- protons of the cyclopentyl ring appeared as multiplet peaks in the range of 1.96 – 2.46 ppm in **5** and 1.48 – 1.69 ppm in **6**.

The IR spectra of compounds **5** and **6** show a broad peak at 1801 and 1779 cm^{-1} region absorption respectively, this peak can be attributed to the Al–H stretching vibration. The peak lies well in the Al–H stretching vibration reported range [91].

Compound	^{1}HNMR(C_6D_6) (ppm)			^{13}C-NMR (C_6D_6) (ppm)			IR cm^{-1} (Al-H)
	Al-H	CH-	-CH_2 (ring)	(-C1)	(-C2)	(C3)	
$[H_2Al(O\text{-}C_5H_9)]_6[H(Cl)Al(O\text{-}C_5H_9)]_2$ **(1)**	4.72	4.36	1.74 –2.14	77.06	34.93	23.46	1807
$[H_6Al_4(OC_5H_9)_6]$ **(2)**	4.86	4.48	1.83 –2.14	76.32	34.84	23.88	1814
$[Cl_6Al_4(OC_5H_9)_6]$ **(3)**	-	4.66	1.60 –1.99	80.91	34.95	23.62	-
$[Al(OC_5H_9)_3]_4$ **(4)**	-						-
$[H_5Al_5(O)(OC_5H_9)_8]$ **(5)**	4.83	4.51	1.96-2.46	74.51	35.87	23.56	1801
$[H_{4.5}Cl_{0.5}Al_5(O)(OC_5H_9)_8]$ **(6)**	4.47	4.02	1.48 –1.69	74.51	35.88	23.65	1779

Table 3.1: Spectroscopic data of the compounds **1-6**

3.1.3 Crystals structure characterization:

The solid state structures of **1-6** have been determined using X-ray diffraction methods. Colourless crystals of compounds **1-6** suitable for XRD measurements were grown at +5°C in the refrigerator.

3.1.3 .1 Structure of compound 1:

The molecule **1** is a coordination oligomer of discrete composition and can be classified by the interaction of two entities of $[H(Cl)Al(O\text{-}C_5H_9)]$ with six entities of $[H_2Al(O\text{-}C_5H_9)]$. In the crystal structure the chlorine atoms are not unique, as they are exchanged with hydride at several positions, creating a positional disorder. The occupancies of the chloride positions follow from the refinement of the structure. Atom Cl1 is found at two very narrow positions, A (0.254) and B (0.419), which sum up to 0.67, Cl2 has an occupancy factor of 0.229 and Cl3 of 0.098. As the molecule is centro-symmetric the sum of the occupancies is 2x(0.254+0.419) + 2x(0.229+0.0.098)= 2.0. All chloride atoms are exclusively engaged in terminal Al-Cl bonds. A drawing of the structure of **1** with the chloride disorder is depicted in Figure 3.1[99].

From this disorder it can be concluded that several structure isomers of **1** could be assumed to be present in the solid or that even other composition $[H(Cl)Al(O\text{-}C_5H_9)]_n\,[H2Al(O\text{-}C_5H_9)]_m$ with n = 1 or 3 and m = 8-1 or 8-3 are mixed up with **1** in the same crystal[99]. The most populated isomer of **1**emphasizing the inner central polycyclic is shown in Figure 3.2.

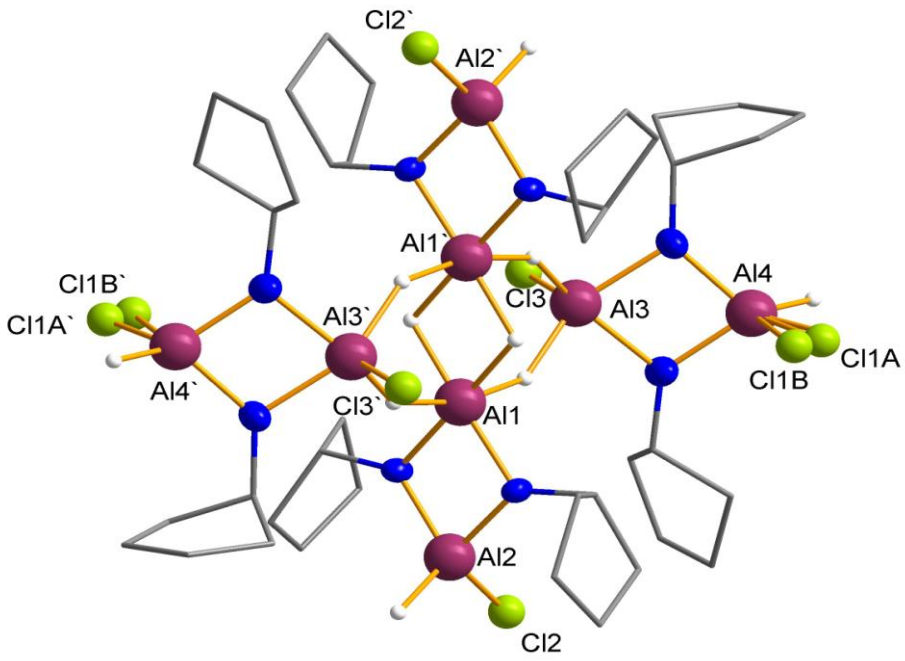

Figure 3.1: Molecular structure of compound **1,** the hydrogen atoms at the carbon atoms are omitted for clarity. The side occupancy factors for Cl1A = 0.254, Cl1B = 0.419, Cl2 = 0.229 and Cl3 = 0.098.

As already mentioned, the coordination octamer **1** combines 6 [H_2Al (O-C_5H_9)] with 2 [H(Cl)Al(O-C_5H_9)] entities. More precisely, two [H(Cl)Al(O-C_5H_9)$_2$$AlH_2$] units and two dimeric [H_2Al(O-C_5H_9)$_2$$AlH_2$] unit, all displaying Al_2O_2 four membered rings by Lewis acid-base interactions, are connected together by 6 Al-H-Al bridges forming a central Al_4H_6 hetero-atomic cluster. This cluster may also be described as an Al_4H_4 eight membered cycle spanned in the middle with two hydride bridges[99].

Identification code	sh3420	
Empirical formula	C40 H86 Al8 Cl2 O8	
Formula weight	981.82	
Temperature	182(2) K	
Wavelength	0.71073 Å	
Crystal system	Triclinic	
Space group	P-1	
Unit cell dimensions	a = 10.6125(4) Å	α = 76.687(2)°.
	b = 11.1194(4) Å	β = 76.385(2)°.
	c = 12.2034(5) Å	γ = 88.487(2)°.

Volume	1361.39(9) $Å^3$
Z	1
Density (calculated)	1.198 Mg/m^3
Absorption coefficient	0.291 mm^{-1}
F(000)	528
Crystal size	0.656 x 0.184 x 0.138 mm^3
Theta range for data collection	1.765 to 26.372°.
Index ranges	-13<=h<=13, -13<=k<=13, -15<=l<=15
Reflections collected	23996
Independent reflections	5562 [R(int) = 0.0239]
Completeness to theta = 25.242°	99.8 %
Absorption correction	Semi-empirical from equivalents
Max. and min. transmission	0.7461 and 0.7006
Refinement method	Full-matrix least-squares on F^2
Data / restraints / parameters	5562 / 99 / 317
Goodness-of-fit on F^2	1.032
Final R indices [I>2sigma(I)]	R1 = 0.0428, wR2 = 0.1085
R indices (all data)	R1 = 0.0550, wR2 = 0.1183
Extinction coefficient	n/a
Largest diff. peak and hole	0.446 and -0.283 $e.Å^{-3}$

Table 3.2: Crystal data and structure refinement for compound **1**

The molecular structure of **1** Figure 3.2 shows three different geometries of aluminium atoms, a highly distorted octahedron geometry for hexa coordinated aluminium atoms (Al1), pseudo trigonal bipyramidal geometry for the penta coordinated aluminium atoms (Al3), and distorted tetrahedron geometry for the quad coordinated aluminium atoms (Al2 &Al4). In the octahedron geometry, the central aluminium atom (Al1) is surrounded by 4 hydrogen atoms and 2 oxygen atoms. In the trigonal bipyramidal geometry, the central aluminium atom (Al3) is surrounded by 3 hydrogen (one of them is terminal) atoms and 2 oxygen atoms. The bipyarmidal are connected through hydride or alkoxide bridges to (Al1) or (Al4). The tetrahedral geometry is composed of two hydrogen atoms (Al2) or hydrogen and chorine atoms (Al4) which are terminal, and two oxygen atoms shared with to other aluminium centres. The bridged Al-O bond lengths of the Al_2O_2 rings are different due to the diversity of the coordination numbers of the shared Al atoms, the difference is not significant. The mean of Al-O bond

length is 1.832(1) Å which lies well on the reported range of Al_2O_2 ring of similar alkoxides [47]. The bridging Al- H bonds are as expected considerably longer compared to the terminal Al-H bonds. The bridging hydrides bond length have an average of 1.71(1)Å , while for the terminal one is 1.53(1)Å is found , these values are within the reported range of similar hydride alkoxides of aluminium [100, 101].

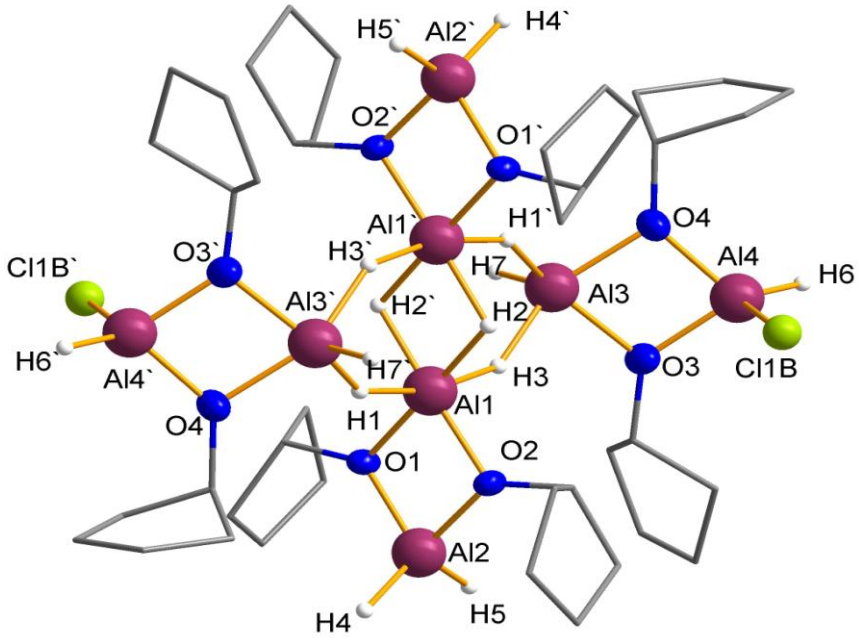

Figure 3.2: The most probable structural isomer of compound **1,** the hydrogen atoms at the carbon atoms are omitted as well as the atoms Cl1A, Cl1A', Cl2, Cl2', Cl3 and Cl3' for clarity.

Bond	Length [Å]	Bond	Angle [°]
Al1-O1	1.851(1)	O1-Al1-H1	94.1(7)
Al1-O2	1.848(1)	H2-Al1-H3	86.3(1)
Al2-O1	1.815(1)	O2-Al1-O1	79.63(6)
Al2-O2	1.821(1)	O2-Al1-H2	100.3(7)
Al3-O3	1.864(2)	O1-Al2-O2	81.63
Al3-O4	1.878(2)	H5-Al2-H4	117.6(2)
Al4-O3	1.786(2)	O3-Al3-O4	77.16(7)
Al4-O4	1.794(2)	O3-Al3-H3	86.0(7)
Al1-H1	1.73(2)	O3 –Al3-H7	110.9(2)
Al2-H4	1.65(2)	O3-Al4-O4	81.37(7)

Al3-H3	1.72(2)	Cl1B-Al4-H6	102.0(1)
Al3-H7	1.49(1)		
Al4-H6	1.52(3)		
Al4-Cl1B	2.318(5)		

Table 3.3: Selected characteristic bond lengths (Å) and angles (°) for the compound **1**

3.1.3 .2 Structures of compounds 2, 3, and 4:

Compounds **2**, **3**, and **4** are very similar, and their structural features are quite identical to the reported tetrameric alkoxides of aluminium with other alcohols like iso-propanol, ethanol, and etc.[54, 102]. The molecular structures of these compounds are adapted to what is called a Mitsubishi motif, a term introduced firstly by Folting et al. for the description of the structure of aluminium isopropoxide [102] .

The crystal data of **2**, **3**, and **4** are presented in Tables 3.4, 3.5, and 3.6 respectively, while the most relevant bond lengths and angles are shown in Tables 3.7, 3.8, and 3.9.

Identification code	sh3462	
Empirical formula	C30 H60 Al4 O6	
Formula weight	624.70	
Temperature	132(2) K	
Wavelength	0.71073 Å	
Crystal system	Orthorhombic	
Space group	Pbcn	
Unit cell dimensions	a = 17.760(2) Å	α = 90°.
	b = 18.562(2) Å	β = 90°.
	c = 10.7416(10) Å	γ = 90°.
Volume	3541.3(7) $Å^3$	
Z	4	
Density (calculated)	1.172 Mg/m^3	
Absorption coefficient	0.169 mm^{-1}	
F(000)	1360	
Crystal size	0.80 x 0.56 x 0.38 mm^3	
Theta range for data collection	1.59 to 29.19°.	
Index ranges	-24<=h<=24, -25<=k<=25, -13<=l<=14	
Reflections collected	64280	

Independent reflections	4765 [R(int) = 0.0468]
Completeness to theta = 29.19°	99.3 %
Absorption correction	Semi-empirical from equivalents
Max. and min. transmission	0.9387 and 0.8771
Refinement method	Full-matrix least-squares on F^2
Data / restraints / parameters	4765 / 0 / 270
Goodness-of-fit on F^2	1.178
Final R indices [I>2sigma(I)]	R1 = 0.0734, wR2 = 0.1660
R indices (all data)	R1 = 0.0841, wR2 = 0.1737
Largest diff. peak and hole	0.610 and -0.363 e.$Å^{-3}$

Table 3.4: Crystal data and structure refinement for compound **2**

Identification code	sh3427	
Empirical formula	C30 H54 Al4 Cl6 O6	
Formula weight	831.35	
Temperature	132(2) K	
Wavelength	0.71073 Å	
Crystal system	Orthorhombic	
Space group	Pbcn	
Unit cell dimensions	a = 14.4625(9) Å	α = 90°.
	b = 17.1676(11) Å	β = 90°.
	c = 15.7325(11) Å	γ = 90°.
Volume	3906.2(4) $Å^3$	
Z	4	
Density (calculated)	1.414 Mg/m^3	
Absorption coefficient	0.569 mm^{-1}	
F(000)	1744	
Crystal size	0.54 x 0.15 x 0.12 mm^3	
Theta range for data collection	1.84 to 27.65°.	
Index ranges	-17<=h<=18, -22<=k<=22, -20<=l<=20	
Reflections collected	63114	
Independent reflections	4551 [R(int) = 0.0446]	
Completeness to theta = 27.65°	99.6 %	
Absorption correction	Semi-empirical from equivalents	
Max. and min. transmission	0.9364 and 0.7475	
Refinement method	Full-matrix least-squares on F^2	
Data / restraints / parameters	4551 / 0 / 309	
Goodness-of-fit on F^2	1.030	
Final R indices [I>2sigma(I)]	R1 = 0.0270, wR2 = 0.0628	
R indices (all data)	R1 = 0.0374, wR2 = 0.0678	
Largest diff. peak and hole	0.489 and -0.418 e.$Å^{-3}$	

Table 3.5: Crystal data and structure refinement for compound **3**

Identification code	sh3419a
Empirical formula	C48 H108 Al4 O12
Formula weight	985.26
Temperature	163(2) K
Wavelength	0.71073 Å
Crystal system	Trigonal
Space group	P 3
Unit cell dimensions	a = 23.9617(6) Å α = 90°. b = 23.9617(6) Å β = 90°. c = 10.1935(3) Å γ = 120°.
Volume	5068.6(3) $Å^3$
Z	4
Density (calculated)	1.291 Mg/m^3
Absorption coefficient	0.152 mm^{-1}
F(000)	2176
Crystal size	0.425 x 0.375 x 0.210 mm^3
Theta range for data collection	0.981 to 26.371°.
Index ranges	-29<=h<=29, -29<=k<=29, -12<=l<=12
Reflections collected	81992
Independent reflections	13846 [R(int) = 0.0497]
Completeness to theta = 25.242°	100.0 %
Absorption correction	None
Refinement method	Full-matrix least-squares on F^2
Data / restraints / parameters	13846 / 216 / 676
Goodness-of-fit on F^2	2.989
Final R indices [I>2sigma(I)]	R1 = 0.1505, wR2 = 0.3864
R indices (all data)	R1 = 0.1663, wR2 = 0.3962
Absolute structure parameter	0.30(4)
Extinction coefficient	n/a
Largest diff. peak and hole	4.986 and -0.909 $e.Å^{-3}$

Table 3.6: Crystal data and structure refinement for compound **4**

The molecular structures of compounds **2**, **3** and **4** (Figure 3.4, 3.5, and 3.6) are built up of three planar Al_2O_2 four membered rings. Compounds 2 and 3 have a crystallographic C2 symmetry, and deviate only to minor extent from D3 symmetry which has to be attributed to these molecules in solutions [99]. Compound **4** has a final point of symmetry D3 as it possesses three two fold axis of rotation C2 passing through hexa coordinated Al1 centre, this besides

another three fold axis of rotation C3 which is the principal axis of rotation and it is perpendicular to the plane of the four Al atoms.

The central aluminium atom Al1 in **2** or **3** or **4 is** almost octahedrally coordinated by six oxygen atoms which are part of the cyclo-pentanolate ligands. The three other aluminium atoms of the compounds, are in almost tetrahedral coordination sites and have either hydrogen (**2**) or chlorine (**3**) or O-^{c}Pen (**4**) as terminating substituents.

Due to the differences of the electronegativity of the attached ligands to the terminal aluminum atoms, the dimensions of the Al_2O_2 rings of **2**, **is** quite different than that of **3**, and **4**. This also has an effect on the Al-O bonds adjacent to hydride or chloride or oxide Al (2, 3)-O which shows a mean value of 1.814(1) Å in hydride alkoxide **1** compared to 1.782(2) Å in the chlorine derivative **2** and 1.788(2) Å. in the alkoxide derivative **4**. The shortening of this bond in **3** and 4 may thus be due to the higher electron withdrawal capabilities of the terminating ligands in **3** and **4** compared to those in **2**. The mean Al1-O on the octahedron aluminium atoms centre is compare well in all compounds: 1.914(3) Å (**2**) versus 1.919(3) Å (**3**) and 1.9135(6) Å (**4**) and all are within the reported range for similar structures [102].

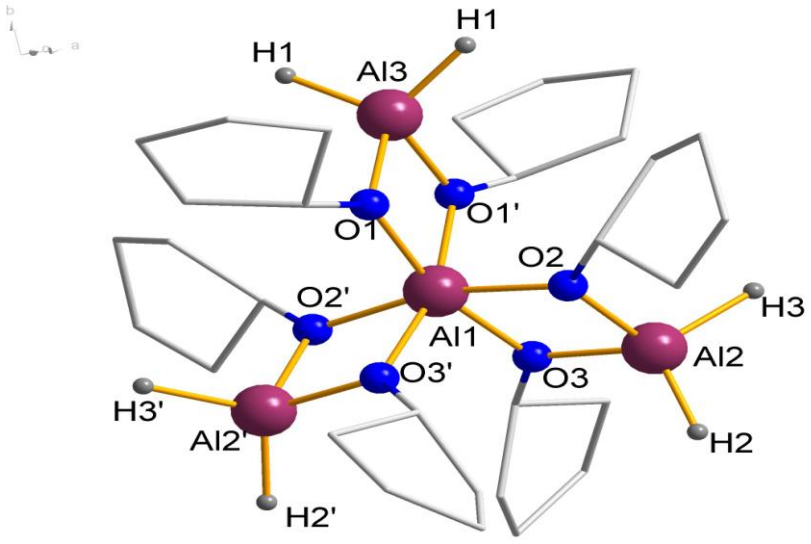

Figure 3.3: Molecular structure of compound **2,** the hydrogen atoms at the carbon atoms are omitted for clarity

Bond	Length [Å]	Bond	Angle [°]
Al1-O1	1.907(2)	O1-Al1-O1'	76.00(6)
Al1-O2	1.919(2)	O2-Al1-O3	75.81(6)
Al1-O3	1.917(2)	O1-Al1-O3	93.50(6)
Al2-O2	1.815(2)	O1-Al1-O2	98.12(7)
Al2-O3	1.813(2)	O3-Al1-O3’	98.73(7)
Al2-H2	1.54(4)	O1-Al1-O2'	94.64(6)
Al2-H3	1.71(3)	O2-Al1-O3'	93.53(7)
Al3-O1	1.814(2)	O2-Al1-O2’	163.79(7)
Al3-H1	1.55(4)	O1-Al1-O3’	164.86(7)
		O2-Al2-O3	81.00(7)
		H2-Al2-H3	111.2(2)
		O1-Al3-O1’	80.66(7)
		H1-Al3-H1’	109.4(2)

Table 3.7: Selected characteristic bond lengths (Å) and angles (°) for the compound **2**

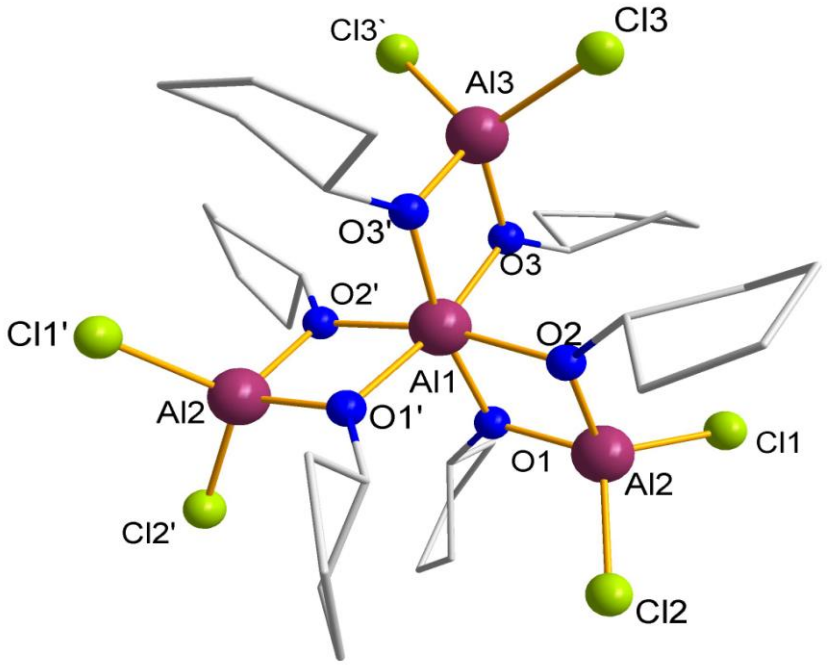

Figure 3.4: Molecular structure of compound **3,** the hydrogen atoms at the carbon atoms are omitted for clarity

Bond	Length [Å]	Bond	Angle [°]
Al1-O1	1.918(9)	O3-Al1-O3’	76.30(7)
Al1-O2	1.927(9)	O1-Al1-O2	76.39(7)
Al1-O3	1.912(9)	O1-Al1-O1'	93.55(6)
Al2-O1	1.779(9)	O1-Al1-O3	95.42(4)
Al2-O3	1.783(9)	O2-Al1-O3	93.00(6)
Al2-Cl1	2.115(6)	O2-Al1-O1’	94.68(6)
Al2-Cl2	2.103(6)	O2-Al1-O3’	97.13(6)
Al3-O3	1.782(9)	O1-Al1-O3'	169.36(5)
Al3-Cl3	2.107(5)	O2-Al1-O2’	167.12(5)
		O1-Al2-O2	83.75(5)
		Cl1-Al2-Cl2	110.62(2)
		O3-Al3-O3’	82.99(5)
		Cl3-Al2-Cl3’	109.85(2)

Table 3.8: Selected characteristic bond lengths (Å) and angles (°) for the compound **3**

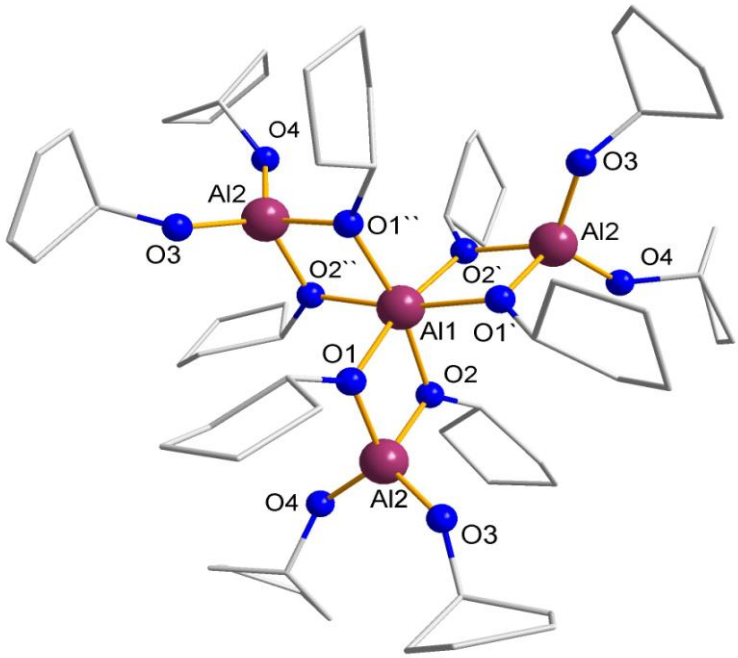

Figure 3.5: Molecular structure of compound **4,** the hydrogen atoms at the carbon atoms are omitted for clarity.

Bond	Length [Å]	Bond	Angle [°]
Al1-O1	1.916(6)	O1-Al1-O2	75.56 (3)
Al1- O1'	1.914 (8)	O1'-Al1-O2'	75.60(3)
Al1-O2	1.911 (6)	O2"-Al1-O1'	75.51(3)
Al2-O1	1.79 (6)	O2'-Al1-O1"	92.95(3)
Al2- O2	1.78 (6)	O1'-Al1-O1	96.0 (3)
Al2-O3	1.72 (7)	O1'-Al1-O2	93.00(3)
		O1"-Al1-O2"	94.64(6)
		O1'-Al1-O2"	168.30(3)
		O1-Al2-O2	81.99(4)
		O3-Al2-O4	116.57(4)

Table 3.9: Selected characteristic bond lengths (Å) and angles (°) for the compound **4**

There is a remarkable differences in Al-O bond distances between central octahedron Al1 and terminal Al2/Al3 and they increase in the order $^{n=4}$Al-O < $^{n=4}$Al–(μ-O) < $^{n=6}$Al–(μ-O) (n = coordination number) What is in a good agreement with that reported for similar alkoxides of aluminium [102].

The hexa coordinated central aluminium Al1 atom posses a distorted octahedron. The deviation from an ideal octahedron around Al1 is more pronounced in **2** than in **3** and **4** , as may be concluded from the corresponding axial bond O1-Al1-O3' or O2-Al1-O2' angles (Figures 3.3, 3.4 and 3.5), which are closer to linear in **3** and **4** than in **2**. On the same line the Al_2O_2 cycles in **2** and **4** have more acute angles at the aluminium atoms (mean: 75.88(7)/80.89(9)° and 75.57(3)/81.99(9)° respectively) than **3** (mean: 76.33(4)/83.50(8)°.

The tetrahedra terminal aluminium centres are highly distorted due to the nature of the ligands attached to aluminium, since two of the ligands are free for rotation as terminal groups and two are bridged with the central hexa-coordinated aluminium centre.

3.1.3.3 Structures of compounds 5 and 6:

The structural analysis of the crystals of compounds **5** $[H_5Al_5(\mu_5\text{-}O)(\mu_2\text{-}OC_5H_9)_8]*OC_4H_{10}$ and **6** $[H_{4.5}Cl_{0.5}Al_5(\mu_5\text{-}O)(\mu_2\text{-}OC_5H_9)_8].OC_4H_{10}$ (Figure 3.6 and Figure 3.8) shows that their molecular structures are very similar as both contain five aluminium atoms bridged by cyclopentanolate entities and being linked to a central oxygen lacking any organic substituent. Four of the five aluminium atoms (Al2,3, 4, 5) have coordination number 5 and one that is Al1 has coordination number 6. Each of the former is attached to four oxygen atoms making the bridges between the Al centres, and one terminal hydrogen atom. These Al atoms show pseudo trigonal bipyramidal geometry where the bond angles have a high degree of distortion. The fifth Al atom having coordination number 6 is attached to five bridging oxygen and one terminal hydrogen atom in **5** or chlorine atom in case of **6** forming distorted octahedron geometry.

Several Similar pentanuclear aluminium alkoxides have been reported with different alcohols and different halide: in $[F_5Al_5(\mu_5\text{-}O)(\mu_2\text{-}O^iPr)_8]$ the ligands at aluminium are fluoride [97] , in $[(^tBuO)_5Al_5(\mu_5\text{-}O)(\mu_2\text{-}O^tBu)_8]$ [103], they are tert-butanolates, and $[H_4ClAl_5(\mu_5\text{-}O)(\mu_2\text{-}O^iPr)_8]$ [98] is (with the exception of a different alcoholate group) very similar to our synthesized compound **6** $[H_4ClAl_5(\mu_5\text{-}O)(\mu_2\text{-}OC_5H_9)_8]$ which is described below. The structure of **5** indicates that it is unique as no structure of a hydride compound with exclusive terminal hydride ligands at the aluminium atoms has been found in the published literature, although quite similar compounds like $[H_6Al_5(\mu_4\text{-}O)(\mu_2\text{-}O^iPr)_7]$ have been isolated [98].

The crystal data of **5** are organized in Table 3.10 and the pertinent bond lengths and angles are presented in Table 3.11.

Identification code	sh3364
Empirical formula	C40 H77 Al5 O9 x C4 H10 O
Formula weight	911.04
Temperature	123(2) K
Wavelength	0.71073 Å
Crystal system	Triclinic
Space group	P-1
Unit cell dimensions	a = 11.6740(15) Å α = 79.248(7)°. b = 11.7380(15) Å β = 78.824(7)°. c = 18.481(2) Å γ = 89.398(5)°.
Volume	2440.0(5) $Å^3$
Z	2
Density (calculated)	1.240 Mg/m^3
Absorption coefficient	0.166 mm^{-1}
F(000)	992
Crystal size	0.25 x 0.23 x 0.13 mm^3
Theta range for data collection	1.14 to 26.36°.
Index ranges	-14<=h<=14, -14<=k<=14, 0<=l<=23
Reflections collected	8032
Independent reflections	8032 [R(int) = 0.0000]
Completeness to theta = 26.36°	79.9 %
Absorption correction	Semi-empirical from equivalents
Max. and min. transmission	0.9793 and 0.9596
Refinement method	Full-matrix least-squares on F^2
Data / restraints / parameters	8032 / 408 / 616
Goodness-of-fit on F^2	1.023
Final R indices [I>2sigma(I)]	R1 = 0.0771, wR2 = 0.1752
R indices (all data)	R1 = 0.1547, wR2 = 0.2127
Largest diff. peak and hole	0.512 and -0.344 $e.Å^{-3}$

Table 3.10: Crystal data and structure refinement for compound **5**

From the crystals analysis data, it is shown that the molecule has no crystallographic symmetry but the deviation from C_4 is almost negligible. This can be shown measuring the dihedral angle between the four basal aluminum atoms Al2, Al3, Al4 and Al5 which is only 0.41°. The oxygen atom O1 is situated a little bit above that plane, as may be seen from the Al2-O1-Al4 or Al3-O1-Al5 angles which both are approximately 14° away from a linear arrangement [99]. The Al–O bond lengths can be categorized in several groups: the bond with central oxygen atom (Al1 -O1) 1.885(6) Å for the hexa -

coordinated aluminium centre (Al1) is shorter than the penta coordinated aluminium centre (Al2, 3, 4, 5–O1) (mean: 2.09(2) Å).

The average Al-O bond length of the penta-coordinated Al centres and the central oxo-group is 1.914(1) Å, while the average Al to the bridging oxygen atoms bond length is 1.851(1)Å. The other four Al-O bond lengths around Al1 result from alkoxide ligands and have a mean value of 1.957(9) Å, again emphasizing the short Al1-O1 bond. The bond lengths of the other four aluminium atoms Al2, Al3, Al4, Al5 to the alkoxide groups may be divided in those, which are oriented parallel to O1-Al1 (mean: Al-O 1.798(7) Å) and those which are almost in the basal plane (mean: Al-O 1.829(9) Å). The general shortness of the distances may be explained by the lower coordination numbers at Al2, Al3, Al4, Al5 compared to Al1. The O1-Al2,3,4,5-O angles are all around 78° which is far from orthogonal and explain the long Al2,3,4,5-O1 distances mentioned above [99]. The Al-H bond lengths have an average bond length of 1.514(3) Å.

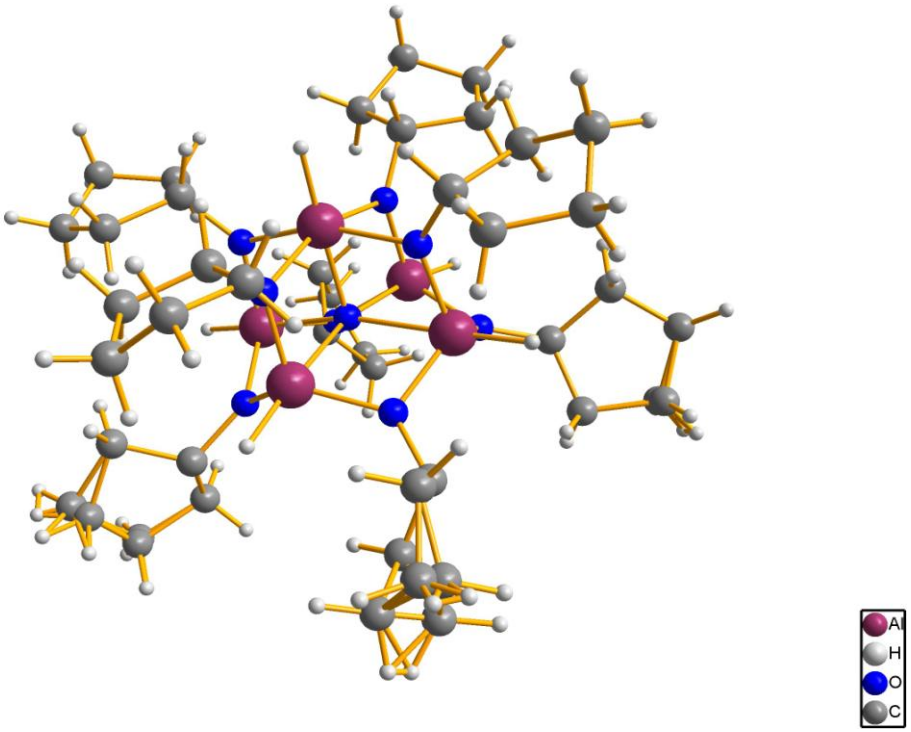

Figure 3.6: Molecular structure of compound **5.** **(**Disorder by super position of some organic ligands)

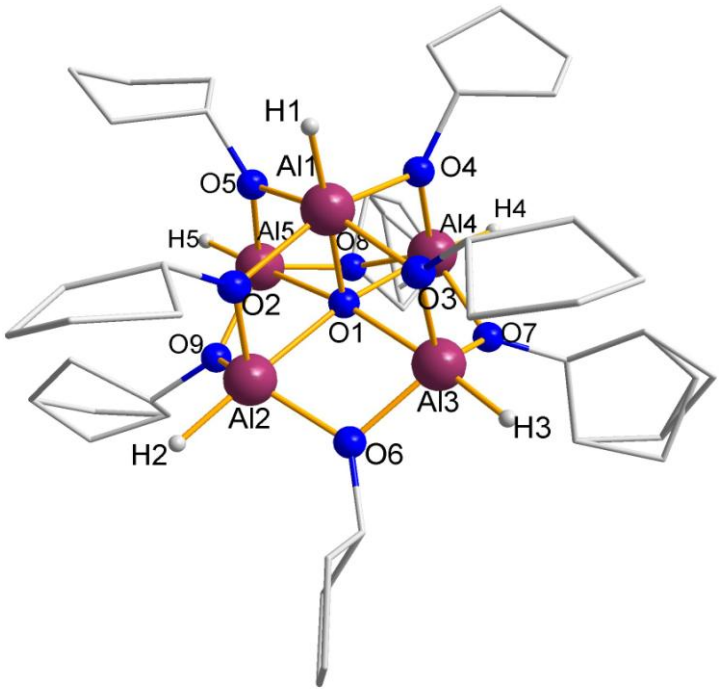

Figure 3.7: Molecular structure of compound **5,** the hydrogen atoms at the carbon atoms are omitted for clarity. **(**Disorder by super position of some organic ligands)

Bond	Length [Å]	Bond	Angle [°]
Al1 - O1	1.885(4)	O1-Al1-O2	79.1(2)
Al1- O2	1.954(5)	O1-Al1-O4	79.9(2)
Al1 - O3	1.944(4)	O2-Al2-O9	110.9(2)
Al1 - O4	1.960(5)	O2-Al2-O6	113.9(2)
Al1 - O5	1.971(4)	O6-Al2-O1	78.6(2)
Al2 - O1	2.057(4)	O9-Al2-O1	78.7(2)
Al2 - O2	1.788(5)	O9-Al2-O6	123.5(2)
Al2 - O6	1.848(5)	O3-Al3-O1	78.3(2)
Al2 - O9	1.845(4)	O6-Al3-O1	78.8(2)
Al3 - O1	2.058(4)	O3-Al3-O7	114.7(2)
Al3 - O3	1.807(5)	O3-Al3-O6	111.4(2)
Al3 - O6	1.827(5)	O6-Al3-O7	122.0(2)
Al3 - O7	1.831(6)	O8-Al4-O1	79.0(2)
Al4- O1	2.077(4)	O4-Al4-O1	78.7(2)
Al4 - O4	1.800(5)	O4-Al4-O8	114.3(3)
Al4 - O7	1.825(6)	O4-Al4-O7	111.9(2)

Al4- O8	1.817(5)	O8-Al4-O7	122.1(2)
Al5 - O1	2.155(4)	O5-Al5-O1	77.4(2)
Al5 - O5	1.796(5)	O5-Al5-O9	114.6(2)
Al5 - O8	1.812(6)	O5-Al5-O8	110.6(2)
Al5 - O(9)	1.810(5)	O9-Al5-O8	120.1(2)
Al1- H1	1.52(3)	O2-Al1-H1	100.0(2)
Al2 - H2	1.51(3)	O3-Al1-H1	102.0(2)
Al3 - H3	1.51(3)	O4-Al1-H1	101.0(2)
Al4 - H4	1.51(3)	O6-Al2-H2	102.0(2)
Al5 - H5	1.52(3)		

Table 3.11: Selected characteristic bond lengths (Å) and angles (°) for the compound **5**

As mentioned above, the crystals of **6** contain a 1:1 mixture of compound **5 (**$[H_5Al_5(\mu_5\text{-}O)(\mu_2\text{-}OC_5H_9)_8]*OC_4H_{10}$) and $[H_4ClAl_5(\mu_5\text{-}O)(\mu_2\text{-}OC_5H_9)_8]*OC_4H_{10}$ **6**. The crystal data of **6** are organized in Table 3.12 and the pertinent bond lengths and angles are presented in Table 3.13.

Identification code	sh3348	
Empirical formula	C40 H76.5 Al5 Cl0.5 O9 x C4 H10 O	
Formula weight	928.26	
Temperature	122(2) K	
Wavelength	0.71073 Å	
Crystal system	Tetragonal	
Space group	P4/n	
Unit cell dimensions	a = 16.4933(14) Å	α = 90°.
	b = 16.4933(14) Å	β = 90°.
	c = 9.1291(8) Å	γ = 90°.
Volume	2483.4(4) $Å^3$	
Z	2	
Density (calculated)	1.241 Mg/m^3	
Absorption coefficient	0.191 mm^{-1}	
F(000)	1008	
Crystal size	0.28 x 0.26 x 0.16 mm^3	
Theta range for data collection	1.75 to 26.37°.	
Index ranges	-20<=h<=12, -12<=k<=19, -10<=l<=11	
Reflections collected	10759	
Independent reflections	2553 [R(int) = 0.0250]	
Completeness to theta = 26.37°	99.8 %	
Absorption correction	Semi-empirical from equivalents	

Max. and min. transmission	0.9701 and 0.9485
Refinement method	Full-matrix least-squares on F^2
Data / restraints / parameters	2553 / 25 / 187
Goodness-of-fit on F^2	1.122
Final R indices [I>2sigma(I)]	R1 = 0.0714, wR2 = 0.1754
R indices (all data)	R1 = 0.0772, wR2 = 0.1790
Largest diff. peak and hole	0.426 and -1.148 e.$Å^{-3}$

Table 3.12: Crystal data and structure refinement for compound **6**

The result of the X-ray structure determination (space group P4/n) shows a superposition of both compounds and a detailed description of the structure is therefore not possible. The point symmetry is C_4 (4) and to Al1 either a hydride (H1) or a chloride is bonded.

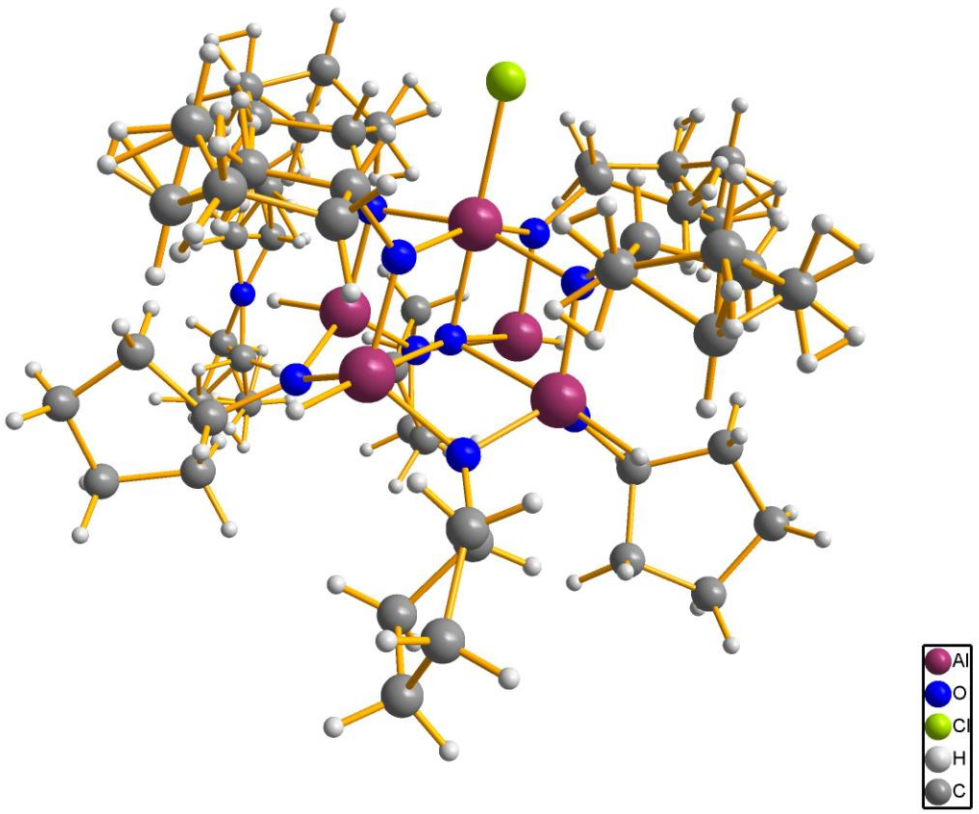

Figure 3.8: Molecular structure of compound **6, (**Disorder by super position of some organic ligands)

The molecular dimensions are very similar to those found for pure hydride compound **5** (see Table). Although the alkoxo ligands in **6** are cyclopentanolates the overall structure of the inner cage compares quite well within standard

deviations with the same cage found in the reported similar structure $[H_4ClAl_5(\mu5\text{-}O)(\mu2\text{-}OiPr)_8]$ [98] which differs only in the ligand (iso-propanol).

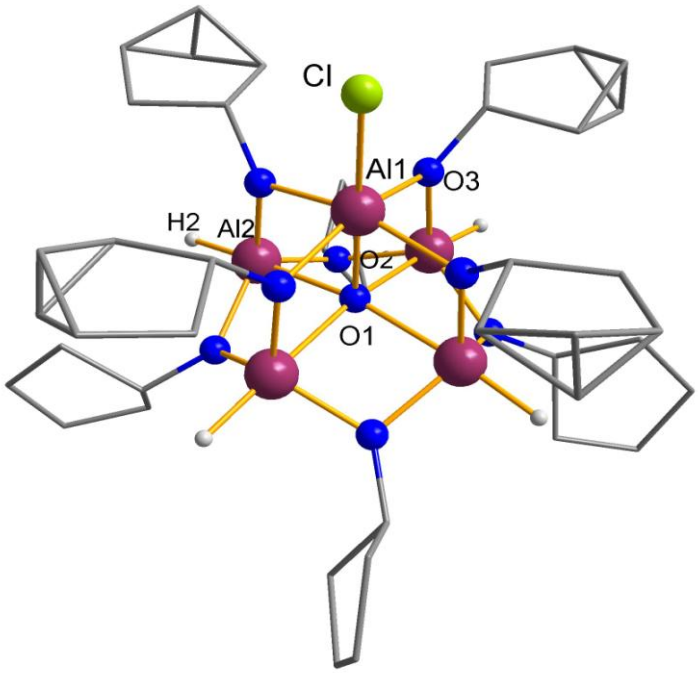

Figure 3.9: Molecular structure of compound **6** the hydrogen atoms at the carbon atoms are omitted for clarity. **(**Disorder by super position of some organic ligands)

Bond	Length [Å]	Bond	Angle [°]
Al1 - O1	1.885(5)	O1-Al1-O3	80.36(8)
Al1 - O3	1.951(2)	O3-Al1-O3'	80.36(8)
Al2 - O1	2.090(2)	O3-Al1-O3"	88.39(3)
Al2 - O2	1.830(2)	O2-Al2-O1	78.15(9)
Al2 - O3	1.815(2)	O3-Al2-O1	78.4(1)
Al1- H1	1.56(2)	O3-Al2-O2	113.9(1)
Al2 - H(2)	1.55(4)	O2-Al2-O2'	122.2(2)
Al1 - Cl	2.233(3)	O2-Al2-H2	98.0(1)
		O3-Al2-H2	107.0(1)
		O3-Al1-Cl	99.64(8)

Table 3.13: Selected characteristic bond lengths (Å) and angles (°) for the compound **6**

3.2 Super hydrophobic surface development:

3.2.1 Deposition of Al/Al_2O_3 NWs

The CVD reaction of the volatile precursor $[H_2Al\ (O^tBu)]_2$ for producing nano materials was extensively studied by Prof. Veith and his co workers in the last two decades. As has been shown in the first chapter changing of the parameters such as temperature, rate flow, etc. in CVD reactions of the same precursors will lead to a significant effect upon the final product. The CVD of $[H_2Al(O^tBu)]_2$ gives different nano-materials in terms of morphology and chemical compositions at different decomposition temperatures and pressure. Below 330°C, a transparent metastable amorphous material of the composition HAlO is obtained. At a temperature above 400°C first core/shell nano-balls are obtained, while above 470°C, a core shell nano-wires form [23, 61, 63, 64]. Their composition in all cases is Al/Al_2O_3 The surfaces decorated with nano-wires, optimum for our purpose, use of synergetic effect of surface topography and surface chemistry to achieve a superhydrophobic surface, were obtained by the CVD of $[H_2Al(O^tBu)]$ at 630°C temperature , 8.0 x 10^{-2} mbar pressure and 30 mints deposition time upon a glass substrate. These parameters were maintained for getting high density highly porous nano-wires as thin film on substrates [68].

3.2.2 Al/Al_2O_3 NWs functionalization by PTFEP coating:

For the functionalization of the deposited Al/Al_2O_3 nano wires with PTFEP we used the dip coating techniques, this procedure known as a very simple, flexible and cost efficient coating technique. PTFEP was dissolved in acetone as a

solvent which due to it's a moderate volatility gives the liquid film enough time to level out and which keeps the drying time short.

The thickness of the coating using dip coating techniques can be basically controlled via the withdrawal speed of the dip and the concentration of the coated liquid [27]. In order to get a homogenous coating, different concentrations in the range of 1-5 weight/volume % were applied. We found that using a concentration of 2.5 % weight/volume is optimum for getting a highly homogenous coating; a concentration above 3 % led to formation of thick and none homogenous coatings. The withdrawal rate of the substrates from the solution was set between 1 mm/min and 7 mm/min. Higher withdrawal speed than 3 mm/min led to a none homogenous coating while a lower withdrawing speed led to the formation of a thick and none homogenous coating (see Figure 3.11). A withdrawal rate of 2 mm/min is optimum for getting highly homogenous coatings. In the following the drying stage we did not see any trace of excess PTFEP layer or webbing.

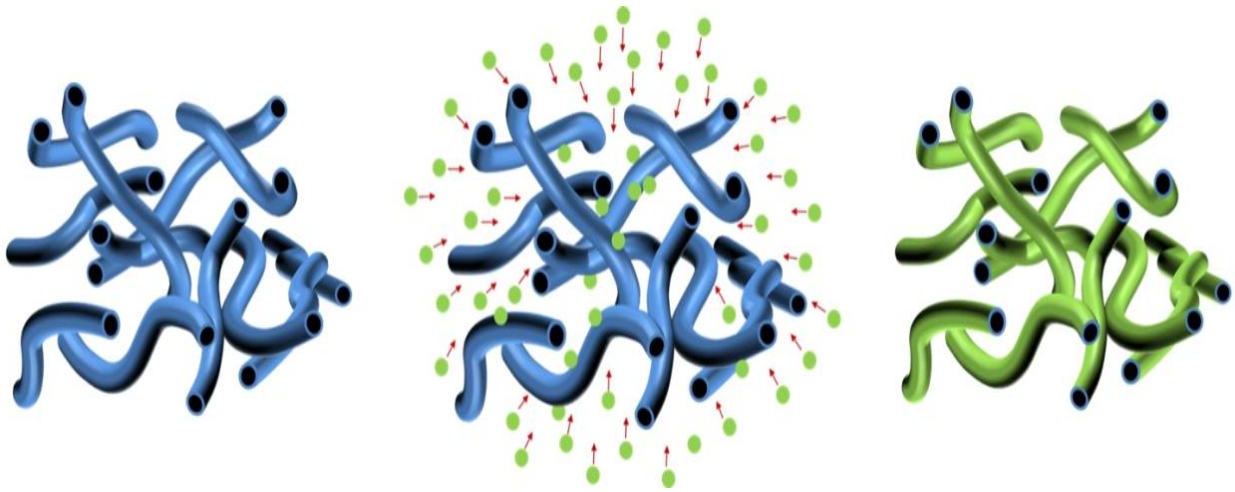

Figure 3.10: Schematic illustration of the coating process, starting from the left with the random 3D network of the 1D Al/Al_2O3 nanostructures (blue labeled), followed by the dip-coating with the PTFEP solution (green labeled) to end up with the stable ultra-porous superhydrophobic surface.

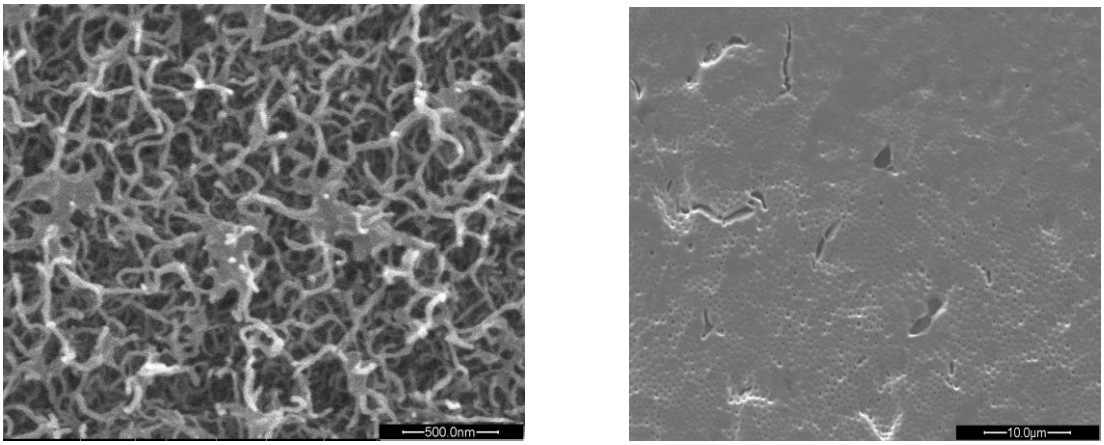

Figure 3.11 SEM micrographs, none homogenous coating when using a high concentration of PTFEP in modifying Al/Al2O3 NWs.

3.2.3 Characterizations of the surfaces:

3.2.3.1 Morphology determination:

The deposition of 1D Al/Al_2O_3 composite nano-wires at a temperature 450°C were shown to exhibit a core shell structure where the core is composed of metallic Al and the shell is formed of the Al_2O_3 ceramic[104]. The nano-wires for the present study have been obtained at 630°C and at a precursor flow of 8.0 x 10-2 mbar pressure. Applying these two parameters led to the formation of a highly porous structure with strict composition of Al/Al_2O_3 as shown in pervious studies in Veith's research group [68]. Maintaining these parameters led to the formation of identical coatings in terms of morphology and chemistry in repeated trials.

The SEM images of deposited 1D Al/Al_2O_3 nano-wires assemblies are shown in Figure 3.12. The diameter of randomly grown nano-wires is about 20-30 nm. Since deposited nanowires are highly tangled and interpenetrated, the thickness of the layer is only about 400 nm although the length of a single nano-wire can reach several micrometers. The texture of the nano-wires is highly porous with small pores and holes.

Upon the coating of the Al/Al_2O_3 nano-wires surface with PTFEP, the morphology of the Al/Al_2O_3 nano-wires and overall topography does not change drastically after modifying them with PTFEP (as shown Figure 3.12). It is

believed that highly diluted polymer solution is able to penetrate inside the complex 3D nano-wire network and thus covering the surface without any webbing. Therefore this coating with PTFEP can be referred to surface functionalization rather than to coating or infusion (see Fig. 3.10).

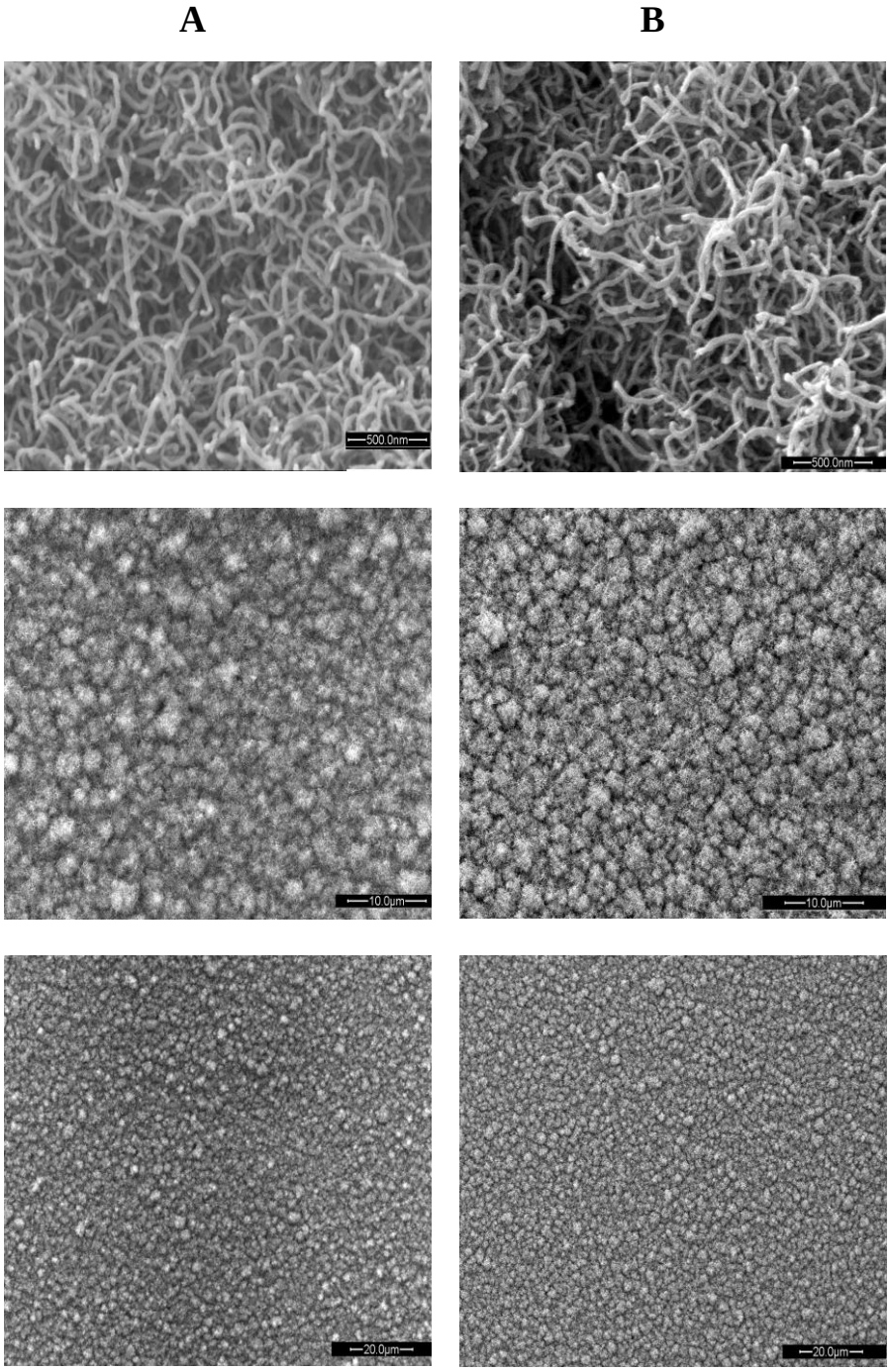

Figure 3.12 SEM micrographs showing identical topography of the (A) as-deposited 1D Al/Al_2O_3 nanostructures (NWs) and (B) modified surface (NWs+PTFEP).

3.2.3.2 Surface chemistry

One of the challenges in applying PTFEP as a coating or thin film is its poor adhesion to the substratum because of its highly hydrophobic character [82]. As we discussed in the first chapter there were two approaches to tackle this problem: either by altering the chemistry of the polymer by introducing a hydroxyl group or by oxidizing the substrate surface to introduce a free hydroxyl group. Remember the trifluoroethoxy side group, can undergo nucleophilic exchange reactions because of its electron-withdrawing character, and relatively small size. In our case we have Al/Al_2O_3 nano-wires which are supposed to accommodate high amounts of active hydroxyl (-OH) groups due to their extremely high surface area. Therefore it is believed that a hydrolysis reaction takes place as expressed through eqn. (3.1)

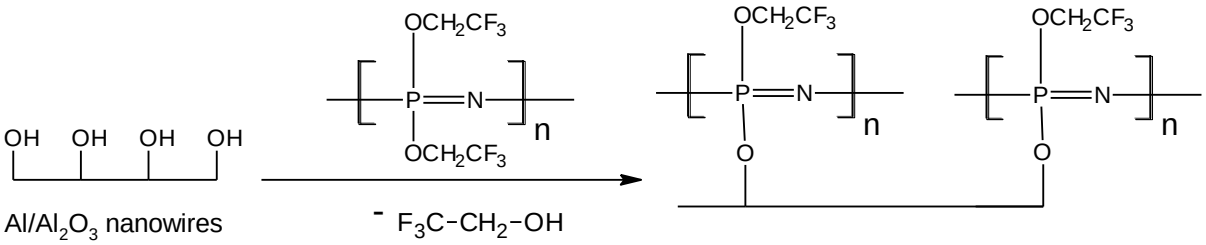

Equation 3.1: surface functinlaizarion by PTFEP.

Different techniques have been applied to prove the presence and bonding of the PTFEP to the Al/Al_2O_3 nano-wires. The elemental composition of the nano-wires surfaces before and after functionlaization with PTFEP has been determined with energy dispersive X-ray spectroscopy (EDX). The EDX spectrum in Figure 3.13 shows the elemental composition of the surfaces qualitatively. The small peaks for gold appeared due to the sample preparation process. The surfaces have to be sputtered with gold to avoid the charging on the surfaces in order to get better resolution and the presence of carbon peak on the nano-wires spectrum is due to the carbon tape used for supporting the samples for analysis.

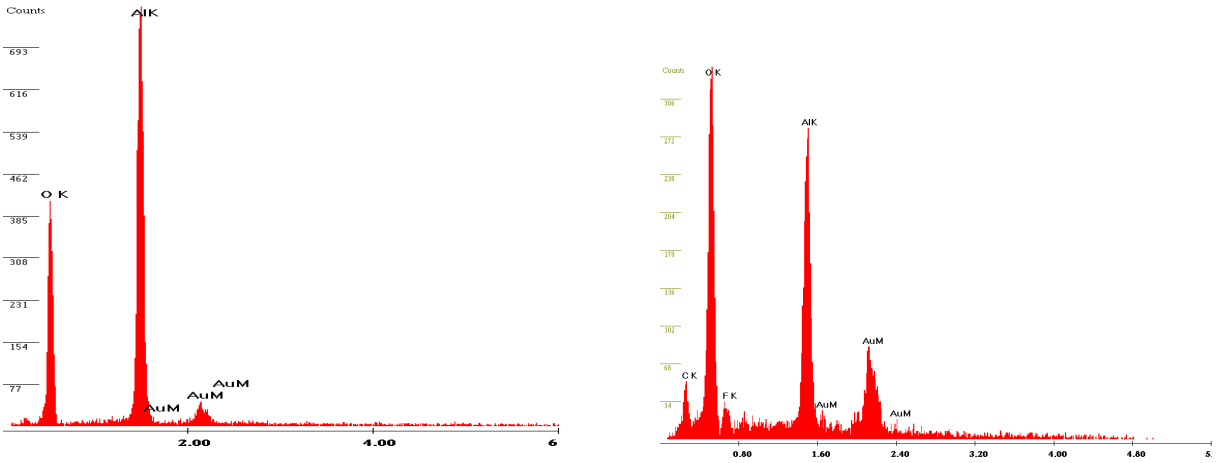

A **B**

Figure 3.13: EDX spectrum of Al/Al_2O_3 NWs surface **A** before and B after modification with PTFEP. The carbon peak in **A** is due to the carbon tape and the Au peak due to gold sputtering used in sample preparations.

XPS measurements were performed also for the nano-wires surfaces, before and after functionalization, in order to determine their surface chemistry. Figure 3.14 shows the XPS results of the nano-wires. The binding energies at 75.5 eV and 72.3 eV were assigned to Al 2p of Al_2O_3 shell and Al 2p of metallic Al for both as-deposited and PTFEP modified Al/Al_2O_3 nano-wires. These peaks are in accordance with the reported ones [105]. Furthermore, the P2p, C 1s, and F1S orbitals appear at 136 eV, 298 eV and 694 eV respectively, clearly indicative for the presence of PTFEP on Al/Al_2O_3 nano-wires surfaces.

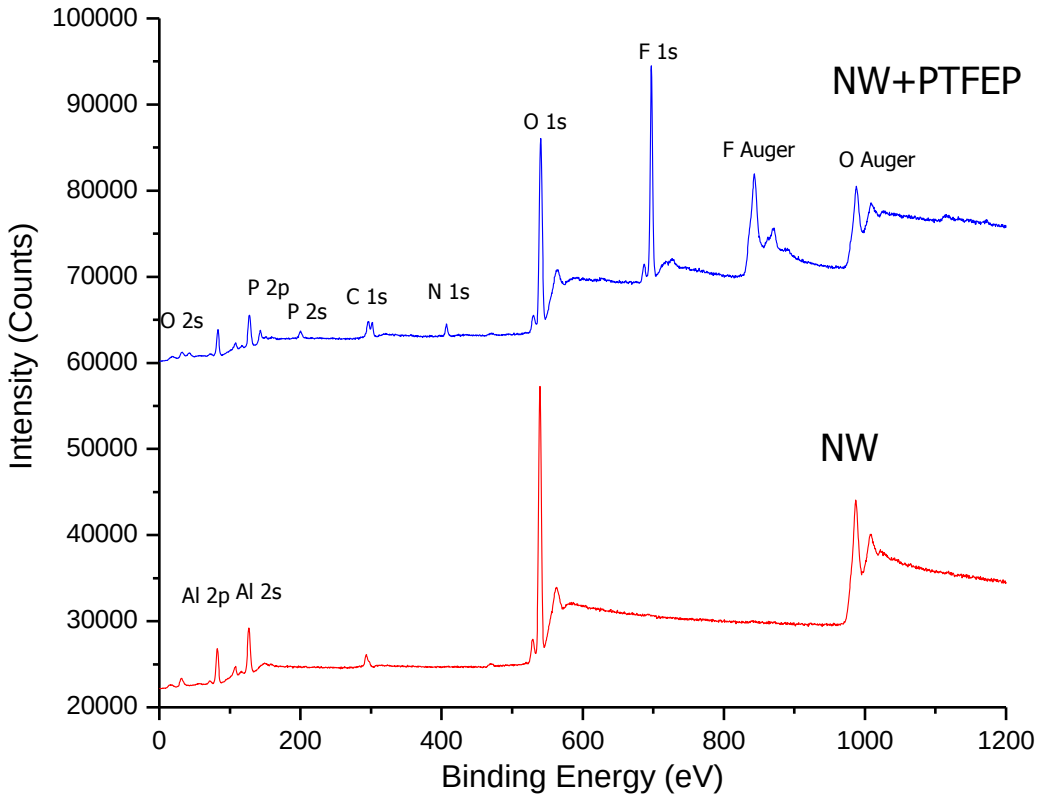

Figure 3.14 XPS analysis, comparing the chemical composition of the NWs and NWs +PTFEP surfaces.

In order to confirm the bonding of the PTFEP to the Al/Al_2O_3 nano-wires, ^{1}H and ^{13}C NMR analysis of the solution of the polymer before and after the immersion of Al/Al_2O_3 nano-wires were carried out. New peaks were observed on ^{1}H NMR spectra using the solution of the polymer after the immersion of Al/Al_2O_3: a broad peak showing a multiplet at 3.9 ppm is observed in the spectra of the solution after immersion. This peak can be assigned to the OH of the liberated by-product 2, 2, 2, trifluroethaol (see Figure 3.15). In the FT-IR spectrum of the hybrid composite an absorption band at 985 cm^{-1} is observed which can be correlated to the stretching vibration of Al-O-P[106].

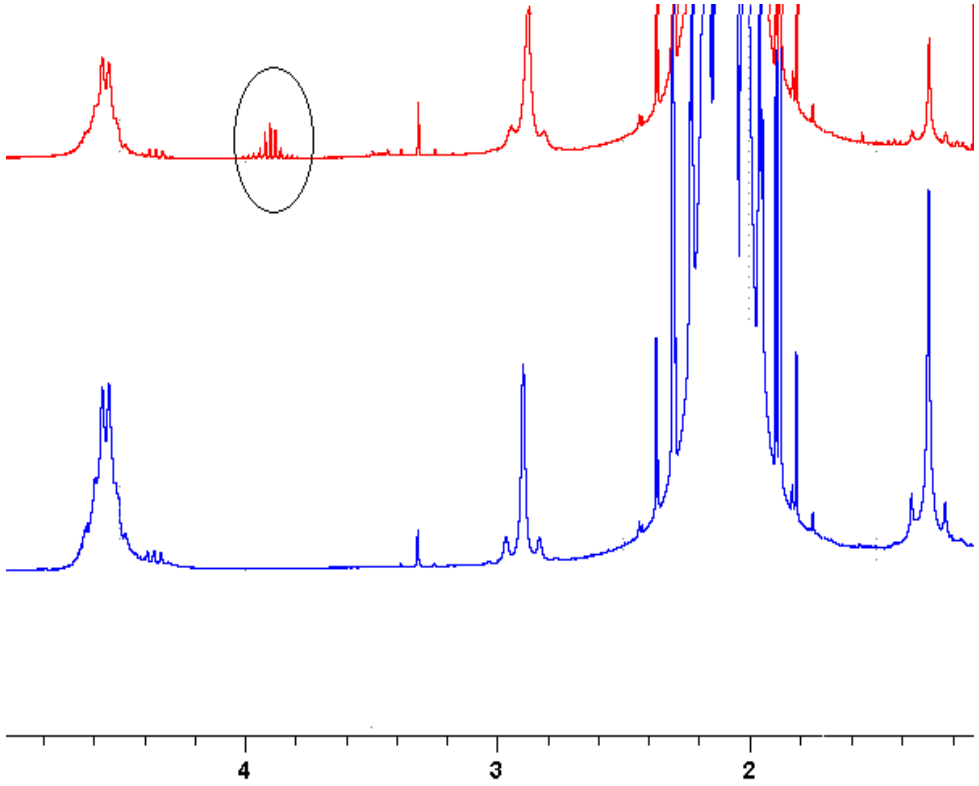

Figure 3.15 ^{1}H NMR spectra of the PTFEP acetone solution before (blue) and after (red) immersion of Al/Al_2O_3 nano-wires

For further confirmation of the chemical bonding of the PTFEP to Al/Al_2O_3 nano-wires, we did the so called "acetone test"[107], as the polymer is highly soluble in acetone. Extraction of the polymer from the hybrid surface of Al/Al_2O_3 and PTFEP, with a calibrated amount of acetone gave a solution that contained high quantities of the PTFEP removed from the surface once the PTFEP is not chemically bonded to the Al/Al_2O_3 NWs. The hybrid surfaces were immersed in acetone and stirred for 72 hrs at room temperature and pressure. This solution was later analysed by ^{1}H and ^{13}C NMR spectroscopy, no PTFEP could be detected in the acetone solutions used, the extraction process indicating that the acetone is unable to remove PTFEP from the hybrid surfaces. This proves the existence of strong chemical bonds between the Al/Al_2O_3 NWs network and PTFEP.

3.2.3.3 Contact Angle Measurements

Static contact angles of the prepared surfaces were measured using a classical static method. The precise values of contact wetting angel in case of PTEFP modified Al/Al_2O_3 nano-wires can not be measured using this method, as the results suggest that the receding angle is indistinguishable from the advancing angle. It is clear that conventional contact angle measurements are not useful in determining contact angle differences when the angles are higher than 175° and, in particular, distinguishing between 180° and values slightly less than this. As all our attempted measurements show angles higher than 175° we have to assume that the hybrid surfaces of Al/Al_2O_3/PTFEP have a highly superhydrophobic character.

The high density coated Al/Al_2O_3 nanoporous layer on a glass substrate shows a static contact angle below 8° (Figure 3.16) which matches with earlier reported values for these surfaces [108], a planar Al_2O_3 surface exhibits a water contact angle around 55-65°, and PTFEP covered glass substrate exhibits a contact angle around 65°. The super-hydrophobic nature of the modified surfaces can be attributed to the combination of nano nanostructure surface topography and the surface chemistry. Captured photos of the water drops on the surfaces substrates are presented in Figure 3.17. Measurement results of tested liquids are given in Figure 3.16.

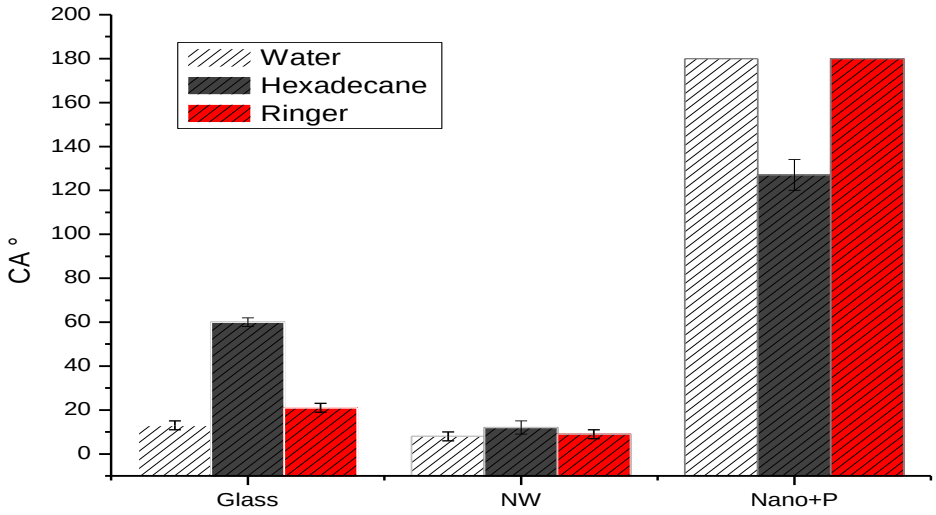

Figure 3.16: Wetting angle curve maximal values representing the contact angle of three different liquids used (water, hexadecane and ringer solution on the Glass surface, Al/Al_2O_3 coated glass (NW), Hybrid surfaces of PTFEP modified Al/Al_2O_3 nano-wires +PTFEP.

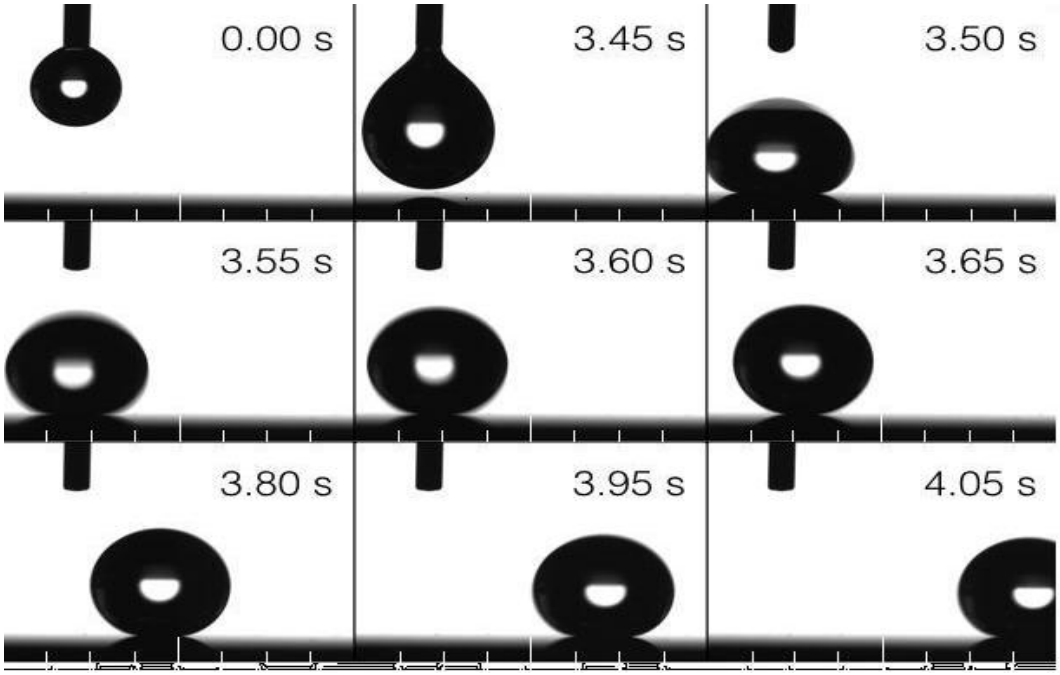

Figure 3.17: showing falling and rolling of water droplets on PTFEP modified Al/Al_2O_3 nano-wires at different time laps. As soon as the water droplets contact with our super hydrophobic surface it does not stick and starts moving.

3.2.4 Anti-adhesive properties of the modified surface:

To test the anti-adhesive properties of modified surfaces, we examined the surface adhesion of water, Ringer solution, hexadecane, and fresh human blood on Al/Al_2O_3 with or without PTFEP. The modified nanoporous coatings were brought into slope at an angle of 30 degrees Figure 3.18. None of the droplets exhibited any wetting on the modified surface. There was only a difference in the speed of droplets sliding over the substrate as shown in Figure 3.17. With the help of a fast camera recording it has been observed that, the water droplet slid off the surface after 0.14s whereas the rolling of ringer solution from the substrate took 0.16s. On the other hand the same droplets behave differently on non modified NWs substrates as may be seen in supplementary videos (1.2, and 3). Blood droplets behave differently: they immediately adhere to the surface and leave a trail of blood components over the time course of 5s (Supplementary video 3). In contrast, when the same surface was coated with PTEFP modified nanoporous layer, the blood droplet almost immediately slid off the surface and, remarkably, there was no evidence of any residual blood trail (Figure 3.18, Supplementary video 3). In comparison uncoated surfaces exhibited considerable blood adhesion as shown in Supplementary video 3 and in Figure 3.19.

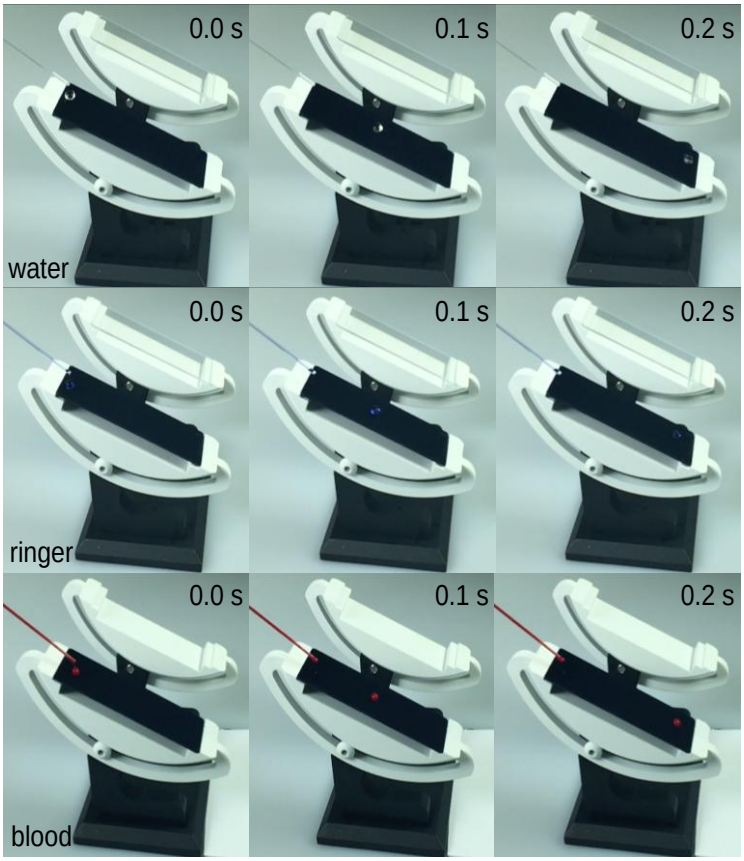

Figure 3.18: Snapshots images taken by a high speed camera, presenting the droplet speed of different liquids (water, ringer solution and blood) on the modified surface (NWs+PTFEP) which is the figure are black.

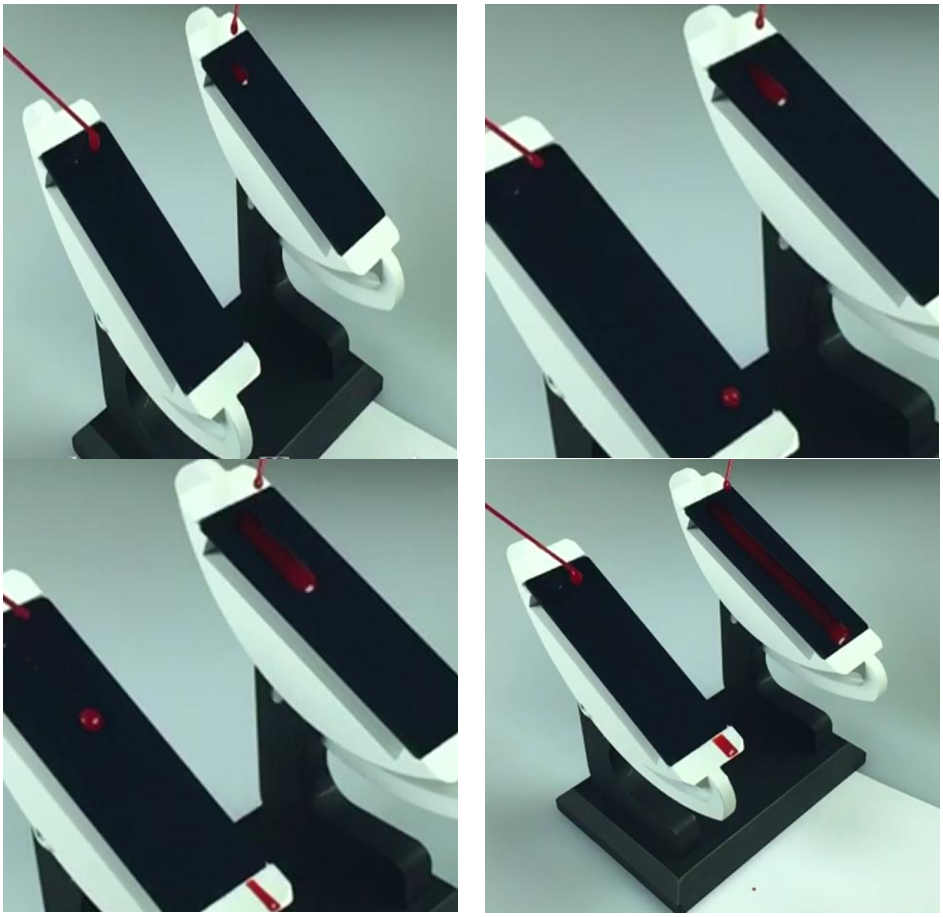

Figure 3.19: Blood droplets behaviour on modified Al/Al2O3 NWs with PTFEP and none modified Al/Al2O3 Nws.

3.2.5 Stability of hydrophobicity under dynamic conditions

In the supplementary video 4 and in the figure 3.20 one can observe the water jet bouncing on our superhydrophobic surface . The water jet impinges on the surface and reflects back with the same angle Figure 3.19. This may also be considered as the stability of hydrophobicity under dynamic conditions. We tested the static hydrophobicity performance of the surface by immersing the prepared sample into deionized water for 120 minutes (see the supplementary

video 5) and found that the coated surface stayed totally dry without any detoriation.

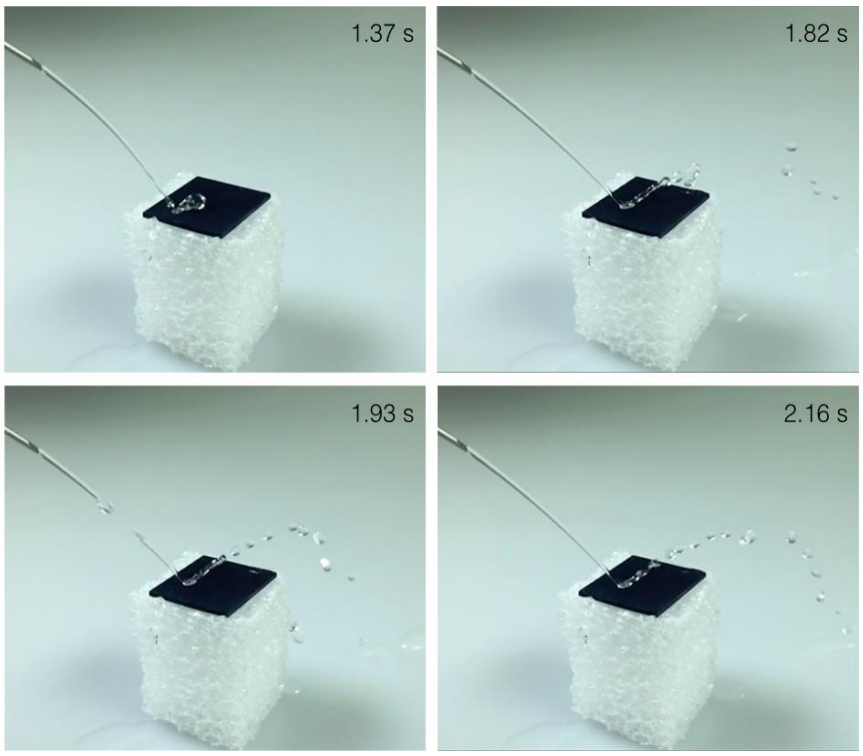

Figure 3.20: The water jet impinges on the surface and reflects back with the same angle.

3.3 Possible applications of the modified Al/Al_2O_3 +PTFEP surface:

Since the here presented modified surfaces consist of PTFEP which is known as hemocomatible and biodegradable polymer with unique properties such as anti-inflammatory and anti-thrombotic, and of Al/Al_2O_3 nano-wires assemblies which were proven as a biocompatibile material, this besides its proven superhydrophobicity toward blood and protein. The surface may be used for the coating of implants which have contact with blood and tissue and may bring significant improvement in view of blood surface interaction. Another point in the hemo-compatibility of such coated devices used as mechanical heart valves , stent or stents, and etc. These surfaces may reduce the intensity of

anticoagulation which reduces the severe associate complications such as bleeding or thrombosis. The preliminary results of the biological interactions of these surfaces are very promising.

The control of adhesion of fibroplast and osteoplast cells on Al/Al_2O_3 nano-wires [67] which should be influenced through further coating of PTFEP. One of my ideas of using PTFEP was to (for example) invert the biological properties due to the new outside chemistry always by maintaining the original 3D structure of the Al/Al_2O_3 assemblies.

Surfaces, which have typically large water contact angles above 150° and exhibit no or very little sticking to water drops, have numerous applications in self-cleaning coatings, non-wetting textiles, anti-fogging, anti-icing and microfluidic devices and antifouling bio surfaces [109].

In nature self-cleaning occurs on superhydrophobic surfaces with water from rain, dew, and fog. Self-cleaning surfaces should have the following properties: (i) large water contact angle exceeding 150°, (ii) small sliding angle (<10°) to cause water drops easily roll off the surface, and (iii) the adhesion between the surface and dust particles on the surface should be smaller than that between the dust particles and water. In supplementary video 5 we show that by dropping water the dust particles are taken away, and afterwards superhydrophobic surface becomes virtually clean and remains completely dry (see also Figure 3.21).

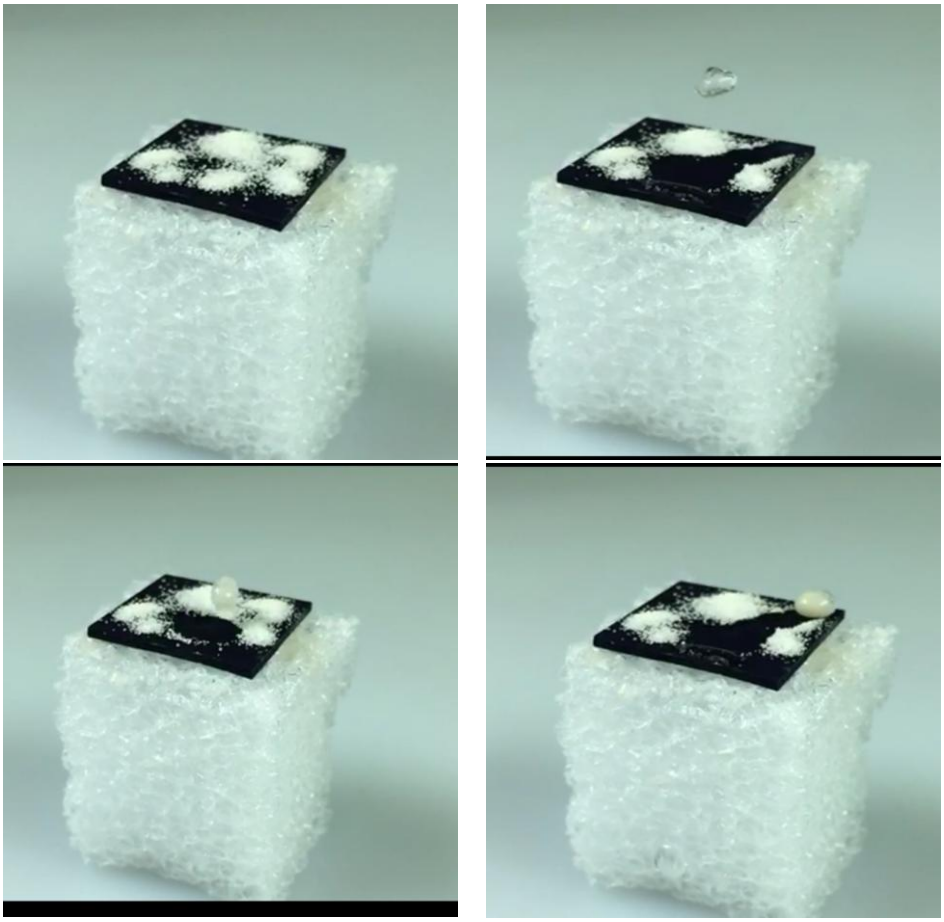

Figure 3.21: The self-cleaning property of Al/Al_2O_3 Nws +PTFEP, water droplets take the dust particles away.

4. Conclusions:

The primary aim of this work was the synthesis and characterization of new potential aluminium hydride/ alkoxides for their use as precursors in high purity CVD or sol/gel processes for formation of alumina or aluminium/alumina composites. This goal was fulfilled through the preparation of six different new precursors from the reaction of lithium aluminium hydride with aluminium chloride and cyclopentanol in different molar ratios.

The structures of the synthesized compounds were elucidated on the basis of spectroscopic data (IR. ^{1}H and ^{13}C NMR) , and by X-ray diffraction XRD.

The synthesized compounds shows different types structures:

The octameric Compound **1** is combines the dimeric dihydrido aluminium cyclopentanolate $[H_2Al(O\text{-}C_5H_9)]_2$ and Chloro-hydrido aluminium cyclopentanolate $[H(Cl)Al(O\text{-}C_5H_9)]_2$ as 6:2 aggregate via oxide and hydride bridges (Figure 3.21).

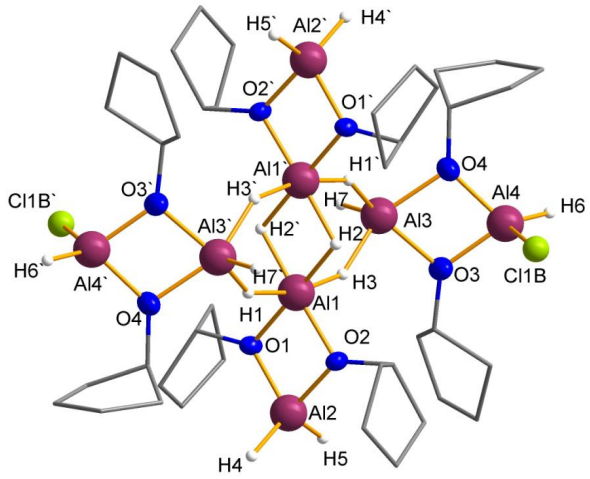

Figure 3.22: Octanuclear cluster compound **1**

Compounds **2**, **3** and **4** are tetrameric posses comparable structure features and belong to the so called Mitsubishi motif family. All of them displaying a central octahedron aluminium atom coordinated by oxygen atoms of the cyclopentanolates with three AlH_2 or $AlCl_2$ or $Al(O^cPen)_2$ (see Figure 3.22).

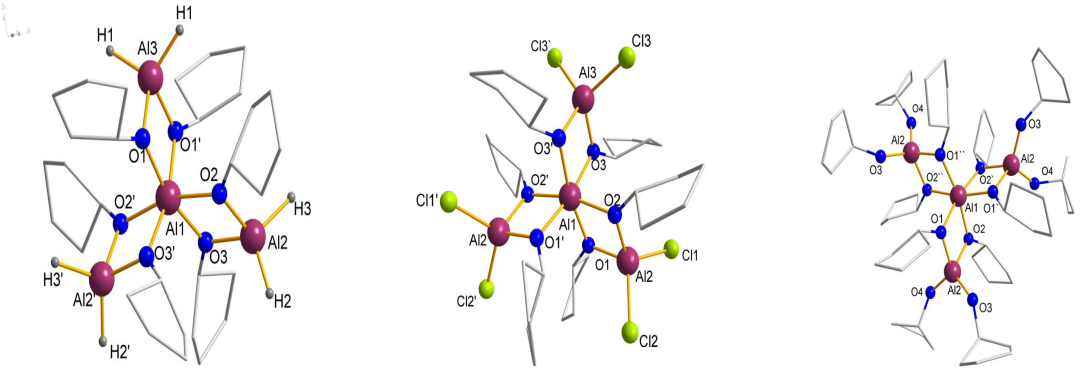

2 **3** **4**

Figure 3.23: Tetraamer structure of **2**, **3**, and **4**.

Compound **5** and **6** are isolated as pentanuclear aluminium/oxo cluster with a central naked oxygen atom connecting 5 aluminium atoms in a square pyramid. In compound **5** all aluminium atoms have terminal hydride ligands, while in compound **6** the aluminium atom situated on the top of the pyramid has a chloride ligand Figure 3.22.

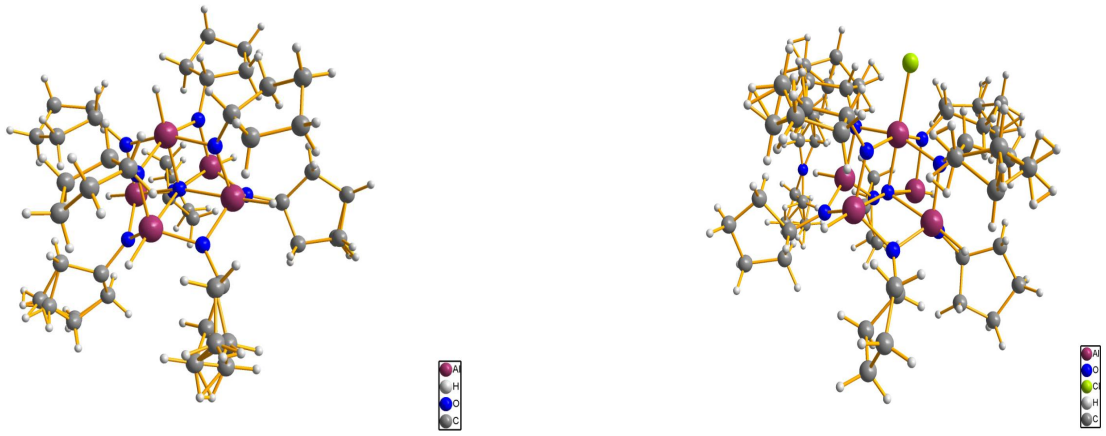

5 **6**

Figure 3.24: Pentanuclear oxo cluster of compounds **5** and **6**

For the second part of the thesis , modifications of the 1D Al/Al2O3 core/shell nano-wires by attachment phosphazenes PTFEP :

High density highly porous Al/Al_2O_3 nano–wires have been synthesized as thin film upon substrates through the CVD reaction of $[H_2Al\ (OtBu)]_2$.

The Al/Al_2O_3 nano–wires assemblies were functionalized by PTFEP. The modified surfaces were fully characterized using different techniques: SEM, XPS, wetting angle measurement, and IR. The modified surface is stable and the chemical bonding of PTFEP to the Al/Al_2O_3 nano-wiress has been proven by ^{1}H and ^{13}C NMR spectroscopy. The modified surface exhibits ultra hydrophobic nature and extreme repellency against several liquids including blood and hexadecane. The combination of Al/Al_2O_3 nano-wires which have been proved as a biocompatible surface for implant applications and of the poly [bis (2,2,2 - trifluoroethoxy)phosphazene] (PTFEP) polymer, a widely used hemocompatible material in clinical applications, has lead to a new composite surface with new extraordinary properties. Especially in implant techniques these new surfaces should add new application possibilities, as the coating modifies the implant in such way that its blood compatibility is raised.

Outlook:

The primary results of vitro investigations of the hybrid materials are promised therefore further in vivo investigation will be carried out , actually it is now started and several cardiovascular implants have been coated. We believe that these modified surfaces particularly, in the paediatric patients may be a significant advantage to overcome several associated morbidities.

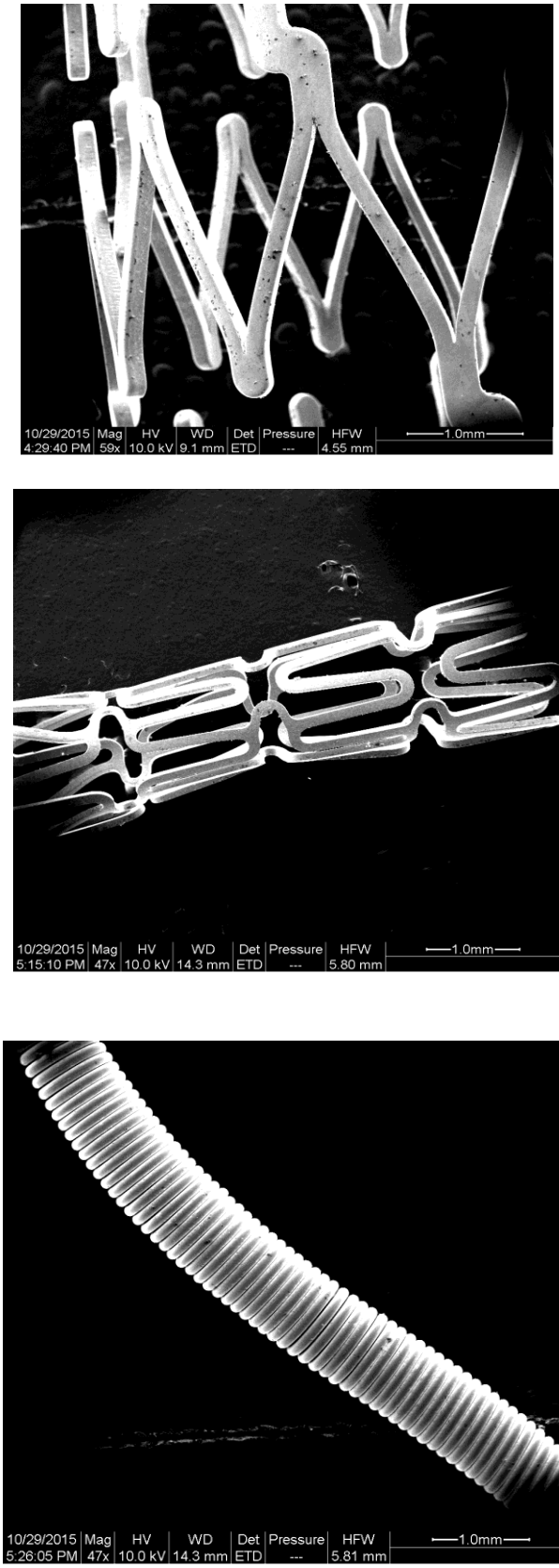

Figure 4.1: Coated vascular implants for future in- vivo applications.

5. References.

1. Park, J. and R.S. Lakes, *Biomaterials: an introduction*. 2007: Springer Science & Business Media.
2. Kasemo, B., *Biological surface science.* Surface science, 2002. **500**(1): p. 656-677.
3. Wen, X., X. Wang, and N. Zhang, *Microrough surface of metallic biomaterials: a literature review.* Bio-medical materials and engineering, 1996. **6**(3): p. 173-189.
4. Cai, K., J. Bossert, and K.D. Jandt, *Does the nanometre scale topography of titanium influence protein adsorption and cell proliferation?* Colloids and Surfaces B: Biointerfaces, 2006. **49**(2): p. 136-144.
5. Denis, F.A., et al., *Protein adsorption on model surfaces with controlled nanotopography and chemistry.* Langmuir, 2002. **18**(3): p. 819-828.
6. Curtis, A. and C. Wilkinson, *Topographical control of cells.* Biomaterials, 1997. **18**(24): p. 1573-1583.
7. Curtis, A.S. and C.D. Wilkinson, *Reactions of cells to topography.* Journal of Biomaterials Science, Polymer Edition, 1998. **9**(12): p. 1313-1329.
8. Curtis, A.S.G., et al., *Substratum nanotopography and the adhesion of biological cells. Are symmetry or regularity of nanotopography important?* Biophysical Chemistry, 2001. **94**(3): p. 275-283.
9. Flemming, R.G., et al., *Effects of synthetic micro- and nano-structured surfaces on cell behavior.* Biomaterials, 1999. **20**(6): p. 573-588.
10. Kane, R.S., et al., *Patterning proteins and cells using soft lithography.* Biomaterials, 1999. **20**(23): p. 2363-2376.
11. Chen, C.S., et al., *Geometric control of cell life and death.* Science, 1997. **276**(5317): p. 1425-1428.
12. Matsuda, T. and T. Sugawara, *Control of cell adhesion, migration, and orientation on photochemically microprocessed surfaces.* Journal of biomedical materials research, 1996. **32**(2): p. 165-173.
13. Hoch, H.C., L.W. Jelinski, and H.G. Craighead, *Nanofabrication and biosystems: integrating materials science, engineering, and biology*. 1996: Cambridge University Press.
14. Ranucci, C.S. and P.V. Moghe, *Substrate microtopography can enhance cell adhesive and migratory responsiveness to matrix ligand density.* Journal of biomedical materials research, 2001. **54**(2): p. 149-161.

15. Hallab, N., et al., *Cell adhesion to biomaterials: correlations between surface charge, surface roughness, adsorbed protein, and cell morphology.* Journal of long-term effects of medical implants, 1994. **5**(3): p. 209-231.
16. Andersson, M., et al., *Microtextured surfaces: towards macrofouling resistant coatings.* Biofouling, 1999. **14**(2): p. 167-178.
17. Ungersböck, A., O. Pohler, and S. Perren, *Evaluation of the soft tissue interface at titanium implants with different surface treatments: experimental study on rabbits.* Bio-medical materials and engineering, 1994. **4**(4): p. 317-325.
18. Rosengren, A., et al., *Tissue reactions evoked by porous and plane surfaces made out of silicon and titanium.* IEEE transactions on biomedical engineering, 2002. **49**(4): p. 392-399.
19. Rosengren, A., et al., *Tissue reactions to porous silicon: A comparative biomaterial study.* physica status solidi (a), 2000. **182**(1): p. 527-531.
20. Davis, J., *Overview of biomaterials and their use in medical devices.* Handbook of materials for medical devices. Illustrated edition, Ohio: ASM International, 2003: p. 1-11.
21. Wälivaara, B., et al., *Titanium with different oxides: in vitro studies of protein adsorption and contact activation.* Biomaterials, 1994. **15**(10): p. 827-834.
22. Veith, M., et al., *Adhesion of fibroblasts on micro- and nanostructured surfaces prepared by chemical vapor deposition and pulsed laser treatment.* Biofabrication, 2010. **2**(3): p. 035001.
23. Veith, M., *Molecular precursors for (nano) materials—a one step strategy.* Journal of the Chemical Society, Dalton Transactions, 2002(12): p. 2405-2412.
24. Turova, N.Y., et al., *The chemistry of metal alkoxides*. 2006: Springer Science & Business Media.
25. Kuhlmann, F., *Untersuchungen über die Aetherbildung.* Justus Liebigs Annalen der Chemie, 1840. **33**(1): p. 97-110.
26. Rehberg, C. and C. Fisher, *Preparation and polymerization of acrylic esters of olefinic alcohols.* The Journal of organic chemistry, 1947. **12**(2): p. 226-231.
27. Aegerter, M.A. and M. Mennig, *Sol-gel technologies for glass producers and users*. 2013: Springer Science & Business Media.
28. Marchand, P. and C.J. Carmalt, *Molecular precursor approach to metal oxide and pnictide thin films.* Coordination Chemistry Reviews, 2013. **257**(23): p. 3202-3221.

29. Mazdiyasni, K.S. and L.M. Brown, *Synthesis and some properties of yttrium and lanthanide isopropoxides.* Inorganic Chemistry, 1970. **9**(12): p. 2783-2786.
30. Turova, N.Y., A. Novoselova, and K. Semenenko, *Beryllium alcoholates.* Zh. Neorg. Khim, 1959. **4**: p. 997.
31. Whitaker, G., *Aluminum Alcoholates and the Commercial Preparation and Uses of Aluminum Isopropylate.* Metal-Organic Compounds, Advances in Chemistry Series, 1959. **23**.
32. Kulpinski, M. and F. Nord, *New Synthesis of Glycolesters.* Nature, 1943. **151**: p. 363-364.
33. Drake, S.R., et al., *Dinuclear barium alkoxides and siloxides displaying variable coordination numbers and asymmetric dispositions of ligands.* Inorganic Chemistry, 1992. **31**(15): p. 3205-3210.
34. Turova, N.Y. and A.V.e. Novoselova, *Alcohol derivatives of the alkali and alkaline earth metals, magnesium, and thallium (i).* Russian Chemical Reviews, 1965. **34**(3): p. 161-185.
35. Wu, Y.-T., et al., *Stepwise Reactions of TiCl4 and Ti (OiPr) Cl3 with 2-Propanol. Variable-Temperature NMR Studies and Crystal Structures of [TiCl2 (OiPr)(HOiPr)(μ-Cl)] 2 and [TiCl2 (OiPr)(HOiPr)(μ-OiPr)] 2.* Inorganic Chemistry, 1996. **35**(20): p. 5948-5952.
36. Caldin, E. and G. Long, *The equilibrium between ethoxide and hydroxide ions in ethanol and in ethanol–water mixtures.* Journal of the Chemical Society (Resumed), 1954: p. 3737-3742.
37. White, G.F., A.B. Morrison, and E.G. Anderson, *REACTIONS OF STRONGLY ELECTROPOSITIVE METALS WITH ORGANIC SUBSTANCES IN LIQUID AMMONIA SOLUTION V. THE SYNTHESIS OF OXYGEN AND SULFUR ETHERS AND OF ALKYL DERIVATIVES OF AMMONO ACIDS.* Journal of the American Chemical Society, 1924. **46**(4): p. 961-968.
38. Coates, G. and P. Roberts, *Some t-butyl and t-butoxy-derivatives of zinc.* Journal of the Chemical Society A: Inorganic, Physical, Theoretical, 1967: p. 1233-1234.
39. Mehrotra, R. and M. Aroda, *Alkoxides and double alkoxides of zinc.* Zeitschrift für anorganische und allgemeine Chemie, 1969. **370**(5‐6): p. 300-309.
40. Mehrotra, R., D. Gaur, and D. Bradley, *Metal alkoxides*. 1978: Academic Press.

41. Sailäard, B., *Über die elektrolytische Darstellung der Alkoholate und der Alkoholat‐Carbonsäureester.* Zeitschrift für Elektrochemie und angewandte physikalische Chemie, 1906. **12**(22): p. 393-395.
42. Lehmkuhl, H. and W. Eisenbach, *ELECTROCHEMICAL SYNTHESIS OF ORGANIC COMPOUNDS OF METALS. 7. ELECTROSYNTHESIS OF ALKOXIDES AND ACETYLACETONATES OF IRON, COBALT AND NICKEL.* ANNALEN DER CHEMIE-JUSTUS LIEBIG, 1975(4): p. 672-691.
43. Kovsman, E., et al., *Electrochemical synthesis of metal alkoxides. Prospects of commercial alkoxides production.* Journal of Sol-Gel Science and Technology, 1994. **2**(1-3): p. 61-66.
44. Grundström, B., *Über die sogenannten überzähligen Terme bei Hydriden.* Zeitschrift für Physik, 1940. **115**(3-4): p. 120-139.
45. Cucinella, S., A. Mazzel, and W. Marconl, *Synthesis and reactions of aluminum hydride derivatives.* Inorganica Chimica Acta Reviews, 1970. **4**: p. 51-71.
46. Nöth, H. and H. Suchy, *Über Alkoxyalane und Alkoxyaluminium‐boranate.* Zeitschrift für anorganische und allgemeine Chemie, 1968. **358**(1‐2): p. 44-66.
47. Veith, M., et al., *(tert-Butoxy)aluminium and -gallium Hydrides.* Chemische Berichte, 1996. **129**(4): p. 381-384.
48. Veith, M., A. Altherr, and H. Wolfanger, *A Single Source CVD Precursor to MgAl2O4:[Mg {(Ot‐Bu) 2AlH2} 2]*. Chemical Vapor Deposition, 1999. **5**(2): p. 87-90.
49. Bradley, D., et al., *Alkoxo and aryloxo derivatives of metals*. 2001: Academic Press.
50. Dahl, L., et al., *The molecular and crystal structure of thallium (I) methoxide.* Journal of Inorganic and Nuclear Chemistry, 1962. **24**(4): p. 357-363.
51. Cunnington, M.J., *Alkoxy and related derivatives of main group elements*. 1993, Durham University.
52. Weiss, E., *Die kristallstruktur des kaliummethylats.* Helvetica Chimica Acta, 1963. **46**(6): p. 2051-2054.
53. Bradley, D., *Metal alkoxides.* Prog. Inorg. Chem, 1960. **2**: p. 303-361.
54. Turova, N.Y., et al., *Physico-chemical and structural investigation of aluminium isopropoxide.* Journal of Inorganic and Nuclear Chemistry, 1979. **41**(1): p. 5-11.
55. Wijk, M., et al., *Synthesis, Characterization, and Structural Determination of the Bimetallic Alkoxide ErAl3 (OC3H7i) 12.* Inorganic Chemistry, 1996. **35**(4): p. 1077-1079.

56. Healy, M.D., et al., *Sterically crowded aryloxide compounds of aluminium: hydrides and homoleptic aryloxides.* Journal of the Chemical Society, Dalton Transactions, 1993(3): p. 441-454.
57. Nöth, H., et al., *Di ‐, Tri ‐, and Tetranuclear Alkoxyaluminum Hydrides.* Angewandte Chemie International Edition in English, 1997. **36**(23): p. 2640-2643.
58. Koutsantonis, G.A., F.C. Lee, and C.L. Raston, *Reduction of Bu2 tC¯ O by H3MNMe3 (M= Al or Ga): Product Association via Bridging Alkyloxides (M= Al, Ga) and Hydrides (M= Al).* Main Group Chemistry, 1995. **1**(1): p. 21-28.
59. Yan, X.-T. and Y. Xu, *Chemical vapour deposition: an integrated engineering design for advanced materials*. 2010: Springer Science & Business Media.
60. Hampden ‐ Smith, M.J. and T.T. Kodas, *Chemical vapor deposition of metals: Part 1. An overview of CVD processes.* Chemical Vapor Deposition, 1995. **1**(1): p. 8-23.
61. Veith, M. and S. Kneip, *New metal-ceramic composites grown by metalorganic chemical vapour deposition.* Journal of materials science letters, 1994. **13**(5): p. 335-337.
62. Veith, M., et al., *Synthesis and microstructure of nanostructured Al/Al2O3 (H)-composite.* Journal of materials science, 1996. **31**(8): p. 2009-2017.
63. Veith, M., et al., *The Metastable, Glasslike Solid ‐State Phase of HAlO and Its Transformation to Al/Al2O3 Using a CO2 Laser.* European Journal of Inorganic Chemistry, 2003. **2003**(24): p. 4387-4393.
64. Petersen, C., et al., *SEM/TEM characterization of periodical novel amorphous/nano-crystalline micro-composites obtained by laser interference structuring: The system HAlO–Al· Al 2 O 3.* Applied surface science, 2007. **253**(19): p. 8022-8027.
65. Carradò, A., et al. *A perspective of pulsed laser deposition (PLD) in surface engineering: alumina coatings and substrates*. in *Key Engineering Materials*. 2008: Trans Tech Publ.
66. Sykaras, N., et al., *Implant materials, designs, and surface topographies: their effect on osseointegration. A literature review.* International Journal of Oral & Maxillofacial Implants, 2000. **15**(5).
67. Veith, M., et al., *Adhesion of fibroblasts on micro-and nanostructured surfaces prepared by chemical vapor deposition and pulsed laser treatment.* Biofabrication, 2010. **2**(3): p. 035001.
68. Veith, M., et al., *Bi-phasic nanostructures for functional applications.* Chemical Society Reviews, 2012. **41**(15): p. 5117-5130.

69. Kiefer, K., et al., *Al 2 O 3 micro-and nanostructures affect vascular cell response.* RSC Advances, 2016. **6**(21): p. 17460-17469.
70. Lee, J., et al., *Recombinant Phage Coated 1D Al2O3 Nanostructures for Controlling the Adhesion and Proliferation of Endothelial Cells.* BioMed research international, 2015. **2015**.
71. Andrianov, A.K., *Polyphosphazenes for biomedical applications*. 2009: John Wiley & Sons.
72. Allcock, H. and R. Kugel, *Synthesis of high polymeric alkoxy-and aryloxyphosphonitriles.* Journal of the American Chemical Society, 1965. **87**(18): p. 4216-4217.
73. Tian, Z., C. Chen, and H.R. Allcock, *New Mixed-Substituent Fluorophosphazene High Polymers and Small Molecule Cyclophosphazene Models: Synthesis, Characterization, and Structure Property Correlations.* Macromolecules, 2015. **48**(5): p. 1483-1492.
74. Deng, M., et al., *Polyphosphazene polymers for tissue engineering: an analysis of material synthesis, characterization and applications.* Soft Matter, 2010. **6**(14): p. 3119-3132.
75. Allcock, H.R., S.Y. Cho, and L.B. Steely, *New amphiphilic poly [bis (2, 2, 2-trifluoroethoxy) phosphazene]/poly (propylene glycol) triblock copolymers: Synthesis and micellar characteristics.* Macromolecules, 2006. **39**(24): p. 8334-8338.
76. Tian, Z., et al., *Synthesis and Micellar Behavior of Novel Amphiphilic Poly [bis (trifluoroethoxy) phosphazene]-co-poly [(dimethylamino) ethyl methacrylate] Block Copolymers.* Macromolecules, 2012. **45**(5): p. 2502-2508.
77. Allcock, H.R., J.S. Rutt, and R.J. Fitzpatrick, *Surface reaction of poly [bis (trifluoroethoxy) phosphazene] films by basic hydrolysis.* Chemistry of Materials, 1991. **3**(3): p. 442-449.
78. Allcock, H.R., L.B. Steely, and A. Singh, *Hydrophobic and superhydrophobic surfaces from polyphosphazenes.* Polymer international, 2006. **55**(6): p. 621-625.
79. Singh, A., L. Steely, and H.R. Allcock, *Poly [bis (2, 2, 2-trifluoroethoxy) phosphazene] superhydrophobic nanofibers.* Langmuir, 2005. **21**(25): p. 11604-11607.
80. Nagai, K., et al., *Gas permeability of poly (bis-trifluoroethoxyphosphazene) and blends with adamantane amino/trifluoroethoxy (50/50) polyphosphazene.* Journal of Membrane Science, 2000. **172**(1): p. 167-176.

81. Singh, A., L. Steely, and H.R. Allcock, *Electrospinning nanofiber membranes of poly [bis (trifluoroethoxy) phosphazene]*. Polym Prepr (ACS Div. Polym Chem), 2005. **46**(2): p. 599-600.
82. Welle, A., M. Grunze, and D. Tur, *Blood compatibility of poly [bis (trifluoroethoxy) phosphazene]*. Journal of Applied Medical Polymers, 2000. **4**(1): p. 6-10.
83. Ohkawa, K., T. Matsuki, and N. Saiki, *Phosphazene article and process for producing the same*. 1990, Google Patents.
84. Lora, S., et al., *Polyphosphazenes as biomaterials: surface modification of poly (bis (trifluoroethoxy) phosphazene) with polyethylene glycols.* Biomaterials, 1993. **14**(6): p. 430-436.
85. Kolich, C.H., W.D. Klobucar, and J.T. Books, *Process for surface treating phosphonitrilic fluoroelastomers*. 1990, Google Patents.
86. Allcock, H.R., R.J. Fitzpatrick, and L. Salvati, *Functionalization of the Surface of Poly [bis (trifluoroethoxy) phosphazene] by Reactions with Alkoxide Nucleophiles.* Chemistry of Materials, 1991. **3**(3): p. 450-454.
87. Tur, D., et al., *Investigation of the thermostability of poly [bis (trifluoroethoxy) phosphazene]*. Acta Polymerica, 1985. **36**(11): p. 627-631.
88. Welle, A., M. Grunze, and D. Tur, *Plasma Protein Adsorption and Platelet Adhesion on Poly[bis(trifluoroethoxy)phosphazene] and Reference Material Surfaces.* Journal of Colloid and Interface Science, 1998. **197**(2): p. 263-274.
89. Gleria, M., R. Bertani, and R. De Jaeger, *Fluorinated Polyphosphazenes: A Survey.* Journal of Inorganic and Organometallic Polymers, 2004. **14**(1): p. 1-28.
90. Gleria, M., et al., *Fluorine containing phosphazene polymers.* Journal of Fluorine Chemistry, 2004. **125**(2): p. 329-337.
91. Richter, G.M., et al., *A new polymer concept for coating of vascular stents using PTFEP (poly (bis (trifluoroethoxy) phosphazene) to reduce thrombogenicity and late in-stent stenosis.* Investigative radiology, 2005. **40**(4): p. 210-218.
92. Grunze, M. and C. Gries. *CA, 2,408,997, 2002*. in *Chem. Abstr*. 2001.
93. Nagel, S. and M. Boxberger, *Implants with a phosphazene-containing coating*. 2001, Google Patents.
94. Henn, C., et al., *Efficacy of a Polyphosphazene Nanocoat in Reducing Thrombogenicity, In-stent Stenosis, and Inflammatory Response in Porcine Renal and Iliac Artery Stents.* Journal of Vascular and Interventional Radiology, 2008. **19**(3): p. 427-437.

95. Schüssler, A., M. Grunze, and R. Denk, *Device based on nitinol, a process for its production, and its use*. 2012, Google Patents.

96. Veith, M., et al., *Structural Aspects of Chlorine‐Aluminium Alkoxides.* Zeitschrift für anorganische und allgemeine Chemie, 2011. **637**(7‐8): p. 923-929.

97. König, R., et al., *New crystalline aluminum alkoxide oxide fluorides: Evidence of the mechanism of the fluorolytic sol–gel reaction.* Dalton Transactions, 2011. **40**(34): p. 8701-8710.

98. Carmalt, C.J., et al., *Pentanuclear alkoxyaluminium hydrides.* New journal of chemistry, 2002. **26**(7): p. 902-905.

99. Ali, A.A., et al., *Cyclopentanolates of Aluminum Hydride/Aluminum Chloride forming Aluminum-Oxygen-Hetero-Cages and Mixed Coordination Oligomers.* Zeitschrift für anorganische und allgemeine Chemie, 2016. **642**(18): p. 973-978.

100. Jones, C., G.A. Koutsantonis, and C.L. Raston, *Lewis base adducts of alane and gallane.* Polyhedron, 1993. **12**(15): p. 1829-1848.

101. Raston, C.L., *Recent developments in the chemistry of alane (AlH 3) and gallane (GaH 3).* Journal of organometallic chemistry, 1994. **475**(1): p. 15-24.

102. Folting, K., et al., *Characterization of aluminium isopropoxide and aluminosiloxanes.* Polyhedron, 1991. **10**(14): p. 1639-1646.

103. Lichtenberger, R. and U. Schubert, *Chemical modification of aluminium alkoxides for sol–gel processing.* Journal of Materials Chemistry, 2010. **20**(42): p. 9287-9296.

104. Veith, M., et al., *The transformation of core/shell aluminium/alumina nanoparticles into nanowires.* European Journal of Inorganic Chemistry, 2008. **2008**(33): p. 5181-5184.

105. Muilenberg, G. and C. Wagner, *Handbook of X-ray photoelectron spectroscopy: a reference book of standard data for use in x-ray photoelectron spectroscopy*. 1979: Physical Electronics Division, Perkin-Elmer Corporation.

106. John, A., et al., *IR and Raman spectra of two layered aluminium phosphates Co (en) 3 Al 3 P 4 O 16· 3H 2 O and [NH 4] 3 [Co (NH 3) 6] 3 [Al 2 (PO 4) 4] 2· 2H 2 O.* Spectrochimica Acta Part A: Molecular and Biomolecular Spectroscopy, 2000. **56**(14): p. 2715-2723.

107. Guglielmi, M., et al., *Hybrid materials based on metal oxides and poly(organophosphazenes).* Journal of Inorganic and Organometallic Polymers, 1996. **6**(3): p. 221-236.

108. Aktas, O.C., *Functional applications of Al· Al2O3 nanowires: laser assisted α-Al2O3 synthesis and fabrication of micro-/nanostructured surfaces for cell compatibility studies.* 2009.
109. Barthlott, W., M. Mail, and C. Neinhuis, *Superhydrophobic hierarchically structured surfaces in biology: evolution, structural principles and biomimetic applications.* Phil. Trans. R. Soc. A, 2016. **374**(2073): p. 20160191.

6. Appendix

1: List of figures:

2. List of tables:

3. List of abbreviations

1D	one dimensional
2D	Three Dimensional
^{t}Bu	tertiary butyl
^{c}Pen	Cyclo pentyl
°C	degree centrigrade
CVD	chemical Vapour Deposition
EDX	energy Dispersive X-ray Analysis
Eq	equation
et. al.	and others (latin: et alii or et alteri)
FT-IR	fourier transform infra red
HAlO	oxoaluminiumhydride
IR	infra red
MOCVD	metal-organic chemical vapor deposition
NMR	nuclear Magnetic Resonance
NWs	nano-wires
ppm	ppm parts per millions
PTFEP	poly [bis (2, 2, 2-trifluoroethoxy) phosphazene]
Pr	iso-propyl
SEM	scanning Electron Microscopy
SSP	single source precursors
XPS	X-ray Photoelectron Spectroscopy
XRP	X-Ray Diffractometry

4. Crystallography Data:

Compound 1

Table 1: Atomic coordinates (x 10^4) and equivalent isotropic displacement parameters ($Å^2$x 10^3) for sh3420. U(eq) is defined as one third of the trace of the orthogonalized U^{ij} tensor.

	x	y	z	U(eq)
Al(1)	4723(1)	174(1)	6060(1)	23(1)
Al(3)	3959(1)	2444(1)	4171(1)	28(1)
Al(2)	4149(1)	386(1)	8359(1)	33(1)
Al(4)	1384(1)	3031(1)	4066(1)	60(1)
O(1)	5459(1)	777(1)	7067(1)	27(1)
O(2)	3363(1)	-121(1)	7361(1)	28(1)
O(4)	2850(1)	2642(1)	3153(1)	37(1)
O(3)	2422(1)	2927(1)	5040(1)	39(1)
C(1)	6792(2)	1235(2)	6801(2)	37(1)
C(2)	6911(3)	2559(2)	6130(2)	58(1)
C(3)	6467(4)	3278(3)	7052(3)	79(1)
C(4)	6896(3)	2560(2)	8104(2)	59(1)
C(5)	7214(2)	1280(2)	7904(2)	44(1)
C(6)	2072(2)	-560(2)	7398(2)	37(1)
C(7)	2026(2)	-1941(2)	7607(2)	49(1)
C(8)	1890(3)	-2380(2)	8901(2)	60(1)
C(9)	1177(3)	-1364(3)	9437(2)	60(1)
C(10)	1092(2)	-300(2)	8437(2)	47(1)
Cl(2)	3319(3)	1825(3)	8933(3)	54(1)
C(12)	2219(2)	3142(2)	6186(2)	38(1)
C(13)	807(3)	3159(3)	6798(2)	59(1)
C(14)	874(3)	3767(3)	7778(2)	69(1)
C(15)	1982(4)	4662(3)	7312(3)	90(1)
C(16)	2764(4)	4363(3)	6191(3)	81(1)
C(17)	3181(2)	2436(2)	1991(2)	47(1)
C(18)	2002(3)	2348(3)	1528(3)	69(1)
C(19)	1739(4)	3630(4)	969(3)	88(1)
C(20)	2914(5)	4373(3)	787(4)	115(2)
C(21)	3932(3)	3523(3)	1158(2)	71(1)
Cl(1A)	-43(6)	1899(12)	4544(7)	96(2)

Cl(1B)	186(3)	1185(6)	4749(3)	78(1)
Cl(3)	5203(10)	3822(9)	3572(9)	90

Table 2: Bond lengths [Å] and angles [°] for sh3420.

Al(1)-O(2)	1.8483(13)	C(3)-C(4)	1.509(4)	C(1)-C(5)	1.526(3)
Al(1)-O(1)	1.8512(13)	C(3)-H(3A)	0.9900	C(1)-H(1A)	1.0000
Al(1)-Al(1)#1	2.6313(10)	C(3)-H(3B)	0.9900	C(2)-C(3)	1.508(4)
Al(1)-Al(2)	2.7913(8)	C(4)-C(5)	1.515(4)	C(2)-H(2A)	0.9900
Al(1)-H(1)	1.73(2)	C(4)-H(4A)	0.9900	C(15)-H(15B)	0.9900
Al(1)-H(2)	1.71(2)	C(4)-H(4B)	0.9900	C(16)-H(16A)	0.9900
Al(1)-H(3)	1.68(2)	C(5)-H(5A)	0.9900	C(16)-H(16B)	0.9900
Al(3)-O(3)	1.8638(15)	C(5)-H(5B)	0.9900	C(17)-C(21)	1.494(4)
Al(3)-O(4)	1.8779(15)	C(6)-C(7)	1.497(3)	C(17)-C(18)	1.504(4)
Al(3)-Cl(3)	1.939(7)	C(6)-C(10)	1.519(3)	C(17)-H(17)	1.0000
Al(3)-Al(4)	2.8183(9)	C(6)-H(6A)	1.0000	C(18)-C(19)	1.482(5)
Al(3)-H(7)	1.493(10)	C(7)-C(8)	1.515(4)	C(18)-H(18A)	0.9900
Al(3)-H(3)	1.72(2)	C(7)-H(7A)	0.9900	C(18)-H(18B)	0.9900
Al(2)-O(1)	1.8148(13)	C(7)-H(7B)	0.9900	C(19)-C(20)	1.458(6)
Al(2)-O(2)	1.8209(14)	C(8)-C(9)	1.529(4)	C(19)-H(19A)	0.9900
Al(2)-Cl(2)	1.994(3)	C(8)-H(8A)	0.9900	C(19)-H(19B)	0.9900
Al(2)-H(5)	1.506(9)	C(8)-H(8B)	0.9900	C(20)-C(21)	1.499(5)
Al(2)-H(4)	1.649(18)	C(9)-C(10)	1.509(4)	C(20)-H(20A)	0.9900
Al(4)-O(3)	1.7857(16)	C(9)-H(9A)	0.9900	C(20)-H(20B)	0.9900
Al(4)-O(4)	1.7936(16)	C(9)-H(9B)	0.9900	C(21)-H(21A)	0.9900
Al(4)-Cl(1A)	1.888(7)	C(10)-H(10A)	0.9900	C(21)-H(21B)	0.9900
Al(4)-Cl(1B)	2.318(5)	C(10)-H(10B)	0.9900	O(2)-Al(1)-O(1)	79.93(6)
Al(4)-H(8)	1.503(10)	C(12)-C(16)	1.492(4)	O(2)-Al(1)-Al(1)#1	138.95(5)
Al(4)-H(6)	1.52(3)	C(12)-C(13)	1.510(3)	O(1)-Al(1)-Al(1)#1	141.09(5)
O(1)-C(1)	1.454(2)	C(12)-H(12)	1.0000	O(2)-Al(1)-Al(2)	40.11(4)
O(2)-C(6)	1.454(2)	C(13)-C(14)	1.519(4)	O(1)-Al(1)-Al(2)	39.93(4)
O(4)-C(17)	1.448(3)	C(13)-H(13A)	0.9900	Al(1)#1-Al(1)-Al(2)	176.43(4)
O(3)-C(12)	1.438(2)	C(13)-H(13B)	0.9900	O(2)-Al(1)-H(1)	97.2(7)
C(1)-C(2)	1.504(3)	C(14)-C(15)	1.477(5)	O(1)-Al(1)-H(1)	94.1(7)
Al(1)#1-Al(1)-H(1)	81.5(7)	Al(1)-Al(2)-H(5)	121.6(13)	Al(4)-O(3)-Al(3)	101.09(8)
Al(2)-Al(1)-H(1)	95.1(7)	O(1)-Al(2)-H(4)	116.1(6)	O(1)-C(1)-C(2)	110.40(19)
O(2)-Al(1)-H(2)	100.3(7)	O(2)-Al(2)-H(4)	112.3(7)	O(1)-C(1)-C(5)	111.11(16)

O(1)-Al(1)-H(2)	177.6(7)	Cl(2)-Al(2)-H(4)	113.8(7)	C(2)-C(1)-C(5)	103.97(18)
Al(1)#1-Al(1)-H(2)	38.7(7)	Al(1)-Al(2)-H(4)	120.5(6)	O(1)-C(1)-H(1A)	110.4
Al(2)-Al(1)-H(2)	140.1(7)	H(5)-Al(2)-H(4)	117.6(15)	C(2)-C(1)-H(1A)	110.4
C(14)-H(14A)	0.9900	H(1)-Al(1)-H(2)	83.5(10)	O(3)-Al(4)-O(4)	81.37(7)
C(14)-H(14B)	0.9900	O(2)-Al(1)-H(3)	93.9(7)	O(3)-Al(4)-Cl(1A)	116.3(3)
C(15)-C(16)	1.527(4)	O(1)-Al(1)-H(3)	96.1(7)	O(4)-Al(4)-Cl(1A)	118.6(3)
C(15)-H(15A)	0.9900	Al(1)#1-Al(1)-H(3)	84.6(7)	O(3)-Al(4)-Cl(1B)	103.28(12)
Al(2)-Al(1)-H(3)	98.8(7)	O(4)-Al(4)-Cl(1B)	104.00(14)	C(1)-C(2)-H(2B)	111.0
H(1)-Al(1)-H(3)	166.1(10)	O(3)-Al(4)-Al(3)	40.46(5)	C(3)-C(2)-H(2B)	111.0
H(2)-Al(1)-H(3)	86.3(10)	O(4)-Al(4)-Al(3)	40.97(5)	H(2A)-C(2)-H(2B)	109.0
O(3)-Al(3)-O(4)	77.16(7)	Cl(1A)-Al(4)-Al(3)	125.7(4)	C(2)-C(3)-C(4)	105.8(2)
O(3)-Al(3)-Cl(3)	110.4(4)	Cl(1B)-Al(4)-Al(3)	106.36(14)	C(2)-C(3)-H(3A)	110.6
O(4)-Al(3)-Cl(3)	106.0(3)	O(3)-Al(4)-H(8)	125(3)	C(4)-C(3)-H(3A)	110.6
O(3)-Al(3)-Al(4)	38.45(5)	O(4)-Al(4)-H(8)	123(5)	C(2)-C(3)-H(3B)	110.6
O(4)-Al(3)-Al(4)	38.77(5)	Al(3)-Al(4)-H(8)	136.3(18)	C(4)-C(3)-H(3B)	110.6
Cl(3)-Al(3)-Al(4)	115.2(3)	O(3)-Al(4)-H(6)	119.9(12)	H(3A)-C(3)-H(3B)	108.7
O(3)-Al(3)-H(7)	110.9(17)	O(4)-Al(4)-H(6)	119.2(12)	C(3)-C(4)-C(5)	106.5(2)
O(4)-Al(3)-H(7)	113.7(9)	Cl(1A)-Al(4)-H(6)	102.0(13)	C(3)-C(4)-H(4A)	110.4
Al(4)-Al(3)-H(7)	120.6(14)	Cl(1B)-Al(4)-H(6)	121.3(12)	C(5)-C(4)-H(4A)	110.4
O(3)-Al(3)-H(3)	86.0(7)	Al(3)-Al(4)-H(6)	132.3(12)	C(3)-C(4)-H(4B)	110.4
O(4)-Al(3)-H(3)	141.3(7)	H(8)-Al(4)-H(6)	91(2)	C(5)-C(4)-H(4B)	110.4
Cl(3)-Al(3)-H(3)	112.5(8)	C(1)-O(1)-Al(2)	135.63(12)	H(4A)-C(4)-H(4B)	108.6
Al(4)-Al(3)-H(3)	115.9(7)	C(1)-O(1)-Al(1)	124.60(11)	C(4)-C(5)-C(1)	105.80(19)
H(7)-Al(3)-H(3)	104.9(12)	Al(2)-O(1)-Al(1)	99.17(6)	C(4)-C(5)-H(5A)	110.6
O(1)-Al(2)-O(2)	81.63(6)	C(6)-O(2)-Al(2)	136.14(12)	C(1)-C(5)-H(5A)	110.6
O(1)-Al(2)-Cl(2)	115.19(12)	C(6)-O(2)-Al(1)	124.68(11)	C(4)-C(5)-H(5B)	110.6
O(2)-Al(2)-Cl(2)	113.87(10)	Al(2)-O(2)-Al(1)	99.06(6)	C(1)-C(5)-H(5B)	110.6
O(1)-Al(2)-Al(1)	40.90(4)	C(17)-O(4)-Al(4)	133.88(14)	H(5A)-C(5)-H(5B)	108.7
O(2)-Al(2)-Al(1)	40.84(4)	C(17)-O(4)-Al(3)	125.76(13)	O(2)-C(6)-C(7)	110.32(17)
Cl(2)-Al(2)-Al(1)	125.56(10)	Al(4)-O(4)-Al(3)	100.26(7)	O(2)-C(6)-C(10)	110.79(17)
O(1)-Al(2)-H(5)	114.3(17)	C(12)-O(3)-Al(4)	132.49(13)	C(7)-C(6)-C(10)	103.65(18)
O(2)-Al(2)-H(5)	109.2(12)	C(12)-O(3)-Al(3)	126.43(13)	O(2)-C(6)-H(6A)	110.6
C(7)-C(6)-H(6A)	110.6	C(12)-C(13)-H(13B)	111.3	C(18)-C(19)-H(19A)	110.3
C(10)-C(6)-H(6A)	110.6	C(14)-C(13)-H(13B)	111.3	C(20)-C(19)-H(19B)	110.3
C(6)-C(7)-C(8)	104.1(2)	H(13A)-C(13)-H(13B)	109.2	C(18)-C(19)-H(19B)	110.3
C(6)-C(7)-H(7A)	110.9	C(15)-C(14)-C(13)	105.7(2)	H(19A)-C(19)-H(19B)	108.6
C(8)-C(7)-H(7A)	110.9	C(15)-C(14)-H(14A)	110.6	C(19)-C(20)-C(21)	107.9(3)

C(6)-C(7)-H(7B)	110.9	C(13)-C(14)-H(14A)	110.6	C(19)-C(20)-H(20A)	110.1
C(5)-C(1)-H(1A)	110.4	C(8)-C(7)-H(7B)	110.9	C(15)-C(14)-H(14B)	110.6
C(1)-C(2)-C(3)	103.6(2)	H(7A)-C(7)-H(7B)	109.0	C(13)-C(14)-H(14B)	110.6
C(1)-C(2)-H(2A)	111.0	C(7)-C(8)-C(9)	105.8(2)	H(14A)-C(14)-H(14B)	108.7
C(3)-C(2)-H(2A)	111.0	C(7)-C(8)-H(8A)	110.6	C(14)-C(15)-C(16)	107.4(2)
C(9)-C(8)-H(8A)	110.6	C(14)-C(15)-H(15A)	110.2	C(17)-C(21)-C(20)	104.3(3)
C(7)-C(8)-H(8B)	110.6	C(16)-C(15)-H(15A)	110.2	C(17)-C(21)-H(21A)	110.9
C(9)-C(8)-H(8B)	110.6	C(14)-C(15)-H(15B)	110.2	C(20)-C(21)-H(21A)	110.9
H(8A)-C(8)-H(8B)	108.7	C(16)-C(15)-H(15B)	110.2	C(21)-C(20)-H(20A)	110.1
C(10)-C(9)-C(8)	106.2(2)	H(15A)-C(15)-H(15B)	108.5	C(19)-C(20)-H(20B)	110.1
C(10)-C(9)-H(9A)	110.5	C(12)-C(16)-C(15)	104.4(2)	C(21)-C(20)-H(20B)	110.1
C(8)-C(9)-H(9A)	110.5	C(12)-C(16)-H(16A)	110.9	H(20A)-C(20)-H(20B)	108.4
C(10)-C(9)-H(9B)	110.5	C(15)-C(16)-H(16A)	110.9	C(17)-C(21)-H(21B)	110.9
C(8)-C(9)-H(9B)	110.5	C(12)-C(16)-H(16B)	110.9	C(20)-C(21)-H(21B)	110.9
H(9A)-C(9)-H(9B)	108.7	C(15)-C(16)-H(16B)	110.9	H(21A)-C(21)-H(21B)	108.9
C(9)-C(10)-C(6)	105.40(19)	H(16A)-C(16)-H(16B)	108.9		
C(9)-C(10)-H(10A)	110.7	O(4)-C(17)-C(21)	110.6(2)		
C(6)-C(10)-H(10A)	110.7	O(4)-C(17)-C(18)	112.2(2)		
C(9)-C(10)-H(10B)	110.7	C(21)-C(17)-C(18)	103.5(2)		
C(6)-C(10)-H(10B)	110.7	O(4)-C(17)-H(17)	110.1		
H(10A)-C(10)-H(10B)	108.8	C(21)-C(17)-H(17)	110.1		
O(3)-C(12)-C(16)	112.85(19)	C(18)-C(17)-H(17)	110.1		
O(3)-C(12)-C(13)	113.9(2)	C(19)-C(18)-C(17)	106.1(3)		
C(16)-C(12)-C(13)	104.3(2)	C(19)-C(18)-H(18A)	110.5		
O(3)-C(12)-H(12)	108.5	C(17)-C(18)-H(18A)	110.5		
C(16)-C(12)-H(12)	108.5	C(19)-C(18)-H(18B)	110.5		
C(13)-C(12)-H(12)	108.5	C(17)-C(18)-H(18B)	110.5		
C(12)-C(13)-C(14)	102.2(2)	H(18A)-C(18)-H(18B)	108.7		
C(12)-C(13)-H(13A)	111.3	C(20)-C(19)-C(18)	107.0(3)		
C(14)-C(13)-H(13A)	111.3	C(20)-C(19)-H(19A)	110.3		

Symmetry transformations used to generate equivalent atoms: #1 -x+1,-y,-z+1

Table 3: Anisotropic displacement parameters ($Å^2 x\ 10^3$) for sh3420. The anisotropic displacement factor exponent takes the form: $-2p^2[\ h^2\ a^{*2}U^{11} + ... + 2\ h\ k\ a^*\ b^*\ U^{12}\ ]$

	U^{11}	U^{22}	U^{33}	U^{23}	U^{13}	U^{12}
Al(1)	25(1)	26(1)	18(1)	-7(1)	-5(1)	5(1)
Al(3)	30(1)	27(1)	26(1)	-6(1)	-7(1)	6(1)
Al(2)	35(1)	44(1)	20(1)	-11(1)	-3(1)	-1(1)
Al(4)	38(1)	101(1)	51(1)	-28(1)	-19(1)	29(1)
O(1)	29(1)	32(1)	22(1)	-8(1)	-5(1)	-1(1)
O(2)	25(1)	36(1)	22(1)	-9(1)	-2(1)	0(1)
O(4)	37(1)	45(1)	33(1)	-12(1)	-14(1)	13(1)
O(3)	38(1)	48(1)	33(1)	-12(1)	-9(1)	18(1)
C(1)	31(1)	49(1)	32(1)	-11(1)	-5(1)	-8(1)
C(2)	72(2)	58(2)	40(1)	6(1)	-21(1)	-29(1)
C(3)	127(3)	38(1)	81(2)	-8(1)	-46(2)	-2(2)
C(4)	82(2)	54(2)	49(2)	-18(1)	-24(1)	-6(1)
C(5)	45(1)	48(1)	41(1)	-7(1)	-20(1)	-8(1)
C(6)	28(1)	50(1)	31(1)	-7(1)	-6(1)	-1(1)
C(7)	36(1)	51(1)	61(2)	-26(1)	-1(1)	-4(1)
C(8)	59(2)	44(1)	67(2)	6(1)	-13(1)	-1(1)
C(9)	59(2)	76(2)	36(1)	-9(1)	6(1)	-6(1)
C(10)	31(1)	47(1)	58(2)	-15(1)	3(1)	4(1)
Cl(2)	58(2)	70(2)	47(2)	-40(1)	-15(1)	24(1)
C(12)	43(1)	38(1)	29(1)	-7(1)	-4(1)	14(1)
C(13)	50(2)	66(2)	55(2)	-19(1)	3(1)	15(1)
C(14)	77(2)	72(2)	50(2)	-22(1)	4(1)	28(2)
C(15)	143(3)	63(2)	61(2)	-35(2)	4(2)	-11(2)
C(16)	113(3)	72(2)	48(2)	-23(1)	13(2)	-34(2)
C(17)	58(1)	54(1)	36(1)	-18(1)	-21(1)	22(1)
C(18)	77(2)	87(2)	55(2)	-22(2)	-31(2)	-11(2)
C(19)	96(3)	114(3)	77(2)	-39(2)	-55(2)	51(2)
C(20)	179(5)	55(2)	115(3)	8(2)	-68(3)	4(2)
C(21)	60(2)	110(3)	40(1)	-16(2)	-7(1)	-16(2)
Cl(1A)	54(2)	125(6)	105(4)	-24(4)	-12(2)	-24(3)
Cl(1B)	48(1)	101(3)	79(2)	-10(2)	-8(1)	-21(2)

Compund 2

Table 1: Atomic coordinates (x 10^4) and equivalent isotropic displacement parameters ($Å^2$x 10^3) for sh3462. U (eq) is defined as one third of the trace of the orthogonalized U^{ij} tensor.

	x	y	z	U(eq)
Al(1)	0	2704(1)	7500	22(1)
Al(2)	1324(1)	1925(1)	8306(1)	33(1)
Al(3)	0	4258(1)	7500	35(1)
O(1)	510(1)	3513(1)	6805(2)	27(1)
O(2)	639(1)	2558(1)	8918(2)	26(1)
O(3)	743(1)	2031(1)	6930(2)	27(1)
C(1)	1182(2)	3585(2)	6076(3)	36(1)
C(2)	1884(2)	3777(3)	6823(4)	64(1)
C(3)	2298(2)	4338(2)	6100(4)	54(1)
C(4)	1911(2)	4389(2)	4834(3)	45(1)
C(5)	1109(2)	4177(2)	5095(3)	41(1)
C(6)	644(1)	2884(2)	10122(3)	28(1)
C(7)	880(2)	2379(2)	11173(3)	42(1)
C(8)	1096(2)	2868(2)	12250(3)	51(1)
C(9)	1226(2)	3619(2)	11680(3)	48(1)
C(10)	1190(2)	3511(2)	10268(3)	40(1)
C(11)	823(2)	1672(2)	5756(3)	35(1)
C(12)	534(3)	908(2)	5724(7)	78(2)
C(13)	882(3)	587(3)	4560(8)	90(2)
C(14)	1590(2)	1033(2)	4276(5)	57(1)
C(15)	1632(2)	1586(2)	5319(4)	43(1)

Table 2: Bond lengths [Å] and angles [°] for sh3462.

Al(1)-O(1)#1	1.9066(19)	C(3)-H(3B)	0.9900	C(13)-H(23)	0.92(7)
Al(1)-O(1)	1.9066(19)	C(4)-C(5)	1.504(4)	C(13)-H(24)	0.98(5)

Al(1)-O(3)#1	1.9170(18)	C(4)-H(4A)	0.9900	C(14)-C(15)	1.522(5)
Al(1)-O(3)	1.9170(18)	C(4)-H(4B)	0.9900	C(14)-H(25)	0.92(5)
Al(1)-O(2)#1	1.9185(17)	C(5)-H(5A)	0.9900	C(14)-H(26)	0.98(7)
Al(1)-O(2)	1.9186(17)	C(5)-H(5B)	0.9900	C(15)-H(27)	0.93(4)
Al(1)-Al(3)	2.8850(15)	C(6)-C(10)	1.523(4)	C(15)-H(28)	0.98(4)
Al(1)-Al(2)#1	2.8926(9)	C(6)-C(7)	1.526(4)	O(1)#1-Al(1)-O(1)	76.00(12)
Al(1)-Al(2)	2.8926(9)	C(6)-H(11)	0.96(3)	O(1)#1-Al(1)-O(3)#1	93.50(8)
Al(2)-O(3)	1.813(2)	C(7)-C(8)	1.519(6)	O(1)-Al(1)-O(3)#1	164.86(8)
Al(2)-O(2)	1.815(2)	C(7)-H(12)	0.86(4)	O(1)#1-Al(1)-O(3)	164.86(8)
Al(2)-H(2)	1.54(4)	C(7)-H(13)	0.90(4)	O(1)-Al(1)-O(3)	93.50(8)
Al(2)-H(3)	1.71(3)	C(8)-C(9)	1.540(5)	O(3)#1-Al(1)-O(3)	98.73(11)
Al(3)-O(1)	1.814(2)	C(8)-H(14)	0.96(5)	O(1)#1-Al(1)-O(2)#1	98.12(8)
Al(3)-O(1)#1	1.814(2)	C(8)-H(15)	0.85(5)	O(1)-Al(1)-O(2)#1	94.64(8)
Al(3)-H(1)	1.55(4)	C(9)-C(10)	1.532(5)	O(3)#1-Al(1)-O(2)#1	75.81(8)
O(1)-C(1)	1.433(4)	C(9)-H(16)	0.94(5)	O(3)-Al(1)-O(2)#1	93.53(8)
O(2)-C(6)	1.428(3)	C(9)-H(17)	0.99(4)	O(1)#1-Al(1)-O(2)	94.64(8)
O(3)-C(11)	1.433(4)	C(10)-H(18)	0.90(4)	O(1)-Al(1)-O(2)	98.12(8)
C(1)-C(2)	1.525(4)	C(10)-H(19)	0.95(4)	O(3)#1-Al(1)-O(2)	93.53(8)
C(1)-C(5)	1.529(4)	C(11)-C(12)	1.508(5)	O(3)-Al(1)-O(2)	75.81(8)
C(1)-H(4)	0.92(4)	C(11)-C(15)	1.520(4)	O(2)#1-Al(1)-O(2)	163.79(12)
C(2)-C(3)	1.493(5)	C(11)-H(20)	0.97(4)	O(1)#1-Al(1)-Al(3)	38.00(6)
C(2)-H(2A)	0.9900	C(12)-C(13)	1.516(7)	O(1)-Al(1)-Al(3)	38.00(6)
C(2)-H(2B)	0.9900	C(12)-H(21)	0.82(7)	O(3)#1-Al(1)-Al(3)	130.63(6)
C(3)-C(4)	1.527(5)	C(12)-H(22)	0.99(4)	O(3)-Al(1)-Al(3)	130.63(6)
C(3)-H(3A)	0.9900	C(13)-C(14)	1.536(6)	O(2)#1-Al(1)-Al(3)	98.10(6)
O(1)#1-Al(1)-Al(2)	131.52(6)	C(2)-C(1)-C(5)	105.3(2)	C(8)-C(7)-H(12)	119(3)
O(1)-Al(1)-Al(2)	97.19(6)	O(1)-C(1)-H(4)	110(2)	C(6)-C(7)-H(12)	105(3)
O(3)#1-Al(1)-Al(2)	97.95(6)	C(2)-C(1)-H(4)	106(2)	C(8)-C(7)-H(13)	113(2)
O(3)-Al(1)-Al(2)	37.87(6)	C(5)-C(1)-H(4)	108(2)	C(6)-C(7)-H(13)	115(2)
O(2)#1-Al(1)-Al(2)	130.37(6)	C(3)-C(2)-C(1)	107.1(3)	H(12)-C(7)-H(13)	100(3)
O(2)-Al(1)-Al(2)	37.94(6)	C(3)-C(2)-H(2A)	110.3	C(7)-C(8)-C(9)	106.0(3)
Al(3)-Al(1)-Al(2)	120.00(2)	C(1)-C(2)-H(2A)	110.3	C(7)-C(8)-H(14)	112(3)
Al(2)#1-Al(1)-Al(2)	120.00(5)	C(3)-C(2)-H(2B)	110.3	C(9)-C(8)-H(14)	114(3)
O(3)-Al(2)-O(2)	81.00(8)	C(1)-C(2)-H(2B)	110.3	C(7)-C(8)-H(15)	109(3)
O(3)-Al(2)-Al(1)	40.47(6)	H(2A)-C(2)-H(2B)	108.6	C(9)-C(8)-H(15)	112(3)
O(2)-Al(2)-Al(1)	40.53(6)	C(2)-C(3)-C(4)	106.5(3)	H(14)-C(8)-H(15)	104(4)
O(3)-Al(2)-H(2)	114.3(14)	C(2)-C(3)-H(3A)	110.4	C(10)-C(9)-C(8)	105.6(3)
O(2)-Al(2)-H(2)	119.4(14)	C(4)-C(3)-H(3A)	110.4	C(10)-C(9)-H(16)	112(3)
Al(1)-Al(2)-H(2)	126.6(13)	C(2)-C(3)-H(3B)	110.4	C(8)-C(9)-H(16)	111(3)

O(3)-Al(2)-H(3)	115.6(9)	C(4)-C(3)-H(3B)	110.4	C(10)-C(9)-H(17)	108(3)
O(2)-Al(2)-H(3)	112.5(9)	H(3A)-C(3)-H(3B)	108.6	C(8)-C(9)-H(17)	109(3)
Al(1)-Al(2)-H(3)	122.2(9)	C(5)-C(4)-C(3)	104.2(3)	H(16)-C(9)-H(17)	110(4)
H(2)-Al(2)-H(3)	111.2(16)	C(5)-C(4)-H(4A)	110.9	C(6)-C(10)-C(9)	103.2(3)
O(1)-Al(3)-O(1)#1	80.66(12)	C(3)-C(4)-H(4A)	110.9	C(6)-C(10)-H(18)	106(2)
O(1)-Al(3)-Al(1)	40.33(6)	C(5)-C(4)-H(4B)	110.9	C(9)-C(10)-H(18)	113(2)
O(1)#1-Al(3)-Al(1)	40.33(6)	C(3)-C(4)-H(4B)	110.9	C(6)-C(10)-H(19)	112(2)
O(1)-Al(3)-H(1)	114.8(14)	H(4A)-C(4)-H(4B)	108.9	C(9)-C(10)-H(19)	114(2)
O(1)#1-Al(3)-H(1)	117.5(14)	C(4)-C(5)-C(1)	103.7(2)	H(18)-C(10)-H(19)	108(3)
Al(1)-Al(3)-H(1)	125.3(14)	C(4)-C(5)-H(5A)	111.0	O(3)-C(11)-C(12)	115.1(3)
C(1)-O(1)-Al(3)	124.75(16)	C(1)-C(5)-H(5A)	111.0	O(3)-C(11)-C(15)	114.5(2)
C(1)-O(1)-Al(1)	133.02(17)	C(4)-C(5)-H(5B)	111.0	C(12)-C(11)-C(15)	102.6(3)
Al(3)-O(1)-Al(1)	101.67(9)	C(1)-C(5)-H(5B)	111.0	O(3)-C(11)-H(20)	109(2)
C(6)-O(2)-Al(2)	126.80(15)	H(5A)-C(5)-H(5B)	109.0	C(12)-C(11)-H(20)	109(2)
C(6)-O(2)-Al(1)	131.51(15)	O(2)-C(6)-C(10)	114.8(2)	C(15)-C(11)-H(20)	106(2)
Al(2)-O(2)-Al(1)	101.53(10)	O(2)-C(6)-C(7)	114.3(2)	C(11)-C(12)-C(13)	104.4(4)
C(11)-O(3)-Al(2)	127.53(16)	C(10)-C(6)-C(7)	102.5(2)	C(11)-C(12)-H(21)	115(4)
C(11)-O(3)-Al(1)	130.76(16)	O(2)-C(6)-H(11)	106.6(19)	C(13)-C(12)-H(21)	119(4)
Al(2)-O(3)-Al(1)	101.66(10)	C(10)-C(6)-H(11)	108.5(19)	C(11)-C(12)-H(22)	103(2)
O(1)-C(1)-C(2)	114.6(3)	C(7)-C(6)-H(11)	109.9(19)	C(13)-C(12)-H(22)	107(2)
O(1)-C(1)-C(5)	111.9(2)	C(8)-C(7)-C(6)	105.4(3)	H(21)-C(12)-H(22)	107(5)
C(12)-C(13)-C(14)	106.6(4)	C(15)-C(14)-C(13)	104.9(3)	C(11)-C(15)-C(14)	104.5(3)
C(12)-C(13)-H(23)	107(4)	C(15)-C(14)-H(25)	112(3)	C(11)-C(15)-H(27)	115(3)
C(14)-C(13)-H(23)	120(4)	C(13)-C(14)-H(25)	109(3)	C(14)-C(15)-H(27)	111(3)
C(12)-C(13)-H(24)	115(3)	C(15)-C(14)-H(26)	109(4)	C(11)-C(15)-H(28)	105(3)
C(14)-C(13)-H(24)	108(3)	C(13)-C(14)-H(26)	110(4)	C(14)-C(15)-H(28)	110(2)
H(23)-C(13)-H(24)	100(5)	H(25)-C(14)-H(26)	112(5)		

Symmetry transformations used to generate equivalent atoms: #1 -x+1,-y,-z+1

Table 3: Anisotropic displacement parameters ($Å^2 x\ 10^3$) for sh3462. The anisotropic displacement factor exponent takes the form: $-2p^2[\ h^2\ a^{*2}U^{11} + ... + 2\ h\ k\ a^*\ b^*\ U^{12}\ ]$

	U^{11}	U^{22}	U^{33}	U^{23}	U^{13}	U^{12}
Al(1)	17(1)	18(1)	32(1)	0	-7(1)	0
Al(2)	19(1)	34(1)	48(1)	14(1)	-2(1)	6(1)

Al(3)	53(1)	18(1)	34(1)	0	-15(1)	0
O(1)	29(1)	21(1)	31(1)	6(1)	-9(1)	-4(1)
O(2)	18(1)	28(1)	32(1)	7(1)	-5(1)	1(1)
O(3)	18(1)	23(1)	40(1)	2(1)	-1(1)	1(1)
C(1)	33(1)	31(1)	42(2)	13(1)	-5(1)	-7(1)
C(2)	38(2)	96(3)	58(2)	41(2)	-22(2)	-28(2)
C(3)	44(2)	65(2)	52(2)	12(2)	-10(2)	-26(2)
C(4)	41(2)	48(2)	45(2)	17(2)	2(1)	-5(1)
C(5)	44(2)	43(2)	35(2)	15(1)	-12(1)	-10(1)
C(6)	19(1)	36(1)	29(1)	10(1)	-5(1)	-1(1)
C(7)	38(2)	49(2)	40(2)	21(2)	-4(1)	4(1)
C(8)	35(2)	84(3)	36(2)	22(2)	-14(1)	-12(2)
C(9)	48(2)	66(2)	28(2)	1(2)	-10(1)	-7(2)
C(10)	42(2)	50(2)	29(1)	5(1)	-7(1)	-15(1)
C(11)	22(1)	30(1)	54(2)	-9(1)	0(1)	6(1)
C(12)	53(2)	45(2)	136(5)	-43(3)	47(3)	-22(2)
C(13)	58(3)	66(3)	146(6)	-62(3)	37(3)	-13(2)
C(14)	43(2)	45(2)	82(3)	-13(2)	18(2)	12(2)
C(15)	31(1)	42(2)	55(2)	1(2)	12(1)	-1(1)

Compund 3

Table 1: Atomic coordinates (x 10^4) and equivalent isotropic displacement parameters ($Å^2$x 10^3) for sh3427. U(eq) is defined as one third of the trace of the orthogonalized U^{ij} tensor.

	x	y	z	U(eq)
Al(1)	0	2480(1)	2500	10(1)
Al(2)	1066(1)	1634(1)	1301(1)	14(1)
Al(3)	0	4134(1)	2500	14(1)
Cl(1)	1282(1)	1968(1)	22(1)	24(1)
Cl(2)	1713(1)	562(1)	1554(1)	24(1)
Cl(3)	1175(1)	4839(1)	2312(1)	26(1)
O(1)	-111(1)	1715(1)	1618(1)	13(1)
O(2)	1250(1)	2354(1)	2099(1)	13(1)
O(3)	-224(1)	3356(1)	1778(1)	12(1)

C(1)	-903(1)	1239(1)	1382(1)	16(1)
C(2)	-1334(1)	1442(1)	532(1)	23(1)
C(3)	-2003(1)	755(1)	389(1)	31(1)
C(4)	-1626(1)	78(1)	934(1)	29(1)
C(5)	-705(1)	374(1)	1300(1)	23(1)
C(6)	2091(1)	2769(1)	2338(1)	18(1)
C(7)	2823(1)	2260(1)	2758(1)	30(1)
C(8)	3733(1)	2689(2)	2600(2)	51(1)
C(9)	3547(1)	3312(1)	1963(2)	42(1)
C(10)	2592(1)	3139(1)	1594(1)	27(1)
C(11)	-368(1)	3380(1)	864(1)	14(1)
C(12)	-1276(1)	3751(1)	594(1)	22(1)
C(13)	-1134(1)	3904(1)	-357(1)	29(1)
C(14)	-80(1)	3866(1)	-512(1)	25(1)
C(15)	352(1)	3844(1)	377(1)	19(1)

Table 2: Bond lengths [Å] and angles [°] for sh3427.

Al(1)-O(3)#1	1.9118(10)	C(5)-H(9)	0.96(2)	O(3)-Al(1)-O(1)	95.42(4)
Al(1)-O(3)	1.9118(10)	C(6)-C(10)	1.516(2)	O(1)#1-Al(1)-O(1)	93.55(6)
Al(1)-O(1)#1	1.9175(10)	C(6)-C(7)	1.523(2)	O(3)#1-Al(1)-O(2)#1	93.00(4)
Al(1)-O(1)	1.9175(10)	C(6)-H(10)	0.976(17)	O(3)-Al(1)-O(2)#1	97.13(4)
Al(1)-O(2)#1	1.9272(9)	C(7)-C(8)	1.529(2)	O(1)#1-Al(1)-O(2)#1	76.39(4)
Al(1)-O(2)	1.9272(9)	C(7)-H(11)	0.96(2)	O(1)-Al(1)-O(2)#1	94.68(4)
Al(1)-Al(2)	2.8367(5)	C(7)-H(12)	0.95(2)	O(3)#1-Al(1)-O(2)	97.13(4)
Al(1)-Al(2)#1	2.8367(5)	C(8)-C(9)	1.490(3)	O(3)-Al(1)-O(2)	93.00(4)
Al(1)-Al(3)	2.8384(8)	C(8)-H(13)	0.9900	O(1)#1-Al(1)-O(2)	94.68(4)
Al(2)-O(1)	1.7791(10)	C(8)-H(14)	0.9900	O(1)-Al(1)-O(2)	76.39(4)
Al(2)-O(2)	1.7825(11)	C(9)-C(10)	1.527(2)	O(2)#1-Al(1)-O(2)	167.12(6)
Al(2)-Cl(2)	2.1031(6)	C(9)-H(15)	0.90(3)	O(3)#1-Al(1)-Al(2)	134.92(3)
Al(2)-Cl(1)	2.1148(6)	C(9)-H(16)	1.06(3)	O(3)-Al(1)-Al(2)	95.72(3)
Al(3)-O(3)#1	1.7823(10)	C(10)-H(17)	0.95(2)	O(1)#1-Al(1)-Al(2)	94.88(3)
Al(3)-O(3)	1.7823(10)	C(10)-H(18)	0.99(2)	O(1)-Al(1)-Al(2)	38.12(3)
Al(3)-Cl(3)	2.1072(5)	C(11)-C(15)	1.519(2)	O(2)#1-Al(1)-Al(2)	132.07(4)
Al(3)-Cl(3)#1	2.1073(5)	C(11)-C(12)	1.521(2)	O(2)-Al(1)-Al(2)	38.28(3)
O(1)-C(1)	1.4551(17)	C(11)-H(19)	0.985(15)	O(3)#1-Al(1)-Al(2)#1	95.72(3)

O(2)-C(6)	1.4590(17)	C(12)-C(13)	1.533(2)	O(3)-Al(1)-Al(2)#1	134.92(3)
O(3)-C(11)	1.4536(17)	C(12)-H(20)	0.949(18)	O(1)#1-Al(1)-Al(2)#1	38.12(3)
C(1)-C(2)	1.516(2)	C(12)-H(21)	0.95(2)	O(1)-Al(1)-Al(2)#1	94.88(3)
C(1)-C(5)	1.518(2)	C(13)-C(14)	1.547(3)	O(2)#1-Al(1)-Al(2)#1	38.28(3)
C(1)-H(1)	0.987(17)	C(13)-H(22)	0.94(2)	O(2)-Al(1)-Al(2)#1	132.07(4)
C(2)-C(3)	1.542(2)	C(13)-H(23)	0.99(2)	Al(2)-Al(1)-Al(2)#1	118.36(3)
C(2)-H(2)	0.986(18)	C(14)-C(15)	1.532(2)	O(3)#1-Al(1)-Al(3)	38.15(3)
C(2)-H(3)	0.96(2)	C(14)-H(24)	0.962(19)	O(3)-Al(1)-Al(3)	38.15(3)
C(3)-C(4)	1.544(3)	C(14)-H(25)	0.970(19)	O(1)#1-Al(1)-Al(3)	133.23(3)
C(3)-H(4)	0.95(2)	C(15)-H(26)	0.965(18)	O(1)-Al(1)-Al(3)	133.23(3)
C(3)-H(5)	0.93(2)	C(15)-H(27)	0.976(18)	O(2)#1-Al(1)-Al(3)	96.44(3)
C(4)-C(5)	1.536(2)	O(3)#1-Al(1)-O(3)	76.30(6)	O(2)-Al(1)-Al(3)	96.44(3)
C(4)-H(6)	0.97(2)	O(3)#1-Al(1)-O(1)#1	95.42(4)	Al(2)-Al(1)-Al(3)	120.818(13)
C(4)-H(7)	0.96(2)	O(3)-Al(1)-O(1)#1	169.35(4)	Al(2)#1-Al(1)-Al(3)	120.817(13)
C(5)-H(8)	0.946(19)	O(3)#1-Al(1)-O(1)	169.35(4)	O(1)-Al(2)-O(2)	83.75(5)
O(1)-Al(2)-Cl(2)	116.22(4)	C(1)-C(2)-H(2)	114.2(11)	C(9)-C(8)-C(7)	107.39(15)
O(2)-Al(2)-Cl(2)	114.02(4)	C(3)-C(2)-H(2)	112.0(10)	C(9)-C(8)-H(13)	110.2
O(1)-Al(2)-Cl(1)	112.74(4)	C(1)-C(2)-H(3)	110.5(11)	C(7)-C(8)-H(13)	110.2
O(2)-Al(2)-Cl(1)	117.33(4)	C(3)-C(2)-H(3)	110.7(11)	C(9)-C(8)-H(14)	110.2
Cl(2)-Al(2)-Cl(1)	110.62(2)	H(2)-C(2)-H(3)	107.3(15)	C(7)-C(8)-H(14)	110.2
O(1)-Al(2)-Al(1)	41.71(3)	C(2)-C(3)-C(4)	105.80(14)	H(13)-C(8)-H(14)	108.5
O(2)-Al(2)-Al(1)	42.05(3)	C(2)-C(3)-H(4)	110.9(12)	C(8)-C(9)-C(10)	106.21(15)
Cl(2)-Al(2)-Al(1)	124.35(2)	C(4)-C(3)-H(4)	110.5(13)	C(8)-C(9)-H(15)	114.7(16)
Cl(1)-Al(2)-Al(1)	125.00(2)	C(2)-C(3)-H(5)	111.1(14)	C(10)-C(9)-H(15)	117.6(16)
O(3)#1-Al(3)-O(3)	82.99(6)	C(4)-C(3)-H(5)	111.8(14)	C(8)-C(9)-H(16)	103.6(17)
O(3)#1-Al(3)-Cl(3)	111.94(3)	H(4)-C(3)-H(5)	106.9(18)	C(10)-C(9)-H(16)	109.0(17)
O(3)-Al(3)-Cl(3)	119.15(3)	C(5)-C(4)-C(3)	105.44(14)	H(15)-C(9)-H(16)	105(2)
O(3)#1-Al(3)-Cl(3)#1	119.15(3)	C(5)-C(4)-H(6)	111.6(11)	C(6)-C(10)-C(9)	102.74(15)
O(3)-Al(3)-Cl(3)#1	111.95(3)	C(3)-C(4)-H(6)	111.0(12)	C(6)-C(10)-H(17)	109.3(12)
Cl(3)-Al(3)-Cl(3)#1	109.85(3)	C(5)-C(4)-H(7)	109.2(12)	C(9)-C(10)-H(17)	108.9(12)
O(3)#1-Al(3)-Al(1)	41.50(3)	C(3)-C(4)-H(7)	111.5(12)	C(6)-C(10)-H(18)	112.6(12)
O(3)-Al(3)-Al(1)	41.50(3)	H(6)-C(4)-H(7)	108.1(16)	C(9)-C(10)-H(18)	115.3(12)
Cl(3)-Al(3)-Al(1)	125.076(17)	C(1)-C(5)-C(4)	101.07(13)	H(17)-C(10)-H(18)	107.9(16)
Cl(3)#1-Al(3)-Al(1)	125.076(17)	C(1)-C(5)-H(8)	109.7(11)	O(3)-C(11)-C(15)	114.52(12)
C(1)-O(1)-Al(2)	129.58(8)	C(4)-C(5)-H(8)	111.2(11)	O(3)-C(11)-C(12)	114.32(12)
C(1)-O(1)-Al(1)	129.43(8)	C(1)-C(5)-H(9)	113.2(11)	C(15)-C(11)-C(12)	103.35(12)
Al(2)-O(1)-Al(1)	100.17(5)	C(4)-C(5)-H(9)	113.7(11)	O(3)-C(11)-H(19)	105.9(9)
C(6)-O(2)-Al(2)	130.22(9)	H(8)-C(5)-H(9)	107.9(16)	C(15)-C(11)-H(19)	108.6(9)
C(6)-O(2)-Al(1)	129.97(9)	O(2)-C(6)-C(10)	113.78(13)	C(12)-C(11)-H(19)	110.1(9)

Al(2)-O(2)-Al(1)	99.68(5)	O(2)-C(6)-C(7)	114.27(13)	C(11)-C(12)-C(13)	103.26(13)
C(11)-O(3)-Al(3)	129.46(8)	C(10)-C(6)-C(7)	104.03(13)	C(11)-C(12)-H(20)	112.9(11)
C(11)-O(3)-Al(1)	129.34(8)	O(2)-C(6)-H(10)	105.5(10)	C(13)-C(12)-H(20)	113.3(11)
Al(3)-O(3)-Al(1)	100.36(5)	C(10)-C(6)-H(10)	109.6(10)	C(11)-C(12)-H(21)	108.9(12)
O(1)-C(1)-C(2)	114.74(12)	C(7)-C(6)-H(10)	109.7(10)	C(13)-C(12)-H(21)	110.9(12)
O(1)-C(1)-C(5)	115.06(12)	C(6)-C(7)-C(8)	104.60(15)	H(20)-C(12)-H(21)	107.6(15)
C(2)-C(1)-C(5)	103.11(12)	C(6)-C(7)-H(11)	109.6(12)	C(12)-C(13)-C(14)	106.16(13)
O(1)-C(1)-H(1)	107.2(9)	C(8)-C(7)-H(11)	108.9(12)	C(12)-C(13)-H(22)	109.5(14)
C(2)-C(1)-H(1)	108.8(10)	C(6)-C(7)-H(12)	111.9(13)	C(14)-C(13)-H(22)	110.8(13)
C(5)-C(1)-H(1)	107.6(9)	C(8)-C(7)-H(12)	111.7(13)	C(12)-C(13)-H(23)	110.2(13)
C(1)-C(2)-C(3)	102.16(13)	H(11)-C(7)-H(12)	110.1(17)	C(14)-C(13)-H(23)	112.8(12)
C(14)-C(15)-H(26)	114.3(11)	C(15)-C(14)-C(13)	105.02(13)	H(24)-C(14)-H(25)	109.5(15)
C(11)-C(15)-H(27)	109.3(10)	C(15)-C(14)-H(24)	109.4(12)	C(11)-C(15)-C(14)	101.15(13)
C(14)-C(15)-H(27)	109.8(10)	C(13)-C(14)-H(24)	109.0(12)	C(11)-C(15)-H(26)	112.8(10)
H(26)-C(15)-H(27)	109.1(14)	C(15)-C(14)-H(25)	112.0(11)		
H(22)-C(13)-H(23)	107.4(17)	C(13)-C(14)-H(25)	111.8(11)		

Symmetry transformations used to generate equivalent atoms: #1 -x+1,-y,-z+1

Table 3: Anisotropic displacement parameters ($Å^2 x\ 10^3$) for sh3420. The anisotropic displacement factor exponent takes the form: $-2p^2[\ h^2\ a^{*2}U^{11} + ... + 2\ h\ k\ a^*\ b^*\ U^{12}\ ]$

	U^{11}	U^{22}	U^{33}	U^{23}	U^{13}	U^{12}
Al(1)	10(1)	11(1)	10(1)	0	1(1)	0
Al(2)	14(1)	16(1)	13(1)	-1(1)	2(1)	4(1)
Al(3)	14(1)	11(1)	16(1)	0	-2(1)	0
Cl(1)	31(1)	27(1)	15(1)	2(1)	8(1)	8(1)
Cl(2)	25(1)	21(1)	25(1)	1(1)	2(1)	11(1)
Cl(3)	26(1)	23(1)	30(1)	7(1)	-5(1)	-12(1)
O(1)	13(1)	14(1)	13(1)	-2(1)	0(1)	0(1)
O(2)	10(1)	16(1)	14(1)	0(1)	1(1)	0(1)
O(3)	13(1)	13(1)	11(1)	1(1)	-1(1)	1(1)
C(1)	14(1)	16(1)	16(1)	-3(1)	-1(1)	-3(1)
C(2)	25(1)	24(1)	19(1)	-3(1)	-6(1)	-1(1)
C(3)	34(1)	29(1)	32(1)	-9(1)	-15(1)	-2(1)

C(4)	32(1)	21(1)	33(1)	-7(1)	-8(1)	-6(1)
C(5)	25(1)	16(1)	27(1)	-4(1)	-4(1)	0(1)
C(6)	10(1)	22(1)	21(1)	-2(1)	1(1)	-3(1)
C(7)	15(1)	44(1)	30(1)	13(1)	-5(1)	-3(1)
C(8)	19(1)	87(2)	49(1)	29(1)	-10(1)	-19(1)
C(9)	21(1)	54(1)	50(1)	19(1)	-6(1)	-16(1)
C(10)	17(1)	34(1)	29(1)	12(1)	0(1)	-6(1)
C(11)	17(1)	15(1)	11(1)	0(1)	-2(1)	2(1)
C(12)	19(1)	25(1)	21(1)	2(1)	-6(1)	4(1)
C(13)	31(1)	34(1)	22(1)	9(1)	-9(1)	-4(1)
C(14)	36(1)	24(1)	16(1)	6(1)	-1(1)	1(1)
C(15)	20(1)	21(1)	17(1)	4(1)	1(1)	-1(1)

Compund 4

Table 1: Atomic coordinates (x 10^4) and equivalent isotropic displacement parameters ($Å^2$x 10^3) for sh3419(a). U(eq) is defined as one third of the trace of the orthogonalized U^{ij} tensor.

	x	y	z	U(eq)
Al(1)	6667	3333	757(4)	4(1)
Al(2)	5472(1)	2140(1)	761(3)	9(1)
O(1)	5880(3)	2860(3)	1722(6)	7(1)
O(2)	6190(3)	2545(3)	-194(6)	7(1)
O(3)	5347(3)	1509(3)	1762(7)	19(2)
O(4)	4843(3)	2018(3)	-227(7)	19(2)
C(1)	5617(5)	3041(5)	2826(9)	14(2)
C(2)	5555(6)	2672(6)	4069(11)	30(3)
C(3)	4925(10)	2539(9)	4687(19)	78(6)
C(4)	4661(6)	2870(7)	3884(16)	46(3)
C(5)	4939(6)	2930(9)	2492(15)	47(4)
C(6)	6378(5)	2283(5)	-1283(9)	14(2)
C(7)	6007(6)	2225(6)	-2526(11)	32(3)
C(8)	5856(9)	1577(10)	-3130(20)	84(7)
C(9)	6181(8)	1323(7)	-2364(18)	57(4)
C(10)	6247(8)	1599(6)	-1008(15)	43(3)

C(11)	4904(5)	854(5)	1693(10)	22(2)
C(12)	5200(8)	472(6)	2219(12)	39(3)
C(13)	5150(8)	467(8)	3712(13)	47(4)
C(14)	4635(8)	636(7)	4034(13)	45(3)
C(15)	4349(5)	672(7)	2684(14)	43(3)
C(16)	4178(5)	1568(6)	-184(10)	22(2)
C(17)	3804(6)	1866(8)	-729(13)	43(3)
C(18)	3793(9)	1811(8)	-2189(14)	55(4)
C(19)	3979(8)	1307(8)	-2504(13)	50(4)
C(20)	3998(7)	1013(6)	-1167(13)	40(3)
Al(3)	0	0	5845(7)	29(1)
Al(4)	1193(2)	8(2)	5825(4)	30(1)
O(5)	785(4)	315(4)	6802(9)	29(2)
O(6)	475(4)	-315(4)	4875(9)	32(2)
O(7)	1317(4)	-499(4)	6825(10)	41(2)
O(8)	1820(4)	508(4)	4805(9)	37(2)
C(21)	1053(6)	767(6)	7848(13)	35(3)
C(22)	1098(8)	462(8)	9103(16)	54(4)
C(23)	1729(10)	934(9)	9810(20)	82(6)
C(24)	1978(8)	1558(8)	9010(20)	63(5)
C(25)	1732(8)	1331(8)	7594(19)	62(5)
C(26)	306(6)	-763(6)	3770(15)	39(3)
C(27)	660(10)	-452(9)	2470(20)	94(7)
C(29)	581(14)	-1362(16)	2570(30)	147(11)
C(30)	445(10)	-1324(9)	4130(20)	75(5)
C(31)	1766(7)	-716(7)	6844(18)	49(4)
C(32)	1467(10)	-1399(8)	7530(30)	77(5)
C(33)	1501(13)	-1265(11)	8930(30)	98(7)
C(34)	2126(11)	-613(10)	9104(19)	72(5)
C(35)	2309(8)	-327(9)	7724(16)	53(4)
C(36)	2504(6)	757(7)	4863(17)	47(3)
C(37)	2681(7)	375(8)	3915(18)	55(4)
C(38)	2660(10)	674(8)	2530(20)	71(5)
C(39)	2899(11)	1367(9)	2803(18)	75(6)
C(40)	2844(7)	1428(8)	4328(17)	53(4)
Al(5)	3333	6667	5734(5)	18(1)
Al(6)	3338(2)	7860(2)	5738(3)	21(1)
O(9)	3018(4)	7139(4)	6701(7)	22(2)
O(10)	3655(4)	7454(4)	4788(7)	19(2)

O(11)	2832(4)	7984(4)	4736(8)	33(2)
O(12)	3837(4)	8487(4)	6740(8)	31(2)
C(41)	2581(6)	6971(6)	7776(13)	30(3)
C(42)	2901(8)	7308(9)	9032(16)	67(5)
C(43)	2422(10)	7483(12)	9710(20)	118(11)
C(44)	1808(10)	7131(9)	8833(17)	66(5)
C(45)	2010(9)	7107(10)	7482(17)	64(5)
C(46)	4099(6)	7722(6)	3718(11)	32(3)
C(47)	4661(8)	8406(7)	3933(15)	52(4)
C(48)	4882(9)	8660(8)	2566(18)	62(4)
C(49)	4261(13)	8425(12)	1860(20)	108(9)
C(50)	3799(8)	7764(7)	2460(14)	49(4)
C(51)	2625(7)	8443(7)	4778(14)	39(3)
C(52)	3012(8)	8977(7)	3816(14)	46(3)
C(53)	2713(11)	8799(10)	2491(16)	68(5)
C(54)	2049(11)	8189(12)	2700(20)	84(6)
C(55)	1927(8)	8134(10)	4110(20)	65(4)
C(56)	4089(7)	9163(6)	6689(14)	42(3)
C(57)	3715(8)	9348(7)	7605(16)	49(4)
C(58)	4009(8)	9341(8)	9019(17)	54(4)
C(59)	4694(8)	9566(9)	8735(14)	57(4)
C(60)	4748(8)	9501(7)	7253(15)	49(3)

Table 2: Bond lengths [Å] and angles [°] for sh3419a.

Al(1)-O(2)	1.912(6)	Al(2)-O(1)	1.791(7)	C(7)-C(8)	1.538(19)
Al(1)-O(2)#1	1.912(6)	O(1)-C(1)	1.456(11)	C(8)-C(9)	1.44(3)
Al(1)-O(2)#2	1.912(6)	O(2)-C(6)	1.452(10)	C(9)-C(10)	1.51(2)
Al(1)-O(1)#1	1.915(6)	O(3)-C(11)	1.387(12)	C(11)-C(12)	1.510(16)
Al(1)-O(1)	1.915(6)	O(4)-C(16)	1.409(12)	C(11)-C(15)	1.550(16)
Al(1)-O(1)#2	1.915(6)	C(1)-C(2)	1.509(15)	C(12)-C(13)	1.526(18)
Al(1)-Al(2)#1	2.861(2)	C(1)-C(5)	1.549(15)	C(13)-C(14)	1.52(2)
Al(1)-Al(2)	2.861(2)	C(2)-C(3)	1.517(19)	C(14)-C(15)	1.559(19)
Al(1)-Al(2)#2	2.862(2)	C(3)-C(4)	1.48(3)	C(16)-C(17)	1.502(18)
Al(2)-O(4)	1.712(7)	C(4)-C(5)	1.54(2)	C(16)-C(20)	1.546(16)
Al(2)-O(3)	1.722(7)	C(6)-C(7)	1.515(15)	C(17)-C(18)	1.493(19)
Al(2)-O(2)	1.784(7)	C(6)-C(10)	1.533(15)	C(18)-C(19)	1.52(2)

C(19)-C(20)	1.546(18)	C(38)-C(39)	1.49(3)	C(56)-C(57)	1.51(2)
Al(3)-O(5)	1.907(9)	C(39)-C(40)	1.57(3)	C(57)-C(58)	1.61(2)
Al(3)-O(5)#3	1.907(9)	Al(5)-O(10)#5	1.905(7)	C(58)-C(59)	1.48(2)
Al(3)-O(5)#4	1.907(9)	Al(5)-O(10)#6	1.905(7)	C(59)-C(60)	1.53(2)
Al(3)-O(6)#3	1.924(9)	Al(5)-O(10)	1.905(7)	O(2)-Al(1)-O(2)#1	96.6(3)
Al(3)-O(6)#4	1.924(9)	Al(5)-O(9)#5	1.917(8)	O(2)-Al(1)-O(2)#2	96.6(3)
Al(3)-O(6)	1.924(9)	Al(5)-O(9)	1.917(8)	O(2)#1-Al(1)-O(2)#2	96.6(3)
Al(3)-Al(4)#4	2.850(3)	Al(5)-O(9)#6	1.917(8)	O(2)-Al(1)-O(1)#1	92.9(2)
Al(3)-Al(4)#3	2.850(3)	Al(5)-Al(6)	2.853(3)	O(2)#1-Al(1)-O(1)#1	75.6(2)
Al(3)-Al(4)	2.850(3)	Al(5)-Al(6)#5	2.853(3)	O(2)#2-Al(1)-O(1)#1	168.3(2)
Al(4)-O(7)	1.720(10)	Al(5)-Al(6)#6	2.853(3)	O(2)-Al(1)-O(1)	75.6(2)
Al(4)-O(8)	1.724(9)	Al(6)-O(12)	1.714(9)	O(2)#1-Al(1)-O(1)	168.3(2)
Al(4)-O(6)	1.780(9)	Al(6)-O(11)	1.721(9)	O(2)#2-Al(1)-O(1)	92.9(2)
Al(4)-O(5)	1.792(9)	Al(6)-O(10)	1.786(8)	O(1)#1-Al(1)-O(1)	96.0(3)
O(5)-C(21)	1.424(14)	Al(6)-O(9)	1.792(8)	O(2)-Al(1)-O(1)#2	168.3(2)
O(6)-C(26)	1.466(16)	O(9)-C(41)	1.427(14)	O(2)#1-Al(1)-O(1)#2	92.9(2)
O(7)-C(31)	1.410(15)	O(10)-C(46)	1.433(13)	O(2)#2-Al(1)-O(1)#2	75.6(2)
O(8)-C(36)	1.440(15)	O(11)-C(51)	1.414(14)	O(1)#1-Al(1)-O(1)#2	96.0(3)
C(21)-C(22)	1.50(2)	O(12)-C(56)	1.417(15)	O(1)-Al(1)-O(1)#2	96.0(3)
C(21)-C(25)	1.53(2)	C(41)-C(42)	1.50(2)	O(2)-Al(1)-Al(2)#1	95.9(2)
C(22)-C(23)	1.54(2)	C(41)-C(45)	1.59(2)	O(2)#1-Al(1)-Al(2)#1	37.67(19)
C(23)-C(24)	1.54(3)	C(42)-C(43)	1.57(2)	O(2)#2-Al(1)-Al(2)#1	133.7(2)
C(24)-C(25)	1.55(3)	C(43)-C(44)	1.56(3)	O(1)#1-Al(1)-Al(2)#1	37.90(19)
C(26)-C(27)	1.55(2)	C(44)-C(45)	1.47(2)	O(1)-Al(1)-Al(2)#1	133.4(2)
C(26)-C(30)	1.58(2)	C(46)-C(50)	1.50(2)	O(1)#2-Al(1)-Al(2)#1	95.74(19)
C(27)-C(29)	2.09(4)	C(46)-C(47)	1.529(18)	O(2)-Al(1)-Al(2)	37.67(19)
C(29)-C(30)	1.64(4)	C(47)-C(48)	1.51(2)	O(2)#1-Al(1)-Al(2)	133.7(2)
C(31)-C(35)	1.47(2)	C(48)-C(49)	1.49(3)	O(2)#2-Al(1)-Al(2)	95.9(2)
C(31)-C(32)	1.58(2)	C(49)-C(50)	1.54(2)	O(1)#1-Al(1)-Al(2)	95.75(19)
C(32)-C(33)	1.45(3)	C(51)-C(52)	1.51(2)	O(1)-Al(1)-Al(2)	37.90(19)
C(33)-C(34)	1.54(3)	C(51)-C(55)	1.60(2)	O(1)#2-Al(1)-Al(2)	133.4(2)
C(34)-C(35)	1.53(2)	C(52)-C(53)	1.49(2)	Al(2)#1-Al(1)-Al(2)	120.001(1)
C(36)-C(40)	1.50(2)	C(53)-C(54)	1.54(3)	O(2)-Al(1)-Al(2)#2	133.7(2)
C(36)-C(37)	1.53(2)	C(54)-C(55)	1.46(3)	O(2)#1-Al(1)-Al(2)#2	95.9(2)
C(37)-C(38)	1.60(3)	C(56)-C(60)	1.48(2)	O(2)#2-Al(1)-Al(2)#2	37.67(19)
O(1)#1-Al(1)-Al(2)#2	133.4(2)	C(8)-C(9)-C(10)	105.8(12)	O(6)#4-Al(3)-Al(4)#4	37.9(3)
O(1)-Al(1)-Al(2)#2	95.75(19)	C(9)-C(10)-C(6)	102.9(12)	O(6)-Al(3)-Al(4)#4	95.2(3)
O(1)#2-Al(1)-Al(2)#2	37.90(19)	O(3)-C(11)-C(12)	110.0(10)	O(5)-Al(3)-Al(4)#3	96.0(3)
Al(2)#1-Al(1)-Al(2)#2	120.000(1)	O(3)-C(11)-C(15)	110.4(9)	O(5)#3-Al(3)-Al(4)#3	38.2(3)

Al(2)-Al(1)-Al(2)#2	119.998(1)	C(12)-C(11)-C(15)	101.3(10)	O(5)#4-Al(3)-Al(4)#3	133.7(3)
O(4)-Al(2)-O(3)	116.5(4)	C(11)-C(12)-C(13)	107.4(11)	O(6)#3-Al(3)-Al(4)#3	37.9(3)
O(4)-Al(2)-O(2)	107.4(3)	C(14)-C(13)-C(12)	106.6(11)	O(6)#4-Al(3)-Al(4)#3	95.2(3)
O(3)-Al(2)-O(2)	119.9(3)	C(13)-C(14)-C(15)	105.3(11)	O(6)-Al(3)-Al(4)#3	133.4(3)
O(4)-Al(2)-O(1)	119.8(3)	C(11)-C(15)-C(14)	104.5(10)	Al(4)#4-Al(3)-Al(4)#3	119.995(4)
O(3)-Al(2)-O(1)	107.1(3)	O(4)-C(16)-C(17)	109.9(10)	O(5)-Al(3)-Al(4)	38.2(3)
O(2)-Al(2)-O(1)	82.0(3)	O(4)-C(16)-C(20)	111.1(9)	O(5)#3-Al(3)-Al(4)	133.7(3)
O(4)-Al(2)-Al(1)	121.7(3)	C(17)-C(16)-C(20)	101.2(10)	O(5)#4-Al(3)-Al(4)	96.0(3)
O(3)-Al(2)-Al(1)	121.8(3)	C(18)-C(17)-C(16)	108.4(12)	O(6)#3-Al(3)-Al(4)	95.2(3)
O(2)-Al(2)-Al(1)	40.9(2)	C(17)-C(18)-C(19)	106.4(12)	O(6)#4-Al(3)-Al(4)	133.4(3)
O(1)-Al(2)-Al(1)	41.1(2)	C(18)-C(19)-C(20)	105.3(12)	O(6)-Al(3)-Al(4)	37.9(3)
C(1)-O(1)-Al(2)	126.9(5)	C(16)-C(20)-C(19)	103.7(11)	Al(4)#4-Al(3)-Al(4)	119.994(4)
C(1)-O(1)-Al(1)	131.6(5)	O(5)-Al(3)-O(5)#3	96.2(4)	Al(4)#3-Al(3)-Al(4)	119.996(5)
Al(2)-O(1)-Al(1)	101.0(3)	O(5)-Al(3)-O(5)#4	96.2(4)	O(7)-Al(4)-O(8)	116.8(4)
C(6)-O(2)-Al(2)	127.2(5)	O(5)#3-Al(3)-O(5)#4	96.2(4)	O(7)-Al(4)-O(6)	119.1(5)
C(6)-O(2)-Al(1)	130.8(5)	O(5)-Al(3)-O(6)#3	92.8(3)	O(8)-Al(4)-O(6)	106.9(5)
Al(2)-O(2)-Al(1)	101.4(3)	O(5)#3-Al(3)-O(6)#3	76.0(4)	O(7)-Al(4)-O(5)	106.5(5)
C(11)-O(3)-Al(2)	131.4(7)	O(5)#4-Al(3)-O(6)#3	168.7(3)	O(8)-Al(4)-O(5)	120.9(4)
C(16)-O(4)-Al(2)	132.5(7)	O(5)-Al(3)-O(6)#4	168.7(3)	O(6)-Al(4)-O(5)	82.7(4)
O(1)-C(1)-C(2)	113.9(8)	O(5)#3-Al(3)-O(6)#4	92.8(3)	O(7)-Al(4)-Al(3)	121.2(3)
O(1)-C(1)-C(5)	110.6(8)	O(5)#4-Al(3)-O(6)#4	76.0(4)	O(8)-Al(4)-Al(3)	122.1(3)
C(2)-C(1)-C(5)	107.2(10)	O(6)#3-Al(3)-O(6)#4	96.0(4)	O(6)-Al(4)-Al(3)	41.6(3)
C(1)-C(2)-C(3)	105.5(11)	O(5)-Al(3)-O(6)	76.0(4)	O(5)-Al(4)-Al(3)	41.1(3)
C(4)-C(3)-C(2)	107.7(11)	O(5)#3-Al(3)-O(6)	168.7(3)	C(21)-O(5)-Al(4)	126.7(7)
C(3)-C(4)-C(5)	106.1(11)	O(5)#4-Al(3)-O(6)	92.8(3)	C(21)-O(5)-Al(3)	131.7(8)
C(4)-C(5)-C(1)	100.4(11)	O(6)#3-Al(3)-O(6)	96.0(4)	Al(4)-O(5)-Al(3)	100.7(5)
O(2)-C(6)-C(7)	112.6(8)	O(6)#4-Al(3)-O(6)	96.0(4)	C(26)-O(6)-Al(4)	126.1(7)
O(2)-C(6)-C(10)	112.3(8)	O(5)-Al(3)-Al(4)#4	133.7(3)	C(26)-O(6)-Al(3)	132.9(7)
C(7)-C(6)-C(10)	105.0(10)	O(5)#3-Al(3)-Al(4)#4	96.0(3)	Al(4)-O(6)-Al(3)	100.5(5)
C(6)-C(7)-C(8)	105.0(12)	O(5)#4-Al(3)-Al(4)#4	38.2(3)	C(31)-O(7)-Al(4)	134.5(10)
C(9)-C(8)-C(7)	107.9(11)	O(6)#3-Al(3)-Al(4)#4	133.4(3)	C(36)-O(8)-Al(4)	132.8(9)
O(5)-C(21)-C(22)	112.5(12)	O(10)-Al(5)-O(9)	76.1(3)	O(11)-Al(6)-Al(5)	121.5(3)
O(5)-C(21)-C(25)	114.9(12)	O(9)#5-Al(5)-O(9)	95.9(3)	O(10)-Al(6)-Al(5)	40.9(2)
C(22)-C(21)-C(25)	105.6(13)	O(10)#5-Al(5)-O(9)#6	169.1(3)	O(9)-Al(6)-Al(5)	41.4(3)
C(21)-C(22)-C(23)	108.9(14)	O(10)#6-Al(5)-O(9)#6	76.1(3)	C(41)-O(9)-Al(6)	126.3(7)
C(24)-C(23)-C(22)	103.1(14)	O(10)-Al(5)-O(9)#6	92.3(3)	C(41)-O(9)-Al(5)	132.8(7)
C(23)-C(24)-C(25)	104.8(14)	O(9)#5-Al(5)-O(9)#6	95.9(3)	Al(6)-O(9)-Al(5)	100.5(4)
C(21)-C(25)-C(24)	101.6(14)	O(9)-Al(5)-O(9)#6	95.9(3)	C(46)-O(10)-Al(6)	126.3(7)
O(6)-C(26)-C(27)	115.0(11)	O(10)#5-Al(5)-Al(6)	95.5(2)	C(46)-O(10)-Al(5)	132.0(7)

O(6)-C(26)-C(30)	110.0(13)	O(10)#6-Al(5)-Al(6)	134.1(3)	Al(6)-O(10)-Al(5)	101.2(4)
C(27)-C(26)-C(30)	108.1(15)	O(10)-Al(5)-Al(6)	37.9(2)	C(51)-O(11)-Al(6)	131.9(9)
C(26)-C(27)-C(29)	73.5(14)	O(9)#5-Al(5)-Al(6)	133.6(3)	C(56)-O(12)-Al(6)	133.8(8)
C(30)-C(29)-C(27)	84.7(12)	O(9)-Al(5)-Al(6)	38.2(2)	O(9)-C(41)-C(42)	113.5(10)
C(26)-C(30)-C(29)	87.1(17)	O(9)#6-Al(5)-Al(6)	95.4(2)	O(9)-C(41)-C(45)	112.6(10)
O(7)-C(31)-C(35)	111.9(13)	O(10)#5-Al(5)-Al(6)#5	37.9(2)	C(42)-C(41)-C(45)	108.1(13)
O(7)-C(31)-C(32)	110.7(13)	O(10)#6-Al(5)-Al(6)#5	95.5(2)	C(41)-C(42)-C(43)	106.1(16)
C(35)-C(31)-C(32)	100.7(15)	O(10)-Al(5)-Al(6)#5	134.1(3)	C(44)-C(43)-C(42)	102.6(13)
C(33)-C(32)-C(31)	104.9(15)	O(9)#5-Al(5)-Al(6)#5	38.2(2)	C(45)-C(44)-C(43)	108.6(16)
C(32)-C(33)-C(34)	105(2)	O(9)-Al(5)-Al(6)#5	95.4(2)	C(44)-C(45)-C(41)	99.5(14)
C(35)-C(34)-C(33)	105.2(18)	O(9)#6-Al(5)-Al(6)#5	133.6(3)	O(10)-C(46)-C(50)	114.1(11)
C(31)-C(35)-C(34)	108.3(16)	Al(6)-Al(5)-Al(6)#5	120.000(2)	O(10)-C(46)-C(47)	115.4(10)
O(8)-C(36)-C(40)	109.0(13)	O(10)#5-Al(5)-Al(6)#6	134.1(3)	C(50)-C(46)-C(47)	104.2(12)
O(8)-C(36)-C(37)	109.0(12)	O(10)#6-Al(5)-Al(6)#6	37.9(2)	C(48)-C(47)-C(46)	104.1(13)
C(40)-C(36)-C(37)	104.4(13)	O(10)-Al(5)-Al(6)#6	95.5(2)	C(49)-C(48)-C(47)	102.3(14)
C(36)-C(37)-C(38)	102.1(12)	O(9)#5-Al(5)-Al(6)#6	95.4(2)	C(48)-C(49)-C(50)	105.4(16)
C(39)-C(38)-C(37)	104.7(16)	O(9)-Al(5)-Al(6)#6	133.6(3)	C(46)-C(50)-C(49)	106.8(14)
C(38)-C(39)-C(40)	106.6(14)	O(9)#6-Al(5)-Al(6)#6	38.2(2)	O(11)-C(51)-C(52)	109.6(11)
C(36)-C(40)-C(39)	106.7(14)	Al(6)-Al(5)-Al(6)#6	119.999(2)	O(11)-C(51)-C(55)	108.7(12)
O(10)#5-Al(5)-O(10)#6	96.7(3)	Al(6)#5-Al(5)-Al(6)#6	120.000(1)	C(52)-C(51)-C(55)	99.8(12)
O(10)#5-Al(5)-O(10)	96.7(3)	O(12)-Al(6)-O(11)	116.4(4)	C(53)-C(52)-C(51)	110.1(15)
O(10)#6-Al(5)-O(10)	96.7(3)	O(12)-Al(6)-O(10)	120.1(4)	C(52)-C(53)-C(54)	105.7(16)
O(10)#5-Al(5)-O(9)#5	76.1(3)	O(11)-Al(6)-O(10)	107.5(4)	C(55)-C(54)-C(53)	106.4(17)
O(10)#6-Al(5)-O(9)#5	92.3(3)	O(12)-Al(6)-O(9)	107.1(4)	C(54)-C(55)-C(51)	105.2(15)
O(10)-Al(5)-O(9)#5	169.1(3)	O(11)-Al(6)-O(9)	119.6(4)	O(12)-C(56)-C(60)	109.9(12)
O(10)#5-Al(5)-O(9)	92.3(3)	O(10)-Al(6)-O(9)	82.3(4)	O(12)-C(56)-C(57)	109.7(11)
O(10)#6-Al(5)-O(9)	169.1(3)	O(12)-Al(6)-Al(5)	122.1(3)	C(60)-C(56)-C(57)	103.0(11)
C(56)-C(57)-C(58)	103.0(11)	C(58)-C(59)-C(60)	106.9(13)		
C(59)-C(58)-C(57)	103.5(14)	C(56)-C(60)-C(59)	108.5(13)		

Symmetry transformations used to generate equivalent atoms:
#1 -y+1,x-y,z #2 -x+y+1,-x+1,z #3 -y,x-y,z
#4 -x+y,-x,z #5 -y+1,x-y+1,z #6 -x+y,-x+1,z

Table 3: Anisotropic displacement parameters ($Å^2 x\ 10^3$) for sh3420. The anisotropic displacement factor exponent takes the form: $-2p^2[\ h^2\ a^{*2}U^{11} + ... + 2\ h\ k\ a^*\ b^*\ U^{12}\ ]$

	U^{11}	U^{22}	U^{33}	U^{23}	U^{13}	U^{12}

_ Al(1)	6(1)	6(1)	-1(2)	0	0	3(1)
Al(2)	9(1)	10(1)	7(1)	1(1)	1(1)	4(1)
O(1)	12(3)	9(3)	3(3)	-2(2)	1(2)	7(3)
O(2)	12(3)	11(3)	0(3)	-3(2)	0(2)	6(3)
O(3)	19(4)	13(3)	16(3)	7(3)	-1(3)	2(3)
O(4)	12(3)	20(4)	18(4)	0(3)	-9(3)	2(3)
C(1)	13(5)	15(5)	13(5)	-5(3)	1(3)	6(4)
C(2)	39(7)	41(7)	14(5)	14(5)	21(5)	22(6)
C(3)	108(15)	80(12)	74(10)	51(10)	85(11)	66(12)
C(4)	18(6)	48(9)	61(9)	-16(7)	14(6)	8(6)
C(5)	20(6)	88(12)	48(7)	-20(7)	-1(6)	38(8)
C(6)	14(5)	13(5)	9(4)	-6(3)	6(3)	3(4)
C(7)	47(7)	41(7)	9(5)	-12(5)	-5(5)	23(6)
C(8)	78(12)	105(15)	94(12)	-98(12)	-58(11)	64(12)
C(9)	65(10)	18(7)	73(10)	-21(7)	14(8)	11(7)
C(10)	64(9)	19(6)	55(7)	1(5)	21(7)	28(7)
C(11)	29(6)	14(5)	20(5)	6(4)	6(4)	8(4)
C(12)	72(10)	32(7)	24(6)	12(5)	3(6)	34(7)
C(13)	56(9)	68(10)	18(6)	18(6)	6(6)	33(8)
C(14)	54(9)	43(8)	28(6)	12(6)	3(6)	18(7)
C(15)	10(5)	45(8)	50(8)	23(6)	4(5)	-4(5)
C(16)	11(5)	31(6)	14(5)	-4(4)	-3(4)	3(4)
C(17)	24(6)	79(10)	32(6)	0(7)	-4(5)	29(7)
C(18)	84(12)	61(10)	24(6)	7(6)	-14(7)	39(9)
C(19)	57(10)	64(10)	24(6)	5(6)	-9(6)	27(8)
C(20)	50(8)	13(5)	36(7)	1(5)	-20(6)	-1(5)
Al(3)	15(2)	15(2)	55(4)	0	0	8(1)
Al(4)	16(2)	24(2)	51(3)	2(2)	2(2)	11(2)
O(5)	21(4)	20(4)	52(5)	-2(3)	-8(3)	13(3)
O(6)	16(4)	24(4)	52(5)	-2(4)	-5(3)	7(3)
O(7)	22(4)	39(5)	67(6)	6(4)	7(4)	21(4)
O(8)	18(4)	41(5)	51(6)	3(4)	2(4)	14(4)
C(21)	26(6)	35(7)	33(6)	-17(5)	-11(5)	7(5)
C(22)	40(8)	66(10)	41(7)	-14(6)	-6(6)	16(7)
C(23)	66(12)	53(10)	106(14)	-19(9)	-55(11)	14(9)
C(24)	44(9)	52(8)	95(12)	-37(8)	-39(9)	25(7)
C(25)	45(9)	36(8)	75(9)	-15(7)	9(8)	-4(6)

C(26)	29(7)	24(6)	71(9)	-7(5)	8(6)	19(6)
C(27)	76(13)	49(9)	73(10)	-31(7)	36(10)	-30(9)
C(29)	160(30)	230(20)	138(16)	-157(18)	-94(17)	170(20)
C(30)	68(12)	54(10)	120(14)	-24(9)	-9(11)	44(10)
C(31)	35(7)	39(8)	87(10)	-3(7)	-14(7)	29(6)
C(32)	63(11)	23(7)	149(15)	3(8)	18(11)	22(7)
C(33)	97(16)	60(12)	132(14)	20(11)	-10(14)	35(10)
C(34)	97(14)	82(12)	60(9)	12(8)	16(9)	62(10)
C(35)	45(8)	74(10)	58(9)	5(7)	1(6)	42(7)
C(36)	18(6)	48(8)	63(8)	0(6)	7(6)	7(6)
C(37)	34(8)	56(9)	91(11)	30(8)	27(8)	35(7)
C(38)	77(13)	49(9)	82(10)	13(8)	51(10)	29(9)
C(39)	102(16)	48(9)	50(8)	13(7)	-24(10)	18(10)
C(40)	34(8)	47(8)	66(9)	20(7)	17(7)	11(7)
Al(5)	20(2)	20(2)	13(3)	0	0	10(1)
Al(6)	26(2)	19(2)	20(2)	1(1)	-1(1)	13(1)
O(9)	22(4)	21(4)	20(4)	9(3)	5(3)	9(3)
O(10)	29(4)	27(4)	10(3)	5(3)	8(3)	20(3)
O(11)	37(5)	32(5)	38(5)	0(4)	-8(4)	25(4)
O(12)	43(5)	25(4)	30(4)	-2(3)	-6(4)	20(4)
C(41)	31(6)	26(6)	37(6)	0(5)	9(5)	17(5)
C(42)	40(8)	77(12)	45(8)	-20(8)	30(6)	-1(8)
C(43)	52(10)	130(20)	116(15)	-86(16)	38(9)	3(11)
C(44)	84(11)	76(13)	46(9)	-7(8)	22(8)	47(11)
C(45)	79(11)	94(13)	45(7)	27(8)	36(7)	63(11)
C(46)	37(7)	22(6)	20(5)	5(4)	14(5)	2(5)
C(47)	45(8)	36(8)	42(7)	-2(6)	3(6)	-3(6)
C(48)	69(9)	51(9)	66(10)	38(8)	48(8)	31(8)
C(49)	101(15)	97(17)	77(13)	55(13)	9(11)	13(13)
C(50)	63(9)	46(8)	25(6)	0(6)	5(6)	17(7)
C(51)	45(8)	37(7)	49(7)	8(6)	-2(6)	31(6)
C(52)	71(9)	44(8)	39(7)	7(6)	-4(6)	41(7)
C(53)	99(13)	93(13)	37(7)	-14(8)	-7(8)	66(10)
C(54)	80(13)	88(14)	84(11)	-8(11)	-28(10)	42(10)
C(55)	38(8)	75(12)	92(11)	-7(9)	-12(7)	35(8)
C(56)	53(8)	19(6)	36(7)	3(5)	-2(6)	4(6)
C(57)	58(8)	32(7)	72(9)	-25(7)	-36(7)	34(7)
C(58)	47(8)	54(10)	59(8)	-29(8)	-11(7)	23(8)
C(59)	56(9)	77(12)	30(7)	-22(8)	-14(6)	28(9)

C(60)	51(8)	42(8)	44(8)	-18(7)	-13(6)	17(7)

Compund 5

Table 1: Atomic coordinates (x 10^4) and equivalent isotropic displacement parameters ($Å^2$x 10^3) for sh3364. U(eq) is defined as one third of the trace of the orthogonalized U^{ij} tensor.

	x	y	z	U(eq)
Al(1)	6197(2)	6515(2)	8530(1)	22(1)
Al(2)	5846(2)	8416(2)	7295(1)	34(1)
Al(3)	5134(2)	6045(2)	7277(1)	37(1)
Al(4)	7511(2)	5317(2)	7358(1)	40(1)
Al(5)	8242(2)	7685(2)	7388(1)	38(1)
O(1)	6590(3)	6817(3)	7472(2)	22(1)
O(2)	5551(4)	8053(4)	8298(2)	31(1)
O(3)	4834(3)	5845(4)	8290(2)	30(1)
O(4)	7034(4)	5103(4)	8361(2)	33(1)
O(5)	7742(3)	7278(4)	8385(2)	28(1)
O(6)	4969(4)	7555(4)	6848(2)	39(1)
O(7)	6306(5)	5158(4)	6883(3)	44(1)
O(8)	8661(4)	6419(4)	6978(3)	41(1)
O(9)	7406(4)	8802(4)	6927(2)	32(1)
C(1)	4962(5)	8690(6)	8868(4)	30(2)
C(2)	3665(5)	8687(7)	8926(4)	40(2)
C(3)	3279(6)	9756(7)	9247(5)	54(2)
C(4)	4253(7)	10618(7)	8882(7)	79(3)
C(5)	5331(6)	9948(6)	8751(5)	47(2)
C(6)	3871(5)	5229(6)	8837(4)	29(2)
C(7)	3831(6)	3938(6)	8800(4)	34(2)
C(8)	2621(6)	3685(7)	8668(5)	49(2)
C(9)	1890(6)	4618(6)	8942(5)	47(2)
C(10)	2665(6)	5687(6)	8714(5)	42(2)
C(11)	7208(6)	4163(6)	8941(4)	34(2)
C(12)	8479(7)	4105(6)	9039(5)	50(2)
C(13)	8788(7)	2866(8)	9146(6)	68(3)

C(14)	8075(7)	2306(7)	8734(5)	55(2)
C(15)	6911(6)	2964(6)	8810(4)	36(2)
C(16)	8284(5)	7418(6)	8997(4)	32(2)
C(17)	9588(5)	7160(6)	8888(4)	35(2)
C(18)	10208(6)	8303(7)	8875(5)	51(2)
C(19)	9341(6)	8941(7)	9367(4)	52(2)
C(20)	8198(6)	8673(7)	9133(5)	44(2)
C(21)	4078(6)	7899(8)	6409(4)	55(2)
C(22)	2991(6)	8371(7)	6846(5)	49(2)
C(23)	2364(7)	8951(8)	6235(5)	58(2)
C(24)	3287(9)	9206(11)	5522(6)	105(4)
C(25)	4408(8)	8728(9)	5738(4)	63(3)
C(26)	6262(10)	4233(8)	6452(5)	74(3)
C(27)	5582(9)	3171(7)	6847(5)	63(2)
C(28A)	5750(50)	2640(40)	6149(16)	87(4)
C(29A)	5580(60)	3540(20)	5470(20)	86(4)
C(28B)	5460(40)	2470(20)	6255(12)	88(4)
C(29B)	5870(40)	3394(15)	5553(18)	87(4)
C(30)	5938(10)	4590(7)	5746(5)	72(3)
C(31)	9841(7)	6340(9)	6553(5)	63(2)
C(32)	10636(7)	5597(9)	6993(5)	63(3)
C(33A)	11630(30)	5410(30)	6350(20)	73(5)
C(34A)	10878(16)	4890(20)	5895(13)	74(5)
C(33B)	11550(40)	5080(40)	6450(30)	73(5)
C(34B)	11165(18)	5740(30)	5595(13)	74(5)
C(35)	9912(8)	5874(9)	5864(5)	70(3)
C(36)	7787(7)	9973(6)	6503(4)	40(2)
C(37)	8169(7)	10767(7)	6975(4)	46(2)
C(38)	8893(8)	11702(8)	6377(5)	69(3)
C(39A)	9490(20)	11050(20)	5809(15)	53(4)
C(39B)	9150(30)	11270(20)	5657(15)	50(4)
C(40)	8801(7)	9969(7)	5858(4)	52(2)
O(10)	1978(6)	1952(6)	6350(3)	73(2)
C(41A)	2871(11)	2316(15)	5770(7)	73(4)
C(41B)	2150(30)	2856(13)	5754(8)	75(4)
C(42)	2519(8)	2461(8)	5019(5)	74(2)
C(43B)	1860(40)	2240(20)	7060(8)	76(5)
C(43A)	2245(12)	1770(20)	7068(6)	74(4)
C(44)	1302(13)	1380(13)	7677(6)	143(6)

Table 2: Bond lengths [Å] and angles [°] for sh3364.

Al(1)-O(1)	1.885(4)	O(2)-C(1)	1.464(8)	C(9)-H(9B)	0.9900
Al(1)-O(3)	1.944(4)	O(3)-C(6)	1.453(7)	C(10)-H(10A)	0.9900
Al(1)-O(2)	1.954(5)	O(4)-C(11)	1.430(7)	C(10)-H(10B)	0.9900
Al(1)-O(4)	1.960(5)	O(5)-C(16)	1.432(7)	C(11)-C(15)	1.527(9)
Al(1)-O(5)	1.971(4)	O(6)-C(21)	1.449(8)	C(11)-C(12)	1.529(10)
Al(1)-Al(2)	2.967(3)	O(7)-C(26)	1.469(9)	C(11)-H(11)	1.0000
Al(1)-Al(3)	2.968(3)	O(8)-C(31)	1.459(8)	C(12)-C(13)	1.481(11)
Al(1)-Al(4)	2.971(3)	O(9)-C(36)	1.475(8)	C(12)-H(12A)	0.9900
Al(1)-H(1)	1.52(3)	C(1)-C(2)	1.497(9)	C(12)-H(12B)	0.9900
Al(2)-O(2)	1.788(5)	C(1)-C(5)	1.508(10)	C(13)-C(14)	1.465(11)
Al(2)-O(9)	1.845(5)	C(1)-H(1A)	1.0000	C(13)-H(13A)	0.9900
Al(2)-O(6)	1.848(5)	C(2)-C(3)	1.513(10)	C(13)-H(13B)	0.9900
Al(2)-O(1)	2.057(4)	C(2)-H(2A)	0.9900	C(14)-C(15)	1.551(10)
Al(2)-Al(3)	2.921(3)	C(2)-H(2B)	0.9900	C(14)-H(14A)	0.9900
Al(2)-Al(5)	2.945(3)	C(3)-C(4)	1.498(11)	C(14)-H(14B)	0.9900
Al(2)-H(2)	1.51(3)	C(3)-H(3A)	0.9900	C(15)-H(15A)	0.9900
Al(3)-O(3)	1.807(5)	C(3)-H(3B)	0.9900	C(15)-H(15B)	0.9900
Al(3)-O(6)	1.827(5)	C(4)-C(5)	1.480(10)	C(16)-C(17)	1.531(9)
Al(3)-O(7)	1.831(6)	C(4)-H(4A)	0.9900	C(16)-C(20)	1.539(10)
Al(3)-O(1)	2.058(4)	C(4)-H(4B)	0.9900	C(16)-H(16)	1.0000
Al(3)-Al(4)	2.919(3)	C(5)-H(5A)	0.9900	C(17)-C(18)	1.525(10)
Al(3)-H(3)	1.51(3)	C(5)-H(5B)	0.9900	C(17)-H(17A)	0.9900
Al(4)-O(4)	1.800(5)	C(6)-C(7)	1.530(9)	C(17)-H(17B)	0.9900
Al(4)-O(8)	1.817(5)	C(6)-C(10)	1.544(9)	C(18)-C(19)	1.514(10)
Al(4)-O(7)	1.825(6)	C(6)-H(6)	1.0000	C(18)-H(18A)	0.9900
Al(4)-O(1)	2.077(4)	C(7)-C(8)	1.521(9)	C(18)-H(18B)	0.9900
Al(4)-Al(5)	2.930(3)	C(7)-H(7A)	0.9900	C(19)-C(20)	1.532(9)
Al(4)-H(4)	1.51(3)	C(7)-H(7B)	0.9900	C(19)-H(19A)	0.9900
Al(5)-O(5)	1.796(5)	C(8)-C(9)	1.484(10)	C(19)-H(19B)	0.9900
Al(5)-O(9)	1.810(5)	C(8)-H(8A)	0.9900	C(20)-H(20A)	0.9900
Al(5)-O(8)	1.812(6)	C(8)-H(8B)	0.9900	C(20)-H(20B)	0.9900
Al(5)-O(1)	2.155(4)	C(9)-C(10)	1.499(9)	C(21)-C(25)	1.415(11)
Al(5)-H(5)	1.52(3)	C(9)-H(9A)	0.9900	C(21)-C(22)	1.525(11)
C(21)-H(21)	1.0000	C(31)-H(31)	1.0000	C(40)-H(40A)	0.9900

C(22)-C(23)	1.516(10)	C(32)-C(33B)	1.52(4)	C(40)-H(40B)	0.9900
C(22)-H(22A)	0.9900	C(32)-C(33A)	1.54(4)	O(10)-C(41A)	1.351(11)
C(22)-H(22B)	0.9900	C(32)-H(32A)	0.9900	O(10)-C(41B)	1.366(13)
C(23)-C(24)	1.514(12)	C(32)-H(32B)	0.9900	O(10)-C(43B)	1.395(13)
C(23)-H(23A)	0.9900	C(33A)-C(34A)	1.52(5)	O(10)-C(43A)	1.398(11)
C(23)-H(23B)	0.9900	C(33A)-H(33A)	0.9900	C(41A)-C(42)	1.502(12)
C(24)-C(25)	1.513(12)	C(33A)-H(33B)	0.9900	C(41A)-H(41A)	0.9900
C(24)-H(24A)	0.9900	C(34A)-C(35)	1.60(2)	C(41A)-H(41B)	0.9900
C(24)-H(24B)	0.9900	C(34A)-H(34A)	0.9900	C(41B)-C(42)	1.500(14)
C(25)-H(25A)	0.9900	C(34A)-H(34B)	0.9900	C(41B)-H(41C)	0.9900
C(25)-H(25B)	0.9900	C(33B)-C(34B)	1.77(5)	C(41B)-H(41D)	0.9900
C(26)-C(30)	1.416(11)	C(33B)-H(33C)	0.9900	C(42)-H(42A)	0.9800
C(26)-C(27)	1.475(12)	C(33B)-H(33D)	0.9900	C(42)-H(42B)	0.9800
C(26)-H(26)	1.0000	C(34B)-C(35)	1.47(2)	C(42)-H(42C)	0.9800
C(27)-C(28B)	1.511(10)	C(34B)-H(34C)	0.9900	C(42)-H(42D)	0.9800
C(27)-C(28A)	1.514(11)	C(34B)-H(34D)	0.9900	C(42)-H(42E)	0.9800
C(27)-H(27A)	0.9900	C(35)-H(35A)	0.9900	C(42)-H(42F)	0.9800
C(27)-H(27B)	0.9900	C(35)-H(35B)	0.9900	C(43B)-C(44)	1.429(15)
C(28A)-C(29A)	1.523(12)	C(36)-C(40)	1.510(10)	C(43B)-H(43A)	0.9900
C(28A)-H(28A)	0.9900	C(36)-C(37)	1.513(10)	C(43B)-H(43B)	0.9900
C(28A)-H(28B)	0.9900	C(36)-H(36)	1.0000	C(43A)-C(44)	1.422(13)
C(29A)-C(30)	1.514(11)	C(37)-C(38)	1.531(10)	C(43A)-H(43C)	0.9900
C(29A)-H(29A)	0.9900	C(37)-H(37A)	0.9900	C(43A)-H(43D)	0.9900
C(29A)-H(29B)	0.9900	C(37)-H(37B)	0.9900	C(44)-H(44A)	0.9800
C(28B)-C(29B)	1.524(11)	C(38)-C(39A)	1.48(2)	C(44)-H(44B)	0.9800
C(28B)-H(28C)	0.9900	C(38)-C(39B)	1.49(2)	C(44)-H(44C)	0.9800
C(28B)-H(28D)	0.9900	C(38)-H(38A)	0.9900	C(44)-H(44D)	0.9800
C(29B)-C(30)	1.520(10)	C(38)-H(38B)	0.9900	C(44)-H(44E)	0.9800
C(29B)-H(29C)	0.9900	C(39A)-C(40)	1.486(19)	C(44)-H(44F)	0.9800
C(29B)-H(29D)	0.9900	C(39A)-H(39A)	0.9900	O(1)-Al(1)-O(3)	79.52(18)
C(30)-H(30A)	0.9900	C(39A)-H(39B)	0.9900	O(1)-Al(1)-O(2)	79.08(18)
C(30)-H(30B)	0.9900	C(39B)-C(40)	1.54(2)	O(3)-Al(1)-O(2)	89.2(2)
C(31)-C(35)	1.464(12)	C(39B)-H(39C)	0.9900	O(1)-Al(1)-O(4)	79.85(18)
C(31)-C(32)	1.514(11)	C(39B)-H(39D)	0.9900	O(3)-Al(1)-O(4)	88.4(2)
O(2)-Al(1)-O(4)	158.9(2)	O(9)-Al(2)-O(1)	78.67(18)	O(6)-Al(3)-Al(2)	37.59(15)
O(1)-Al(1)-O(5)	80.27(18)	O(6)-Al(2)-O(1)	78.3(2)	O(7)-Al(3)-Al(2)	114.85(19)
O(3)-Al(1)-O(5)	159.8(2)	O(2)-Al(2)-Al(3)	88.14(17)	O(1)-Al(3)-Al(2)	44.77(13)
O(2)-Al(1)-O(5)	88.1(2)	O(9)-Al(2)-Al(3)	115.96(18)	Al(4)-Al(3)-Al(2)	89.20(9)
O(4)-Al(1)-O(5)	86.9(2)	O(6)-Al(2)-Al(3)	37.09(16)	O(3)-Al(3)-Al(1)	39.34(13)

O(1)-Al(1)-Al(2)	43.44(13)	O(1)-Al(2)-Al(3)	44.79(13)	O(6)-Al(3)-Al(1)	97.10(18)
O(3)-Al(1)-Al(2)	82.40(14)	O(2)-Al(2)-Al(5)	85.68(16)	O(7)-Al(3)-Al(1)	96.94(17)
O(2)-Al(1)-Al(2)	35.65(13)	O(9)-Al(2)-Al(5)	35.93(14)	O(1)-Al(3)-Al(1)	39.02(10)
O(4)-Al(1)-Al(2)	123.29(15)	O(6)-Al(2)-Al(5)	117.83(19)	Al(4)-Al(3)-Al(1)	60.62(7)
O(5)-Al(1)-Al(2)	83.74(14)	O(1)-Al(2)-Al(5)	47.02(13)	Al(2)-Al(3)-Al(1)	60.49(7)
O(1)-Al(1)-Al(3)	43.43(13)	Al(3)-Al(2)-Al(5)	90.96(10)	O(3)-Al(3)-H(3)	102(3)
O(3)-Al(1)-Al(3)	36.11(13)	O(2)-Al(2)-Al(1)	39.56(15)	O(6)-Al(3)-H(3)	96(3)
O(2)-Al(1)-Al(3)	83.89(15)	O(9)-Al(2)-Al(1)	96.60(16)	O(7)-Al(3)-H(3)	106(3)
O(4)-Al(1)-Al(3)	81.85(15)	O(6)-Al(2)-Al(1)	96.64(17)	O(1)-Al(3)-H(3)	175(3)
O(5)-Al(1)-Al(3)	123.65(15)	O(1)-Al(2)-Al(1)	39.04(10)	Al(4)-Al(3)-H(3)	140(3)
Al(2)-Al(1)-Al(3)	58.98(7)	Al(3)-Al(2)-Al(1)	60.53(7)	Al(2)-Al(3)-H(3)	130(3)
O(1)-Al(1)-Al(4)	43.93(13)	Al(5)-Al(2)-Al(1)	61.26(7)	Al(1)-Al(3)-H(3)	141(3)
O(3)-Al(1)-Al(4)	83.98(15)	O(2)-Al(2)-H(2)	108(2)	O(4)-Al(4)-O(8)	114.3(3)
O(2)-Al(1)-Al(4)	122.93(15)	O(9)-Al(2)-H(2)	95(2)	O(4)-Al(4)-O(7)	111.9(2)
O(4)-Al(1)-Al(4)	35.95(13)	O(6)-Al(2)-H(2)	102(2)	O(8)-Al(4)-O(7)	122.1(2)
O(5)-Al(1)-Al(4)	80.70(15)	O(1)-Al(2)-H(2)	172(2)	O(4)-Al(4)-O(1)	78.72(18)
Al(2)-Al(1)-Al(4)	87.35(8)	Al(3)-Al(2)-H(2)	138(2)	O(8)-Al(4)-O(1)	79.0(2)
Al(3)-Al(1)-Al(4)	58.87(7)	Al(5)-Al(2)-H(2)	128(2)	O(7)-Al(4)-O(1)	77.8(2)
O(1)-Al(1)-H(1)	178(2)	Al(1)-Al(2)-H(2)	148(2)	O(4)-Al(4)-Al(3)	85.85(17)
O(3)-Al(1)-H(1)	102(2)	O(3)-Al(3)-O(6)	111.4(2)	O(8)-Al(4)-Al(3)	116.31(18)
O(2)-Al(1)-H(1)	100(2)	O(3)-Al(3)-O(7)	114.7(2)	O(7)-Al(4)-Al(3)	37.12(16)
O(4)-Al(1)-H(1)	101(2)	O(6)-Al(3)-O(7)	122.0(2)	O(1)-Al(4)-Al(3)	44.84(13)
O(5)-Al(1)-H(1)	98(2)	O(3)-Al(3)-O(1)	78.34(17)	O(4)-Al(4)-Al(5)	88.16(18)
Al(2)-Al(1)-H(1)	136(2)	O(6)-Al(3)-O(1)	78.75(19)	O(8)-Al(4)-Al(5)	36.09(16)
Al(3)-Al(1)-H(1)	138(2)	O(7)-Al(3)-O(1)	78.1(2)	O(7)-Al(4)-Al(5)	117.00(19)
Al(4)-Al(1)-H(1)	137(2)	O(3)-Al(3)-Al(4)	87.88(16)	O(1)-Al(4)-Al(5)	47.30(13)
O(2)-Al(2)-O(9)	110.9(2)	O(6)-Al(3)-Al(4)	116.41(17)	Al(3)-Al(4)-Al(5)	91.31(10)
O(2)-Al(2)-O(6)	113.9(2)	O(7)-Al(3)-Al(4)	36.97(16)	O(4)-Al(4)-Al(1)	39.73(15)
O(9)-Al(2)-O(6)	123.5(2)	O(1)-Al(3)-Al(4)	45.37(13)	O(8)-Al(4)-Al(1)	96.91(18)
O(2)-Al(2)-O(1)	78.59(18)	O(3)-Al(3)-Al(2)	85.95(17)	O(7)-Al(4)-Al(1)	96.97(18)
O(1)-Al(4)-Al(1)	39.02(10)	Al(2)-O(1)-Al(4)	165.28(19)	C(5)-C(1)-H(1A)	107.8
Al(3)-Al(4)-Al(1)	60.51(7)	Al(3)-O(1)-Al(4)	89.79(19)	C(1)-C(2)-C(3)	104.4(6)
Al(5)-Al(4)-Al(1)	61.38(8)	Al(1)-O(1)-Al(5)	96.19(18)	C(1)-C(2)-H(2A)	110.9
O(4)-Al(4)-H(4)	108(2)	Al(2)-O(1)-Al(5)	88.68(18)	C(3)-C(2)-H(2A)	110.9
O(8)-Al(4)-H(4)	100(2)	Al(3)-O(1)-Al(5)	166.22(19)	C(1)-C(2)-H(2B)	110.9
O(7)-Al(4)-H(4)	97(2)	Al(4)-O(1)-Al(5)	87.60(17)	C(3)-C(2)-H(2B)	110.9
O(1)-Al(4)-H(4)	172(2)	C(1)-O(2)-Al(2)	131.3(4)	H(2A)-C(2)-H(2B)	108.9
Al(3)-Al(4)-H(4)	132(2)	C(1)-O(2)-Al(1)	123.9(4)	C(4)-C(3)-C(2)	103.0(6)
Al(5)-Al(4)-H(4)	134(2)	Al(2)-O(2)-Al(1)	104.8(2)	C(4)-C(3)-H(3A)	111.2

Al(1)-Al(4)-H(4)	148(2)	C(6)-O(3)-Al(3)	130.0(4)	C(2)-C(3)-H(3A)	111.2
O(5)-Al(5)-O(9)	114.6(2)	C(6)-O(3)-Al(1)	125.2(4)	C(4)-C(3)-H(3B)	111.2
O(5)-Al(5)-O(8)	110.6(2)	Al(3)-O(3)-Al(1)	104.5(2)	C(2)-C(3)-H(3B)	111.2
O(9)-Al(5)-O(8)	120.1(2)	C(11)-O(4)-Al(4)	130.8(4)	H(3A)-C(3)-H(3B)	109.1
O(5)-Al(5)-O(1)	77.39(17)	C(11)-O(4)-Al(1)	124.8(4)	C(5)-C(4)-C(3)	106.7(7)
O(9)-Al(5)-O(1)	76.85(19)	Al(4)-O(4)-Al(1)	104.3(2)	C(5)-C(4)-H(4A)	110.4
O(8)-Al(5)-O(1)	77.0(2)	C(16)-O(5)-Al(5)	130.9(4)	C(3)-C(4)-H(4A)	110.4
O(5)-Al(5)-Al(4)	84.59(17)	C(16)-O(5)-Al(1)	123.0(4)	C(5)-C(4)-H(4B)	110.4
O(9)-Al(5)-Al(4)	114.13(19)	Al(5)-O(5)-Al(1)	106.1(2)	C(3)-C(4)-H(4B)	110.4
O(8)-Al(5)-Al(4)	36.20(16)	C(21)-O(6)-Al(3)	122.0(5)	H(4A)-C(4)-H(4B)	108.6
O(1)-Al(5)-Al(4)	45.10(12)	C(21)-O(6)-Al(2)	130.9(5)	C(4)-C(5)-C(1)	107.2(6)
O(5)-Al(5)-Al(2)	87.35(16)	Al(3)-O(6)-Al(2)	105.3(2)	C(4)-C(5)-H(5A)	110.3
O(9)-Al(5)-Al(2)	36.74(14)	C(26)-O(7)-Al(4)	122.0(6)	C(1)-C(5)-H(5A)	110.3
O(8)-Al(5)-Al(2)	113.71(19)	C(26)-O(7)-Al(3)	129.9(6)	C(4)-C(5)-H(5B)	110.3
O(1)-Al(5)-Al(2)	44.30(12)	Al(4)-O(7)-Al(3)	105.9(2)	C(1)-C(5)-H(5B)	110.3
Al(4)-Al(5)-Al(2)	88.53(10)	C(31)-O(8)-Al(5)	120.4(5)	H(5A)-C(5)-H(5B)	108.5
O(5)-Al(5)-H(5)	101(2)	C(31)-O(8)-Al(4)	130.7(5)	O(3)-C(6)-C(7)	111.8(5)
O(9)-Al(5)-H(5)	105(2)	Al(5)-O(8)-Al(4)	107.7(2)	O(3)-C(6)-C(10)	112.9(5)
O(8)-Al(5)-H(5)	103(3)	C(36)-O(9)-Al(5)	129.3(4)	C(7)-C(6)-C(10)	105.5(5)
O(1)-Al(5)-H(5)	178(2)	C(36)-O(9)-Al(2)	121.4(4)	O(3)-C(6)-H(6)	108.8
Al(4)-Al(5)-H(5)	135(2)	Al(5)-O(9)-Al(2)	107.3(2)	C(7)-C(6)-H(6)	108.8
Al(2)-Al(5)-H(5)	136(2)	O(2)-C(1)-C(2)	112.2(5)	C(10)-C(6)-H(6)	108.8
Al(1)-O(1)-Al(2)	97.52(18)	O(2)-C(1)-C(5)	115.4(6)	C(8)-C(7)-C(6)	106.2(5)
Al(1)-O(1)-Al(3)	97.55(18)	C(2)-C(1)-C(5)	105.4(5)	C(8)-C(7)-H(7A)	110.5
Al(2)-O(1)-Al(3)	90.44(18)	O(2)-C(1)-H(1A)	107.8	C(6)-C(7)-H(7A)	110.5
Al(1)-O(1)-Al(4)	97.04(17)	C(2)-C(1)-H(1A)	107.8	C(8)-C(7)-H(7B)	110.5
C(6)-C(7)-H(7B)	110.5	C(14)-C(13)-H(13B)	110.4	C(20)-C(19)-H(19A)	111.5
H(7A)-C(7)-H(7B)	108.7	C(12)-C(13)-H(13B)	110.4	C(18)-C(19)-H(19B)	111.5
C(9)-C(8)-C(7)	104.5(6)	H(13A)-C(13)-H(13B)	108.6	C(20)-C(19)-H(19B)	111.5
C(9)-C(8)-H(8A)	110.9	C(13)-C(14)-C(15)	104.5(7)	H(19A)-C(19)-H(19B)	109.3
C(7)-C(8)-H(8A)	110.9	C(13)-C(14)-H(14A)	110.8	C(19)-C(20)-C(16)	106.0(6)
C(9)-C(8)-H(8B)	110.9	C(15)-C(14)-H(14A)	110.8	C(19)-C(20)-H(20A)	110.5
C(7)-C(8)-H(8B)	110.9	C(13)-C(14)-H(14B)	110.8	C(16)-C(20)-H(20A)	110.5
H(8A)-C(8)-H(8B)	108.9	C(15)-C(14)-H(14B)	110.8	C(19)-C(20)-H(20B)	110.5
C(8)-C(9)-C(10)	105.1(6)	H(14A)-C(14)-H(14B)	108.9	C(16)-C(20)-H(20B)	110.5
C(8)-C(9)-H(9A)	110.7	C(11)-C(15)-C(14)	105.9(6)	H(20A)-C(20)-H(20B)	108.7
C(10)-C(9)-H(9A)	110.7	C(11)-C(15)-H(15A)	110.5	C(25)-C(21)-O(6)	117.2(7)
C(8)-C(9)-H(9B)	110.7	C(14)-C(15)-H(15A)	110.5	C(25)-C(21)-C(22)	105.5(7)
C(10)-C(9)-H(9B)	110.7	C(11)-C(15)-H(15B)	110.5	O(6)-C(21)-C(22)	113.7(6)

H(9A)-C(9)-H(9B)	108.8	C(14)-C(15)-H(15B)	110.5	C(25)-C(21)-H(21)	106.6
C(9)-C(10)-C(6)	103.4(5)	H(15A)-C(15)-H(15B)	108.7	O(6)-C(21)-H(21)	106.6
C(9)-C(10)-H(10A)	111.1	O(5)-C(16)-C(17)	115.0(6)	C(22)-C(21)-H(21)	106.6
C(6)-C(10)-H(10A)	111.1	O(5)-C(16)-C(20)	111.3(5)	C(23)-C(22)-C(21)	103.2(7)
C(9)-C(10)-H(10B)	111.1	C(17)-C(16)-C(20)	105.1(5)	C(23)-C(22)-H(22A)	111.1
C(6)-C(10)-H(10B)	111.1	O(5)-C(16)-H(16)	108.4	C(21)-C(22)-H(22A)	111.1
H(10A)-C(10)-H(10B)	109.1	C(17)-C(16)-H(16)	108.4	C(23)-C(22)-H(22B)	111.1
O(4)-C(11)-C(15)	114.6(5)	C(20)-C(16)-H(16)	108.4	C(21)-C(22)-H(22B)	111.1
O(4)-C(11)-C(12)	112.0(6)	C(18)-C(17)-C(16)	105.8(6)	H(22A)-C(22)-H(22B)	109.1
C(15)-C(11)-C(12)	105.2(5)	C(18)-C(17)-H(17A)	110.6	C(24)-C(23)-C(22)	105.9(7)
O(4)-C(11)-H(11)	108.3	C(16)-C(17)-H(17A)	110.6	C(24)-C(23)-H(23A)	110.6
C(15)-C(11)-H(11)	108.3	C(18)-C(17)-H(17B)	110.6	C(22)-C(23)-H(23A)	110.6
C(12)-C(11)-H(11)	108.3	C(16)-C(17)-H(17B)	110.6	C(24)-C(23)-H(23B)	110.6
C(13)-C(12)-C(11)	107.1(6)	H(17A)-C(17)-H(17B)	108.7	C(22)-C(23)-H(23B)	110.6
C(13)-C(12)-H(12A)	110.3	C(19)-C(18)-C(17)	105.0(6)	H(23A)-C(23)-H(23B)	108.7
C(11)-C(12)-H(12A)	110.3	C(19)-C(18)-H(18A)	110.8	C(25)-C(24)-C(23)	105.8(7)
C(13)-C(12)-H(12B)	110.3	C(17)-C(18)-H(18A)	110.8	C(25)-C(24)-H(24A)	110.6
C(11)-C(12)-H(12B)	110.3	C(19)-C(18)-H(18B)	110.8	C(23)-C(24)-H(24A)	110.6
H(12A)-C(12)-H(12B)	108.6	C(17)-C(18)-H(18B)	110.8	C(25)-C(24)-H(24B)	110.6
C(14)-C(13)-C(12)	106.4(7)	H(18A)-C(18)-H(18B)	108.8	C(23)-C(24)-H(24B)	110.6
C(14)-C(13)-H(13A)	110.4	C(18)-C(19)-C(20)	101.2(6)	H(24A)-C(24)-H(24B)	108.7
C(12)-C(13)-H(13A)	110.4	C(18)-C(19)-H(19A)	111.5	C(21)-C(25)-C(24)	106.5(7)
C(21)-C(25)-H(25A)	110.4	C(29B)-C(28B)-H(28C)	111.9	H(32A)-C(32)-H(32B)	109.5
C(24)-C(25)-H(25A)	110.4	C(27)-C(28B)-H(28D)	111.9	C(34A)-C(33A)-C(32)	97(2)
C(21)-C(25)-H(25B)	110.4	C(29B)-C(28B)-H(28D)	111.9	C(34A)-C(33A)-H(33A)	112.3
C(24)-C(25)-H(25B)	110.4	H(28C)-C(28B)-H(28D)	109.6	C(32)-C(33A)-H(33A)	112.3
H(25A)-C(25)-H(25B)	108.6	C(30)-C(29B)-C(28B)	111.3(19)	C(34A)-C(33A)-H(33B)	112.3
C(30)-C(26)-O(7)	115.0(8)	C(30)-C(29B)-H(29C)	109.4	C(32)-C(33A)-H(33B)	112.3
C(30)-C(26)-C(27)	108.6(8)	C(28B)-C(29B)-H(29C)	109.4	H(33A)-C(33A)-H(33B)	109.9
O(7)-C(26)-C(27)	116.7(7)	C(30)-C(29B)-H(29D)	109.4	C(33A)-C(34A)-C(35)	98(2)
C(30)-C(26)-H(26)	105.1	C(28B)-C(29B)-H(29D)	109.4	C(33A)-C(34A)-H(34A)	112.1
O(7)-C(26)-H(26)	105.1	H(29C)-C(29B)-H(29D)	108.0	C(35)-C(34A)-H(34A)	112.1
C(27)-C(26)-H(26)	105.1	C(26)-C(30)-C(29A)	109.3(16)	C(33A)-C(34A)-H(34B)	112.1
C(26)-C(27)-C(28B)	106.5(13)	C(26)-C(30)-C(29B)	97.3(16)	C(35)-C(34A)-H(34B)	112.1
C(26)-C(27)-C(28A)	93(2)	C(29A)-C(30)-C(29B)	16(2)	H(34A)-C(34A)-H(34B)	109.8
C(28B)-C(27)-C(28A)	15(2)	C(26)-C(30)-H(30A)	109.8	C(32)-C(33B)-C(34B)	99(2)
C(26)-C(27)-H(27A)	113.1	C(29A)-C(30)-H(30A)	109.8	C(32)-C(33B)-H(33C)	111.9
C(28B)-C(27)-H(27A)	101.2	C(29B)-C(30)-H(30A)	106.1	C(34B)-C(33B)-H(33C)	111.9
C(28A)-C(27)-H(27A)	113.1	C(26)-C(30)-H(30B)	109.8	C(32)-C(33B)-H(33D)	111.9

C(26)-C(27)-H(27B)	113.1	C(29A)-C(30)-H(30B)	109.8	C(34B)-C(33B)-H(33D)	111.9
C(28B)-C(27)-H(27B)	112.0	C(29B)-C(30)-H(30B)	124.7	H(33C)-C(33B)-H(33D)	109.6
C(28A)-C(27)-H(27B)	113.1	H(30A)-C(30)-H(30B)	108.3	C(35)-C(34B)-C(33B)	99(2)
H(27A)-C(27)-H(27B)	110.4	O(8)-C(31)-C(35)	115.1(8)	C(35)-C(34B)-H(34C)	111.9
C(27)-C(28A)-C(29A)	111(3)	O(8)-C(31)-C(32)	113.9(7)	C(33B)-C(34B)-H(34C)	111.9
C(27)-C(28A)-H(28A)	109.5	C(35)-C(31)-C(32)	105.1(7)	C(35)-C(34B)-H(34D)	111.9
C(29A)-C(28A)-H(28A)	109.5	O(8)-C(31)-H(31)	107.4	C(33B)-C(34B)-H(34D)	111.9
C(27)-C(28A)-H(28B)	109.5	C(35)-C(31)-H(31)	107.4	H(34C)-C(34B)-H(34D)	109.6
C(29A)-C(28A)-H(28B)	109.5	C(32)-C(31)-H(31)	107.4	C(31)-C(35)-C(34B)	104.9(11)
H(28A)-C(28A)-H(28B)	108.1	C(31)-C(32)-C(33B)	109.2(17)	C(31)-C(35)-C(34A)	105.7(9)
C(30)-C(29A)-C(28A)	97(3)	C(31)-C(32)-C(33A)	100.2(14)	C(34B)-C(35)-C(34A)	40.2(10)
C(30)-C(29A)-H(29A)	112.4	C(33B)-C(32)-C(33A)	15(3)	C(31)-C(35)-H(35A)	110.6
C(28A)-C(29A)-H(29A)	112.4	C(31)-C(32)-H(32A)	111.7	C(34B)-C(35)-H(35A)	73.8
C(30)-C(29A)-H(29B)	112.4	C(33B)-C(32)-H(32A)	96.8	C(34A)-C(35)-H(35A)	110.6
C(28A)-C(29A)-H(29B)	112.4	C(33A)-C(32)-H(32A)	111.7	C(31)-C(35)-H(35B)	110.6
H(29A)-C(29A)-H(29B)	109.9	C(31)-C(32)-H(32B)	111.7	C(34B)-C(35)-H(35B)	140.1
C(27)-C(28B)-C(29B)	99.4(18)	C(33B)-C(32)-H(32B)	117.0	C(34A)-C(35)-H(35B)	110.6
C(27)-C(28B)-H(28C)	111.9	C(33A)-C(32)-H(32B)	111.7	H(35A)-C(35)-H(35B)	108.7
O(9)-C(36)-C(40)	113.4(6)	C(39A)-C(40)-C(39B)	21.2(10)	H(42A)-C(42)-H(42C)	109.5
O(9)-C(36)-C(37)	113.9(6)	C(36)-C(40)-C(39B)	100.5(11)	H(42B)-C(42)-H(42C)	109.5
C(40)-C(36)-C(37)	105.7(6)	C(39A)-C(40)-H(40A)	110.7	C(41B)-C(42)-H(42D)	109.5
O(9)-C(36)-H(36)	107.9	C(36)-C(40)-H(40A)	110.7	C(41A)-C(42)-H(42D)	95.4
C(40)-C(36)-H(36)	107.9	C(39B)-C(40)-H(40A)	130.4	H(42A)-C(42)-H(42D)	19.2
C(37)-C(36)-H(36)	107.9	C(39A)-C(40)-H(40B)	110.7	H(42B)-C(42)-H(42D)	103.7
C(36)-C(37)-C(38)	102.1(7)	C(36)-C(40)-H(40B)	110.7	H(42C)-C(42)-H(42D)	127.9
C(36)-C(37)-H(37A)	111.3	C(39B)-C(40)-H(40B)	94.0	C(41B)-C(42)-H(42E)	109.5
C(38)-C(37)-H(37A)	111.3	H(40A)-C(40)-H(40B)	108.8	C(41A)-C(42)-H(42E)	148.1
C(36)-C(37)-H(37B)	111.3	C(41A)-O(10)-C(41B)	45.7(12)	H(42A)-C(42)-H(42E)	99.7
C(38)-C(37)-H(37B)	111.3	C(41A)-O(10)-C(43B)	124.6(16)	H(42B)-C(42)-H(42E)	46.4
H(37A)-C(37)-H(37B)	109.2	C(41B)-O(10)-C(43B)	116.3(12)	H(42C)-C(42)-H(42E)	70.8
C(39A)-C(38)-C(39B)	21.7(10)	C(41A)-O(10)-C(43A)	116.4(8)	H(42D)-C(42)-H(42E)	109.5
C(39A)-C(38)-C(37)	103.5(10)	C(41B)-O(10)-C(43A)	134.5(15)	C(41B)-C(42)-H(42F)	109.5
C(39B)-C(38)-C(37)	108.2(10)	C(43B)-O(10)-C(43A)	29.5(15)	C(41A)-C(42)-H(42F)	79.0
C(39A)-C(38)-H(38A)	111.1	O(10)-C(41A)-C(42)	113.0(9)	H(42A)-C(42)-H(42F)	98.7
C(39B)-C(38)-H(38A)	89.9	O(10)-C(41A)-H(41A)	109.0	H(42B)-C(42)-H(42F)	144.8
C(37)-C(38)-H(38A)	111.1	C(42)-C(41A)-H(41A)	109.0	H(42C)-C(42)-H(42F)	38.9
C(39A)-C(38)-H(38B)	111.1	O(10)-C(41A)-H(41B)	109.0	H(42D)-C(42)-H(42F)	109.5
C(39B)-C(38)-H(38B)	125.4	C(42)-C(41A)-H(41B)	109.0	H(42E)-C(42)-H(42F)	109.5
C(37)-C(38)-H(38B)	111.1	H(41A)-C(41A)-H(41B)	107.8	O(10)-C(43B)-C(44)	115.9(12)

H(38A)-C(38)-H(38B)	109.0	O(10)-C(41B)-C(42)	112.2(10)	O(10)-C(43B)-H(43A)	108.3
C(38)-C(39A)-C(40)	109.3(12)	O(10)-C(41B)-H(41C)	109.2	C(44)-C(43B)-H(43A)	108.3
C(38)-C(39A)-H(39A)	109.8	C(42)-C(41B)-H(41C)	109.2	O(10)-C(43B)-H(43B)	108.3
C(40)-C(39A)-H(39A)	109.8	O(10)-C(41B)-H(41D)	109.2	C(44)-C(43B)-H(43B)	108.3
C(38)-C(39A)-H(39B)	109.8	C(42)-C(41B)-H(41D)	109.2	H(43A)-C(43B)-H(43B)	107.4
C(40)-C(39A)-H(39B)	109.8	H(41C)-C(41B)-H(41D)	107.9	O(10)-C(43A)-C(44)	116.1(10)
H(39A)-C(39A)-H(39B)	108.3	C(41B)-C(42)-C(41A)	41.1(11)	O(10)-C(43A)-H(43C)	108.3
C(38)-C(39B)-C(40)	105.9(15)	C(41B)-C(42)-H(42A)	128.7	C(44)-C(43A)-H(43C)	108.3
C(38)-C(39B)-H(39C)	110.5	C(41A)-C(42)-H(42A)	109.5	O(10)-C(43A)-H(43D)	108.3
C(40)-C(39B)-H(39C)	110.5	C(41B)-C(42)-H(42B)	68.6	C(44)-C(43A)-H(43D)	108.3
C(38)-C(39B)-H(39D)	110.5	C(41A)-C(42)-H(42B)	109.5	H(43C)-C(43A)-H(43D)	107.4
C(40)-C(39B)-H(39D)	110.5	H(42A)-C(42)-H(42B)	109.5	C(43A)-C(44)-C(43B)	28.9(15)
H(39C)-C(39B)-H(39D)	108.7	C(41B)-C(42)-H(42C)	119.5	C(43A)-C(44)-H(44A)	109.5
C(39A)-C(40)-C(36)	105.0(9)	C(41A)-C(42)-H(42C)	109.5	C(43B)-C(44)-H(44A)	117.0
C(43A)-C(44)-H(44B)	109.5	H(44A)-C(44)-H(44D)	7.5	C(43A)-C(44)-H(44F)	135.6
C(43B)-C(44)-H(44B)	125.4	H(44B)-C(44)-H(44D)	116.1	C(43B)-C(44)-H(44F)	109.5
H(44A)-C(44)-H(44B)	109.5	H(44C)-C(44)-H(44D)	109.0	H(44A)-C(44)-H(44F)	105.8
C(43A)-C(44)-H(44C)	109.5	C(43A)-C(44)-H(44E)	86.2	H(44B)-C(44)-H(44F)	82.4
C(43B)-C(44)-H(44C)	80.9	C(43B)-C(44)-H(44E)	109.5	H(44C)-C(44)-H(44F)	31.3
H(44A)-C(44)-H(44C)	109.5	H(44A)-C(44)-H(44E)	105.4	H(44D)-C(44)-H(44F)	109.5
H(44B)-C(44)-H(44C)	109.5	H(44B)-C(44)-H(44E)	27.5	H(44E)-C(44)-H(44F)	109.5
C(43A)-C(44)-H(44D)	103.1	H(44C)-C(44)-H(44E)	133.4		
C(43B)-C(44)-H(44D)	109.5	H(44D)-C(44)-H(44E)	109.5		

Symmetry transformations used to generate equivalent atoms: #1 -x+1,-y,-z+1

Table 3: Anisotropic displacement parameters ($Å^2 x\ 10^3$) for sh3420. The anisotropic displacement factor exponent takes the form: $-2p^2[\ h^2\ a^{*2}U^{11} + ... + 2\ h\ k\ a^*\ b^*\ U^{12}\ ]$

	U^{11}	U^{22}	U^{33}	U^{23}	U^{13}	U^{12}
_ Al(1)	21(1)	21(1)	25(1)	-6(1)	-5(1)	1(1)
Al(2)	36(1)	29(1)	33(1)	0(1)	-6(1)	1(1)
Al(3)	41(1)	44(1)	26(1)	-4(1)	-11(1)	-10(1)

Al(4)	51(1)	38(1)	28(1)	-9(1)	0(1)	8(1)
Al(5)	36(1)	43(2)	31(1)	-2(1)	2(1)	3(1)
O(1)	26(2)	18(2)	23(2)	-4(2)	-1(2)	-1(2)
O(2)	34(2)	27(3)	32(2)	-9(2)	-1(2)	7(2)
O(3)	22(2)	41(3)	26(2)	-2(2)	-5(2)	-10(2)
O(4)	45(3)	24(2)	30(2)	-5(2)	-7(2)	10(2)
O(5)	24(2)	36(3)	26(2)	-7(2)	-6(2)	0(2)
O(6)	30(2)	57(3)	30(3)	0(2)	-13(2)	-1(2)
O(7)	69(3)	33(3)	30(3)	-16(2)	-4(2)	-8(2)
O(8)	30(2)	50(3)	37(3)	-5(2)	3(2)	14(2)
O(9)	44(3)	20(2)	27(2)	-1(2)	1(2)	-6(2)
C(1)	30(3)	28(4)	40(4)	-18(3)	-13(3)	6(3)
C(2)	23(3)	49(5)	49(5)	-24(4)	6(3)	-1(3)
C(3)	36(4)	63(6)	72(6)	-40(5)	-7(4)	11(4)
C(4)	55(5)	33(5)	149(10)	-26(6)	-14(6)	17(4)
C(5)	32(4)	32(4)	82(6)	-25(4)	-7(4)	5(3)
C(6)	24(3)	27(4)	32(4)	4(3)	-4(3)	-8(3)
C(7)	30(3)	23(4)	44(4)	-7(3)	2(3)	-1(3)
C(8)	40(4)	46(5)	67(6)	-23(4)	-12(4)	-7(3)
C(9)	28(4)	38(5)	74(6)	1(4)	-15(4)	-1(3)
C(10)	27(3)	31(4)	70(6)	-10(4)	-15(4)	3(3)
C(11)	52(4)	26(4)	26(4)	-7(3)	-9(3)	10(3)
C(12)	60(5)	26(4)	69(6)	-8(4)	-30(4)	-1(4)
C(13)	53(5)	55(6)	110(8)	-37(6)	-34(5)	19(4)
C(14)	60(5)	32(5)	79(6)	-21(4)	-17(5)	15(4)
C(15)	48(4)	23(4)	42(4)	-8(3)	-20(4)	6(3)
C(16)	29(3)	33(4)	39(4)	-8(3)	-16(3)	0(3)
C(17)	30(3)	32(4)	47(5)	-8(3)	-16(3)	2(3)
C(18)	33(4)	47(5)	78(6)	-19(5)	-13(4)	-7(3)
C(19)	56(5)	42(5)	71(5)	-29(4)	-28(4)	2(4)
C(20)	41(4)	53(5)	54(5)	-36(4)	-21(4)	16(4)
C(21)	35(4)	82(7)	46(5)	1(4)	-21(3)	11(4)
C(22)	40(4)	52(6)	55(5)	-2(4)	-17(3)	12(4)
C(23)	42(4)	54(6)	75(6)	12(5)	-25(4)	-2(4)
C(24)	96(7)	137(11)	69(6)	22(7)	-23(5)	39(8)
C(25)	66(5)	94(8)	29(4)	-5(4)	-15(4)	18(5)
C(26)	134(9)	44(5)	53(5)	-28(4)	-24(5)	-9(5)
C(27)	111(7)	33(5)	53(5)	-7(4)	-38(5)	-4(4)
C(28A)	178(14)	32(5)	64(6)	-17(5)	-47(7)	-3(6)

C(29A)	177(14)	34(6)	61(6)	-16(5)	-49(7)	-5(6)
C(28B)	179(14)	31(5)	65(6)	-15(5)	-45(7)	-2(6)
C(29B)	179(14)	34(5)	62(5)	-18(5)	-47(7)	-4(6)
C(30)	138(9)	36(5)	49(5)	-19(4)	-28(6)	-7(5)
C(31)	43(4)	93(7)	47(5)	-16(5)	7(4)	27(4)
C(32)	43(5)	95(8)	58(5)	-28(5)	-16(4)	29(5)
C(33A)	50(6)	109(14)	66(8)	-36(9)	-7(5)	30(8)
C(34A)	53(6)	108(14)	66(8)	-38(9)	-5(5)	30(8)
C(33B)	50(6)	108(14)	67(9)	-37(9)	-7(5)	31(9)
C(34B)	52(6)	110(14)	64(8)	-36(9)	-4(5)	29(9)
C(35)	52(5)	120(9)	41(5)	-21(5)	-8(4)	20(5)
C(36)	50(4)	29(4)	36(4)	0(3)	-5(3)	-2(3)
C(37)	64(5)	34(5)	39(4)	-10(4)	-4(4)	-10(4)
C(38)	77(6)	37(5)	80(7)	-12(4)	16(5)	-18(4)
C(39A)	45(5)	53(5)	56(5)	-4(4)	-2(4)	-1(4)
C(40)	73(5)	36(5)	34(4)	8(3)	8(4)	-9(4)
O(10)	82(4)	62(5)	82(3)	-13(4)	-31(4)	-9(4)
C(41A)	60(9)	67(10)	91(6)	-18(7)	-6(6)	-17(7)
C(41B)	62(10)	66(10)	92(6)	-15(6)	-4(8)	-18(8)
C(42)	81(7)	54(7)	95(5)	-16(5)	-30(5)	-10(6)
C(43B)	76(12)	71(13)	86(6)	-49(8)	-2(7)	11(9)
C(43A)	78(11)	71(13)	85(5)	-56(7)	-6(6)	12(8)
C(44)	166(13)	163(14)	89(6)	6(9)	-21(8)	-68(11)

Table 4. Hydrogen coordinates (x 10^4) and isotropic displacement parameters ($Å^2$x 10^3) for sh3364.

	x	y	z	U(eq)
H(1)	5910(40)	6310(50)	9380(14)	22(14)
H(2)	5420(50)	9630(30)	7070(30)	50(20)
H(3)	4010(40)	5590(70)	7130(50)	100(30)
H(4)	8160(40)	4260(30)	7170(30)	25(16)
H(5)	9400(30)	8280(50)	7360(40)	50(20)
H(1A)	5125	8295	9365	37
H(2A)	3294	7977	9263	48
H(2B)	3462	8733	8425	48

H(3A)	2529	10032	9113	65
H(3B)	3194	9601	9800	65
H(4A)	4099	11059	8400	94
H(4B)	4333	11173	9213	94
H(5A)	5835	10058	9107	57
H(5B)	5774	10211	8233	57
H(6)	3967	5308	9351	35
H(7A)	4440	3767	8384	40
H(7B)	3961	3460	9276	40
H(8A)	2636	3711	8127	59
H(8B)	2320	2913	8952	59
H(9A)	1632	4430	9494	57
H(9B)	1192	4727	8708	57
H(10A)	2394	6266	9032	50
H(10B)	2692	6044	8181	50
H(11)	6709	4284	9425	41
H(12A)	8995	4553	8589	59
H(12B)	8569	4434	9481	59
H(13A)	9629	2785	8946	81
H(13B)	8617	2508	9685	81
H(14A)	7937	1473	8958	66
H(14B)	8460	2380	8200	66
H(15A)	6590	3031	8346	43
H(15B)	6327	2552	9238	43
H(16)	7869	6892	9461	38
H(17A)	9746	6559	9307	42
H(17B)	9855	6884	8410	42
H(18A)	10932	8162	9078	62
H(18B)	10411	8754	8357	62
H(19A)	9523	9785	9257	62
H(19B)	9314	8635	9907	62
H(20A)	8108	9215	8669	53
H(20B)	7520	8746	9535	53
H(21)	3821	7181	6259	65
H(22A)	2502	7737	7194	59
H(22B)	3203	8938	7137	59
H(23A)	1741	8429	6176	70
H(23B)	2008	9677	6357	70
H(24A)	3075	8823	5131	127

H(24B)	3374	10052	5327	127
H(25A)	4859	8360	5336	76
H(25B)	4896	9358	5822	76
H(26)	7087	3979	6332	88
H(27A)	4754	3321	7043	75
H(27B)	5939	2719	7250	75
H(28A)	5179	1986	6229	104
H(28B)	6543	2327	6053	104
H(29A)	6104	3419	5002	104
H(29B)	4759	3561	5402	104
H(28C)	4640	2215	6298	105
H(28D)	5969	1796	6272	105
H(29C)	6645	3194	5292	104
H(29D)	5316	3403	5206	104
H(30A)	6603	5006	5380	86
H(30B)	5279	5127	5794	86
H(31)	10193	7143	6406	75
H(32A)	10246	4855	7270	75
H(32B)	10920	6009	7347	75
H(33A)	12023	6147	6067	88
H(33B)	12209	4860	6521	88
H(34A)	10535	4125	6159	89
H(34B)	11315	4834	5388	89
H(33C)	11473	4222	6539	88
H(33D)	12355	5306	6479	88
H(34C)	11578	6495	5385	89
H(34D)	11310	5229	5218	89
H(35A)	10148	6493	5416	84
H(35B)	9148	5536	5845	84
H(36)	7114	10334	6292	48
H(37A)	8647	10354	7324	55
H(37B)	7489	11102	7266	55
H(38A)	8386	12297	6159	83
H(38B)	9465	12086	6591	83
H(39A)	10283	10851	5898	64
H(39B)	9565	11530	5301	64
H(39C)	9994	11373	5430	60
H(39D)	8697	11686	5296	60
H(40A)	9280	9276	5957	63

H(40B)	8521	9971	5385	63
H(41A)	3503	1749	5788	88
H(41B)	3186	3067	5828	88
H(41C)	2748	3398	5815	90
H(41D)	1409	3282	5749	90
H(42A)	3199	2720	4621	111
H(42B)	1910	3039	4992	111
H(42C)	2218	1717	4955	111
H(42D)	3231	2890	4737	111
H(42E)	1897	2604	4728	111
H(42F)	2672	1629	5113	111
H(43A)	1410	2959	7062	91
H(43B)	2648	2414	7142	91
H(43C)	2570	2500	7145	89
H(43D)	2865	1186	7087	89
H(44A)	1569	1330	8152	215
H(44B)	1021	613	7640	215
H(44C)	666	1929	7657	215
H(44D)	1638	1416	8119	215
H(44E)	1422	609	7547	215
H(44F)	463	1523	7788	215

Compund 6

Table 1: Atomic coordinates (x 10^4) and equivalent isotropic displacement parameters ($Å^2$x 10^3) for sh3420. U(eq) is defined as one third of the trace of the orthogonalized U^{ij} tensor.

	x	y	z	U(eq)
Al(1)	7500	7500	583(2)	13(1)
Al(2)	8077(1)	8615(1)	2922(1)	19(1)
O(1)	7500	7500	2649(5)	14(1)
O(3)	8055(1)	8526(1)	941(2)	16(1)
O(2)	7083(1)	8809(1)	3743(2)	19(1)
Cl	7500	7500	-1863(4)	35(1)
C(1)	6904(2)	9530(2)	4595(4)	24(1)

C(2)	6431(3)	9352(2)	5985(4)	33(1)
C(3)	6121(3)	10198(3)	6429(4)	42(1)
C(4)	6059(4)	10690(3)	5004(5)	59(2)
C(5)	6403(3)	10162(2)	3783(4)	33(1)
C(6)	8140(2)	9156(2)	-134(4)	21(1)
C(7)	8947(2)	9625(2)	-38(5)	28(1)
C(8)	8726(3)	10505(3)	-256(8)	65(2)
C(9A)	7950(6)	10626(5)	414(12)	35(2)
C(9B)	7890(4)	10530(4)	-767(9)	36(2)
C(10)	7481(2)	9807(2)	-22(5)	34(1)
O(5)	7500	2500	5000	93(3)
C(12)	7761(10)	2471(15)	3654(19)	116(6)
C(13)	7541(13)	2191(9)	2410(18)	108(6)

Table 2: Bond lengths [Å] and angles [°] for sh3348.

Al(1)-O(1)	1.885(5)	Al(2)-O(2)	1.830(2)	C(1)-C(5)	1.524(5)
Al(1)-O(3)	1.951(2)	Al(2)-O(1)	2.0861(11)	C(1)-H(7)	0.92(4)
Al(1)-O(3)#1	1.952(2)	Al(2)-Al(2)#3	2.9289(14)	C(2)-C(3)	1.539(5)
Al(1)-O(3)#2	1.952(2)	Al(2)-Al(2)#2	2.9290(14)	C(2)-H(3)	0.95(5)
Al(1)-O(3)#3	1.952(2)	Al(2)-H(2)	1.55(4)	C(2)-H(4)	1.06(4)
Al(1)-Cl	2.233(4)	O(1)-Al(2)#1	2.0861(11)	C(3)-C(4)	1.537(6)
Al(1)-Al(2)#2	2.9746(16)	O(1)-Al(2)#2	2.0861(11)	C(3)-H(3A)	0.9900
Al(1)-Al(2)#3	2.9746(16)	O(1)-Al(2)#3	2.0861(11)	C(3)-H(3B)	0.9900
Al(1)-Al(2)#1	2.9746(16)	O(3)-C(6)	1.436(4)	C(4)-C(5)	1.523(5)
Al(1)-Al(2)	2.9746(16)	O(2)-C(1)	1.451(4)	C(4)-H(4A)	0.9900
Al(1)-H(1)	1.557(10)	O(2)-Al(2)#3	1.830(2)	C(4)-H(4B)	0.9900
Al(2)-O(3)	1.815(2)	Cl-H(1)	0.676(11)	C(5)-H(5)	0.91(5)
Al(2)-O(2)#2	1.830(2)	C(1)-C(2)	1.518(5)	C(5)-H(6)	0.96(5)
C(6)-C(10)	1.531(5)	O(1)-Al(1)-O(3)#2	80.36(8)	O(3)#1-Al(1)-Al(2)	124.48(10)
C(6)-C(7)	1.542(5)	O(3)-Al(1)-O(3)#2	88.39(3)	O(3)#2-Al(1)-Al(2)	83.84(8)
C(6)-H(8)	0.92(4)	O(3)#1-Al(1)-O(3)#2	88.39(3)	O(3)#3-Al(1)-Al(2)	82.35(8)
C(7)-C(8)	1.510(5)	O(1)-Al(1)-O(3)#3	80.36(8)	Cl-Al(1)-Al(2)	135.87(3)
C(7)-H(9)	0.95(5)	O(3)-Al(1)-O(3)#3	88.39(3)	Al(2)#2-Al(1)-Al(2)	58.99(4)
C(7)-H(10)	0.97(5)	O(3)#1-Al(1)-O(3)#3	88.39(3)	Al(2)#3-Al(1)-Al(2)	58.99(4)
C(8)-C(9A)	1.433(11)	O(3)#2-Al(1)-O(3)#3	160.72(16)	Al(2)#1-Al(1)-Al(2)	88.25(6)

C(8)-C(9B)	1.457(8)	O(1)-Al(1)-Cl	180.000(1)	O(1)-Al(1)-H(1)	180.000(3)
C(8)-H(8A)	0.9900	O(3)-Al(1)-Cl	99.64(8)	O(3)-Al(1)-H(1)	99.64(8)
C(8)-H(8B)	0.9900	O(3)#1-Al(1)-Cl	99.64(8)	O(3)#1-Al(1)-H(1)	99.64(8)
C(8)-H(8C)	0.9900	O(3)#2-Al(1)-Cl	99.64(8)	O(3)#2-Al(1)-H(1)	99.64(8)
C(8)-H(8D)	0.9900	O(3)#3-Al(1)-Cl	99.64(8)	O(3)#3-Al(1)-H(1)	99.64(8)
C(9A)-C(10)	1.606(10)	O(1)-Al(1)-Al(2)#2	44.13(3)	Cl-Al(1)-H(1)	0.000(1)
C(9A)-H(9A)	0.9900	O(3)-Al(1)-Al(2)#2	82.35(8)	Al(2)#2-Al(1)-H(1)	135.87(3)
C(9A)-H(9B)	0.9900	O(3)#1-Al(1)-Al(2)#2	83.84(8)	Al(2)#3-Al(1)-H(1)	135.87(3)
C(9B)-C(10)	1.528(7)	O(3)#2-Al(1)-Al(2)#2	36.24(7)	Al(2)#1-Al(1)-H(1)	135.87(3)
C(9B)-H(9C)	0.9900	O(3)#3-Al(1)-Al(2)#2	124.48(10)	Al(2)-Al(1)-H(1)	135.87(3)
C(9B)-H(9D)	0.9900	Cl-Al(1)-Al(2)#2	135.87(3)	O(3)-Al(2)-O(2)#2	111.71(11)
C(10)-H(10A)	0.9900	O(1)-Al(1)-Al(2)#3	44.13(3)	O(3)-Al(2)-O(2)	113.88(11)
C(10)-H(10B)	0.9900	O(3)-Al(1)-Al(2)#3	83.84(8)	O(2)#2-Al(2)-O(2)	122.23(15)
C(10)-H(10C)	0.9900	O(3)#1-Al(1)-Al(2)#3	82.35(8)	O(3)-Al(2)-O(1)	78.46(13)
C(10)-H(10D)	0.9900	O(3)#2-Al(1)-Al(2)#3	124.48(10)	O(2)#2-Al(2)-O(1)	78.17(9)
O(5)-C(12)#4	1.303(17)	O(3)#3-Al(1)-Al(2)#3	36.24(7)	O(2)-Al(2)-O(1)	78.15(9)
O(5)-C(12)#5	1.303(17)	Cl-Al(1)-Al(2)#3	135.87(3)	O(3)-Al(2)-Al(2)#3	87.52(7)
O(5)-C(12)#6	1.303(17)	Al(2)#2-Al(1)-Al(2)#3	88.25(6)	O(2)#2-Al(2)-Al(2)#3	115.99(7)
O(5)-C(12)	1.303(17)	O(1)-Al(1)-Al(2)#1	44.13(3)	O(2)-Al(2)-Al(2)#3	36.84(7)
C(12)-C(13)	1.28(2)	O(3)-Al(1)-Al(2)#1	124.48(10)	O(1)-Al(2)-Al(2)#3	45.411(15)
C(12)-H(12A)	0.9900	O(3)#1-Al(1)-Al(2)#1	36.24(7)	O(3)-Al(2)-Al(2)#2	85.89(7)
C(12)-H(12B)	0.9900	O(3)#2-Al(1)-Al(2)#1	82.35(8)	O(2)#2-Al(2)-Al(2)#2	36.86(8)
C(13)-H(13A)	0.9800	O(3)#3-Al(1)-Al(2)#1	83.84(8)	O(2)-Al(2)-Al(2)#2	115.97(7)
C(13)-H(13B)	0.9800	Cl-Al(1)-Al(2)#1	135.87(3)	O(1)-Al(2)-Al(2)#2	45.411(14)
C(13)-H(13C)	0.9800	Al(2)#2-Al(1)-Al(2)#1	58.99(4)	Al(2)#3-Al(2)-Al(2)#2	90.000(1)
O(1)-Al(1)-O(3)	80.36(8)	Al(2)#3-Al(1)-Al(2)#1	58.99(4)	O(3)-Al(2)-Al(1)	39.48(7)
O(1)-Al(1)-O(3)#1	80.36(8)	O(1)-Al(1)-Al(2)	44.13(3)	O(2)#2-Al(2)-Al(1)	96.65(8)
O(3)-Al(1)-O(3)#1	160.72(16)	O(3)-Al(1)-Al(2)	36.24(7)	O(2)-Al(2)-Al(1)	96.64(8)
O(1)-Al(2)-Al(1)	38.99(12)	C(3)-C(2)-H(3)	111(3)	C(9A)-C(8)-C(9B)	44.5(5)
Al(2)#3-Al(2)-Al(1)	60.506(18)	C(1)-C(2)-H(4)	110(2)	C(9A)-C(8)-C(7)	107.0(5)
Al(2)#2-Al(2)-Al(1)	60.506(18)	C(3)-C(2)-H(4)	113(2)	C(9B)-C(8)-C(7)	107.3(4)
O(3)-Al(2)-H(2)	106.6(14)	H(3)-C(2)-H(4)	111(4)	C(9A)-C(8)-H(8A)	110.3
O(2)#2-Al(2)-H(2)	101.1(14)	C(4)-C(3)-C(2)	106.1(3)	C(9B)-C(8)-H(8A)	140.2
O(2)-Al(2)-H(2)	98.0(14)	C(4)-C(3)-H(3A)	110.5	C(7)-C(8)-H(8A)	110.3
O(1)-Al(2)-H(2)	174.6(14)	C(2)-C(3)-H(3A)	110.5	C(9A)-C(8)-H(8B)	110.3
Al(2)#3-Al(2)-H(2)	132.1(14)	C(4)-C(3)-H(3B)	110.5	C(9B)-C(8)-H(8B)	68.9
Al(2)#2-Al(2)-H(2)	135.5(14)	C(2)-C(3)-H(3B)	110.5	C(7)-C(8)-H(8B)	110.3
Al(1)-Al(2)-H(2)	146.0(14)	H(3A)-C(3)-H(3B)	108.7	H(8A)-C(8)-H(8B)	108.6
Al(1)-O(1)-Al(2)	96.88(12)	C(5)-C(4)-C(3)	107.0(3)	C(9A)-C(8)-H(8C)	69.0

Al(1)-O(1)-Al(2)#1	96.88(12)	C(5)-C(4)-H(4A)	110.3	C(9B)-C(8)-H(8C)	110.3
Al(2)-O(1)-Al(2)#1	166.2(2)	C(3)-C(4)-H(4A)	110.3	C(7)-C(8)-H(8C)	110.3
Al(1)-O(1)-Al(2)#2	96.88(12)	C(5)-C(4)-H(4B)	110.3	H(8A)-C(8)-H(8C)	43.6
Al(2)-O(1)-Al(2)#2	89.18(3)	C(3)-C(4)-H(4B)	110.3	H(8B)-C(8)-H(8C)	137.4
Al(2)#1-O(1)-Al(2)#2	89.18(3)	H(4A)-C(4)-H(4B)	108.6	C(9A)-C(8)-H(8D)	140.5
Al(1)-O(1)-Al(2)#3	96.88(12)	C(4)-C(5)-C(1)	103.7(3)	C(9B)-C(8)-H(8D)	110.3
Al(2)-O(1)-Al(2)#3	89.18(3)	C(4)-C(5)-H(5)	111(3)	C(7)-C(8)-H(8D)	110.3
Al(2)#1-O(1)-Al(2)#3	89.18(3)	C(1)-C(5)-H(5)	111(3)	H(8A)-C(8)-H(8D)	68.0
Al(2)#2-O(1)-Al(2)#3	166.2(2)	C(4)-C(5)-H(6)	112(3)	H(8B)-C(8)-H(8D)	43.7
C(6)-O(3)-Al(2)	128.34(19)	C(1)-C(5)-H(6)	110(3)	H(8C)-C(8)-H(8D)	108.5
C(6)-O(3)-Al(1)	123.94(19)	H(5)-C(5)-H(6)	109(4)	C(8)-C(9A)-C(10)	102.0(6)
Al(2)-O(3)-Al(1)	104.28(12)	O(3)-C(6)-C(10)	113.2(3)	C(8)-C(9A)-H(9A)	111.4
C(1)-O(2)-Al(2)#3	129.2(2)	O(3)-C(6)-C(7)	114.1(3)	C(10)-C(9A)-H(9A)	111.4
C(1)-O(2)-Al(2)	123.0(2)	C(10)-C(6)-C(7)	104.9(3)	C(8)-C(9A)-H(9B)	111.4
Al(2)#3-O(2)-Al(2)	106.30(12)	O(3)-C(6)-H(8)	106(2)	C(10)-C(9A)-H(9B)	111.4
Al(1)-Cl-H(1)	0.000(3)	C(10)-C(6)-H(8)	110(2)	H(9A)-C(9A)-H(9B)	109.2
O(2)-C(1)-C(2)	113.2(3)	C(7)-C(6)-H(8)	108(2)	C(8)-C(9B)-C(10)	104.7(5)
O(2)-C(1)-C(5)	114.2(3)	C(8)-C(7)-C(6)	105.5(3)	C(8)-C(9B)-H(9C)	110.8
C(2)-C(1)-C(5)	105.0(3)	C(8)-C(7)-H(9)	111(3)	C(10)-C(9B)-H(9C)	110.8
O(2)-C(1)-H(7)	107(2)	C(6)-C(7)-H(9)	112(3)	C(8)-C(9B)-H(9D)	110.8
C(2)-C(1)-H(7)	109(2)	C(8)-C(7)-H(10)	112(3)	C(10)-C(9B)-H(9D)	110.8
C(5)-C(1)-H(7)	108(2)	C(6)-C(7)-H(10)	113(3)	H(9C)-C(9B)-H(9D)	108.9
C(1)-C(2)-C(3)	102.5(3)	H(9)-C(7)-H(10)	104(4)	C(9B)-C(10)-C(6)	101.8(4)
C(1)-C(2)-H(3)	110(3)	C(6)-C(10)-C(9A)	105.3(4)	C(9B)-C(10)-C(9A)	40.8(5)
C(9B)-C(10)-H(10A)	142.8	C(9A)-C(10)-H(10D)	72.6	O(5)-C(12)-H(12B)	102.3
C(6)-C(10)-H(10A)	110.7	H(10A)-C(10)-H(10D)	39.7	H(12A)-C(12)-H(12B)	104.9
C(9A)-C(10)-H(10A)	110.7	H(10B)-C(10)-H(10D)	134.9	C(12)-C(13)-H(13A)	109.5
C(9B)-C(10)-H(10B)	74.6	H(10C)-C(10)-H(10D)	109.3	C(12)-C(13)-H(13B)	109.5
C(6)-C(10)-H(10B)	110.7	C(12)#4-O(5)-C(12)#5	38.9(16)	H(13A)-C(13)-H(13B)	109.5
C(9A)-C(10)-H(10B)	110.7	C(12)#4-O(5)-C(12)#6	152.8(11)	C(12)-C(13)-H(13C)	109.5
H(10A)-C(10)-H(10B)	108.8	C(12)#5-O(5)-C(12)#6	152.8(11)	H(13A)-C(13)-H(13C)	109.5
C(9B)-C(10)-H(10C)	111.4	C(12)#4-O(5)-C(12)	152.8(11)	H(13B)-C(13)-H(13C)	109.5
C(6)-C(10)-H(10C)	111.4	C(12)#5-O(5)-C(12)	152.8(11)		
C(9A)-C(10)-H(10C)	138.7	C(12)#6-O(5)-C(12)	38.9(16)		
H(10A)-C(10)-H(10C)	73.4	C(13)-C(12)-O(5)	139.1(18)		
H(10B)-C(10)-H(10C)	38.2	C(13)-C(12)-H(12A)	102.3		
C(9B)-C(10)-H(10D)	111.4	O(5)-C(12)-H(12A)	102.3		

Symmetry transformations used to generate equivalent atoms:

#1 -x+3/2,-y+3/2,z #2 y,-x+3/2,z #3 -y+3/2,x,z

#4 -y+1,x-1/2,-z+1 #5 y+1/2,-x+1,-z+1 #6 -x+3/2,-y+1/2,z

Table 3: . Anisotropic displacement parameters ($Å^2 x\ 10^3$) for sh3348. The anisotropic displacement factor exponent takes the form: $-2\pi^2[\ h^2\ a^{*2}U^{11} + ...\ + 2\ h\ k\ a^*\ b^*\ U^{12}\ ]$

	U^{11}	U^{22}	U^{33}	U^{23}	U^{13}	U^{12}
Al(1)	12(1)	12(1)	16(1)	0	0	0
Al(2)	18(1)	21(1)	18(1)	-4(1)	-2(1)	2(1)
O(1)	14(1)	14(1)	16(2)	0	0	0
O(3)	20(1)	13(1)	16(1)	0(1)	0(1)	-2(1)
O(2)	22(1)	14(1)	21(1)	-5(1)	1(1)	4(1)
Cl	36(1)	36(1)	33(2)	0	0	0
C(1)	30(2)	18(2)	24(2)	-7(1)	1(1)	5(1)
C(2)	49(2)	31(2)	19(2)	-3(2)	5(2)	11(2)
C(3)	59(3)	40(2)	27(2)	-10(2)	5(2)	19(2)
C(4)	96(4)	42(3)	37(2)	-5(2)	11(3)	39(3)
C(5)	50(2)	24(2)	25(2)	-4(2)	2(2)	10(2)
C(6)	28(2)	17(2)	19(2)	2(1)	-1(1)	-4(1)
C(7)	24(2)	24(2)	37(2)	6(2)	5(2)	-5(1)
C(8)	38(2)	28(2)	129(5)	21(3)	-8(3)	-10(2)
C(9A)	40(4)	19(3)	46(4)	4(3)	0(4)	3(3)
C(9B)	38(3)	21(3)	49(4)	11(3)	-2(3)	-2(2)
C(10)	24(2)	26(2)	52(2)	18(2)	-3(2)	-1(1)

5: Use of the hybrid surfaces (Al/Al_2O_3 nano-wires +PTFEP):

The in-vitro investigation results of the developed surface will be shown in the Ph.D. thesis of Ayman Haidar.

6:

A.Haidar, **A. A. Ali**, I. Müller, H. Eichler, M. Veith, C. Aktas, H. Abdul-Khaliq: *Novel Compatible Surfaces for Cardiovascular Implants*. The Thoracic and Cardiovascular Surgeon 02/**2016**; 64(S 02-S 02):OP131. DOI:10.1055/s-0036-1571877

7:Awadelkaereem A. Ali, Volker Huc, Cenk Aktas and Michael Veith, Cyclopentanolates of Aluminium Hydride, Aluminium Chloride forming Aluminium-Oxygen-Hetero-Cages and Mixed Coordination Oligomers" , Z. Anorg. Allg. Chem.., **2016**, 642, 18, 973.

8:

Awadelkareem A. Ali, Hassan Nimir, Cenk Aktas, Volker Huch, Ulrich Rauch, Karl-Herbert Schäfer, and Michael Veith, *Organometallics*, **2012**, 31 (6), pp 2256–2262

9:

A patent application have been performed, the draft of the patent was submitted to the patent office at Saarland University.

Acknowledgments

All thanks and praises due to my lord first and last. Thanks to Allah for making this possible and emphasizing more in me that indeed, there is no might or power except in Allah.

This thesis appears in its current form due to the assistance and guidance of several people. I would therefore like to offer my sincere thanks to all of them.

First, I want to thank my supervisors Prof. Dr. Dr. M.E. Hammadeh, Prof. Dr. Hashim Abdul-Khaliq and Prof. Dr. Dr. h.c. Michael Veith for their support, ideas, motivation, and fruitful discussions during my thesis. I did enjoy working with them and indeed they enriched my academic and professional skills by their fruitful scientific discussions, brilliant ideas, and unending motivations.

My gratitude and deep appreciation to all people involved in this research work for being very helpful, friendly, and open to collaboration. Namely, Dr. Cenk Aktas for guiding me during my experimental works and giving me the opportunity to start my experiments in his group CVD/Biosurfaces located in INM, Saarland university, Ayman Haidar for his supports in preparing the videos, offering the blood and bio experiments during the thesis, Alexander May for his helps in translation and . Dr. Volker Huch for his help with X-ray crystallography measurements

Special Thanks to Dr .Peter William de Oliveira, head of optical materials group and Innovationszentrum at INM, for accepting me in his group and offering the opportunity to continue my Ph.D experiments in his labs after the closure of CVD group.

Thanks are also extended to all my colleagues, the former members of Prof. Veith research group and CVD/ Biosurfaces and optical materials group at INM, for

the friendly atmosphere and great work environment, the incredible lovely memories that will always be in mind

Many thanks are due to the DAAD for granting me the DAAD fellowship and for their financial support of this project.

Many thanks to my parents, brothers and sister for their love, their prayer for me, and the unconditional support throughout all these years. Their constant support to me is invaluable and no words could express my feelings towards them.

I owe my deepest gratitude and precious thanks to my lovely wife Marwa for her steadfast moral and spiritual support as well as her understanding for my workload during the whole PhD period. Thank you Marwa for your love and for being the best partner I could have ever wished for. I am also thankful to our sons (Ahmed, Hayder, and Ziad) for being the roses and the lovely part of our life.